Optimization Of Arachidonic Acid Production Through Fermentation

By

Zixuan Ren

Submitted in partial fulfilment of the requirements

for the degree of Master of Applied Science

At

Dalhousie University

Halifax, Nova Scotia

June 2023

Dalhousie University is located in Mi'kma'ki, the ancestral and unceded territory of the Mi'kmaq. We are all Treaty people.

Table of Contents

List of Tables

List of Figures

Abstract

Arachidonic acid (ARA) is an omega-6 fatty acid (C20:4n-6) needed for improving infant memory and eyesight, and an important supplement in infant formula. This project aimed to develop a process to produce ARA from *Mortierella alpina* strain MA2-2 by 1) optimizing the production medium and 2) applying strain improvement techniques.

The optimized medium for MA2-2 resulted in 19–22 g L^{-1} biomass, 30–35 % oil%, 33–42% ARA content and 2.1–2.5 g L^{-1} ARA concentration. Compared to the original medium, this was an improvement of at least 0.9, 0.875, 0.32, 3.7 times, respectively. Random mutagenesis was conducted using UV, cerulenin and staining reagent TTC. However, the mutants did not exhibit significantly beneficial phenotypes. High-temperature ALE was performed on wild-type MA2-2 for up to 90 days (45 ALE cycles). The evolved strain showed greater thermotolerance with ARA final productivity of 0.421 ± 0.04 g L^{-1} d^{-1}, 27.6% higher than the original strain.

List of Abbreviations and Symbols Used

ACC	Acetyl-CoA carboxylase
ACP	Acid Phosphatase
ALE	Adaptive Laboratory Evolution
ANOVA	Analysis of Variance
ARA	Arachidonic Acid (C20:4n-6)
ARASCO	ARA-rich Single Cell Oil
BBD	Box–Behnken Design
C	Carbon
$CaCl_2.2H_20$	Calcium Chloride Dihydrate
CCD	Central Composite Design
cm	Centimeter
CoA	Coenzyme-A
$CoCl_2.6H_20$	Cobalt(II) Chloride Hexahydrate
$CuSO_4.5H_20$	Copper Sulfate Pentahydrate
DCW	Dry Cell Weight
DF	Degree of Freedom
DHA	Docosahexaenoic Acid
DHASCO	DHA Single Cell Oil
DO	Dissolved Oxygen
DOE	Design of Experiments
DNA	Deoxyribonucleic Acid
EFA	Essential Fatty Acid
EMS	Ethyl Methane Sulphonate
EPA	Eicosapentaenoic Acid
FA	Fatty Acid

FAME	Fatty Acid Methyl Esters
F test	Fisher's Test
FID	Flame Ionization Detector
FACS	Fluorescence-Activated Cell Sorting
$FeSo_4.7H_20$	Iron(II) Sulfate Heptahydrate
FFD	Full Factorial 3-Level Design
GC	Gas Chromatography
g	Gram
GMO	Genetically Modified Organism
h	Hour
HCl	Hydrogen Chloride
III	Third
IV	Fourth
Kg	Kilogram
KH_2PO_4	Potassium Dihydrogen Phosphate
L	Liter
LC-PUFA	Long-Chain Polyunsaturated Fatty Acid
M	Molar
M. alpina	*Mortierella alpina*
ME	Malic Enzyme
mg	Milligram
$MgCl_2.6H_20$	Magnesium Chloride Hexahydrate
$MgSO_4.7H_20$	Magnesium Sulfate Heptahydrate
min	Minute
mL	Milliliter
mM	Millimolar
$MnCl_2.4H_20$	Manganese(II) Chloride Tetrahydrate

MS	Mean of Square
MSG	Monosodium Glutamate
MUFA	Monounsaturated Fatty Acid
N	Nitrogen
n-3	Omega-3 Series
n-6	Omega-6 Series
NaCl	Sodium Chloride
NADP	Nicotinamide Adenine Dinucleotide Phosphate
NADPH	Reduced Nicotinamide Adenine Dinucleotide Phosphate
$NaNO_3$	Sodium Nitrate
NaOH	Sodium Hydroxide
$NiSO_4.6H_20$	Nickel Sulfate Hexahydrate
$(NH_4)_2SO_4$	Ammonia Sulfate
nm	Nanometer
NTG	N-methyl-N'-nitro-N'nitrosoguanidine
PB	Plackett-Burman
PBS	Phosphate-Buffered Saline
PDA	Potato Dextrose Agar
PH	Potential of Hydrogen
PKS	Polyketide Synthase
PUFA	Polyunsaturated Fatty Acid
R^2	Coefficient of Determination
RSM	Response Surface Methodology
SCO	Single Cell Oil
SD	Standard Deviation
SFA	Saturated Fatty Acid
SS	Sum of Square

TAG	Triacylglycerols
TCA	Tricarboxylic Acid Cycle
TF	Triphenylformazan
TFA	Total Fatty Acid
TMS	Trace Mineral Solution
TTC	Triphenyltetrazolium Chloride
UNSCN	United Nations System Standing Committee on Nutrition
UV	Ultraviolet
v/v	Volume per Volume
W	Watt
w/w	Weight per Weight
WHO	World Health Organization
WT	Wile-type
$ZnSO_4.7H_20$	Zinc Sulfate Heptahydrate
Δ	Delta
°C	Degree Celsius
µm	Micrometer
µM	Micromolar
µJ	Microjoules
α	Alpha
γ	Gamma

Acknowledgements

I would like to express my deepest gratitude to my supervisors, Dr. Su-Ling Brooks and Dr. Roberto Armenta, for their invaluable guidance, unwavering support, and insightful feedback throughout the course of my Master's degree. Their guidance and support greatly contributed to the success of this research and helped me to grow as a scientist. I am also grateful to my friends and colleagues at Mara Renewables Corporation who have both inspired and supported me over these past two years. I would like to extend a special thanks to Dr. David Woodhall, Dr. Jeremy Benjamin, Kaitlyn Tanner, Denise Muise, Holly Rasmussen, Natalie Weder, Beautisca King, Dr. Marc Grull and Nicole Smith for their encouragement and navigation through many obstacles. I would like to thank my committee members, Dr. Stanislav Sokolenko and Dr. Amina Stoddart, for their continued support and constructive feedback on my project. I am also grateful to Paula Colicchio, Administrative Secretary of the PEAS department, for her patient assistance. Additionally, I would like to acknowledge the Mitacs Accelerate program for their financial support, which has provided me with the opportunity to work with an amazing company, Mara Renewables Corporation, and my incredible mentor, Dr. Su-Ling Brooks from Dalhousie University. The support over the past two years has been greatly appreciated.

Finally, I extend my heartfelt appreciation to my parents for their love, patience, and belief in my abilities. This work would not have been possible without their unwavering support. I am fortunate to have you always loving me unconditionally. I want to extend a special thank you to my fiancé, Lei Wang. During these years in Canada as an international student, the journey would never been easy without your company. Thank you for always being there for me, cheering me up when I was down; cooking for me when I was tired and hungry, and encouraging me when I was lost. Thanks for always being my best teammate and making me a better me!

Chapter 1: Introduction

Polyunsaturated fatty acids (PUFAs) are critical sources of metabolic energy and have an important role in maintaining physiological parameters as the primary structure in a biomembrane (Sakuradani et al., 2013; Kikukawa et al., 2018). Arachidonic acid (ARA) is an n-6 series fatty acid and a precursor to eicosanoids, such as prostaglandins, leukotrienes and thromboxanes, that effectively prevent many human diseases (Ji et al., 2014).

ARA exists in human milk, in neural or functional organs including in the blood, muscles, brain and liver, and is clinically treated as an important nutrient for improving the memory and eyesight of infants (Higashiyama et al., 2002; Zhang et al., 2021). As infants cannot endogenously synthesize ARA, it is a frequent supplementary ingredient in foods or infant formula to facilitate sufficient nutrient intake. In contrast to other fatty acids such as docosahexaenoic acid (DHA) and eicosapentaenoic acid (EPA), ARA only comprises a small portion of food sources such as meat, seafood or dairy foods (Food Standards Australia New Zealand, 2003; Kawashima, 2019). As such, it is not realistic to commercially develop ARA from these sources, despite its importance to health. Therefore, there is a need to find a high-quality alternative for ARA production.

Lipid-accumulating microorganisms, particularly the fungus *Mortierella alpina (M. alpina)*, have been used for several decades as an alternative means for ARA production with the *Mortierella* genus showing promise as a single cell oil (SCO) source rich in various types of C_{20} PUFAs, and especially large amounts of ARA-containing lipids (Sakuradani et al., 2010). The lipid accumulated in total biomass is more than 20% (w/w), and the total amount of ARA varies between 30-70% (w/w) of the total fatty acids, with 70-90% (w/w) of the ARA being present as triacylglycerols (Sakuradani et al., 2013; Kikukawa et al., 2018).

Although some well-studied *M. alpina* strains have been grown commercially for years

(Higashiyama et al., 1998a, 1999, 2002; Sakuradani et al., 2013; Kikukawa et al., 2018), there remains an opportunity to discover, develop and commercialize new strains that may also be highly productive, as many *Mortierella* strains can accumulate ARA (Kikukawa et al., 2018). Various *M. alpina* species have not yet been discovered or fully developed, such as the *M. alpina* MA2-2, newly isolated strains from Mara Renewables Corporation (Mara) strain collection with the potential to be highly productive ARA producers. The search for new SCO producers will continue, and new species with unique characteristics could be discovered and used to replace existing SCOs, or for entirely new applications (Kyle, 2010). Meanwhile, increasing target PUFA yields, reducing fermentation costs, discovering more potential ARA producing strains and expanding the application of *M. alpina*-derived products is still on-going research (Certik, 1998; Chang et al., 2021).

As ARA production by *Mortierella* species can differ significantly with various growth parameters affecting biomass, lipid, and ARA productivities. Culture media selection for each strain is different due to their complicated metabolic characteristics (Nisha & Venkateswaran, 2011). Additionally, combining mutation and genetic breeding with fermentation optimization is still a commonly used method to enhance the lipid yield in *M. alpina* (Chang et al., 2021). The evolutionary engineering strategy is known as Adaptive Laboratory Evolution (ALE) and there are more than 30 research manuscripts on microalgal bacteria, yeast or algae. However, this field is relatively unexplored in fungi (LaPanse et al., 2021). The use of different organisms, such as algae, bacteria or yeast, can achieve evolutionary phenotypes, but relatively few ALE studies have focused on less standard microbial species such as filamentous fungi *M. alpina* (Sandberg et al., 2019). Therefore, there is the opportunity for companies such as Mara to explore the feasibility of industrial ARA production from new *Mortierella* strains derived from ALE.

Mara is a research & development biotechnology company producing nutrient supplements or bio-products from fermentation for fatty acid production, with DHA as the main constituent. Methods of producing oil from microorganisms have been developed by

Mara and include the isolation of novel microorganisms, targeted fermentation strategies and lipid extraction techniques (Dennis & Armenta, 2017). Mara is constantly exploring new microbial-based products for commercialization potential and investigating ARA production aligns with the company's goals.

Therefore, in this work, optimization of fermentation medium composition for ARA production was explored for *M. alpina*. The cell-line performance was analyzed for strain improvements after applying random mutagenesis or ALE strategies. The undeveloped wild-type MA2-2 at Mara produces about 16.7±1.78% (w/w) oil and 26.5±2.22% (w/w) ARA in the original medium, which is not optimal for industrialization and commercialization. In this study, the goal was to improve ARA production by reaching and/or exceeding 40% (w/w) of ARA in total oils and 20% (w/w) of oil accumulation in biomass for industrial development.

Chapter 2: Objectives and Hypotheses

2.1 Objectives and Hypotheses

The overall objective of this project was to develop a process to produce ARA using a selected *M. alpina* strain, MA2-2, from the Mara strain collection by applying medium optimization and strain improvement techniques. The targets for the optimized ARA producer were 40% (w/w) ARA in total fatty acids and 20% (w/w) oil accumulation in biomass.

2.1.1 Subobjectives

The subobjectives of this research were to:

1: Develop a culture media for *M. alpina* MA2-2 by investigating micro- and macro-nutrients using Plackett-Burman Design, Response Surface Methodology and Mixture Optimization design to improve multiple responses including the production of biomass and total lipids, as well as ARA production (ARA percentage and ARA yield). Since multiple response variables were studied in the medium design, the main focus was on balancing between all responses and weighing any drawbacks to bring a final solution that was improved in all response variables.

2: Develop protocols for random mutagenesis and high-throughput screening of ARA-producing strains, to obtain beneficial mutants.

3: Develop protocols for high temperature ALE experimental strategies on ARA-producing strains to improve the temperature tolerance of the strains.

2.1.2 Hypotheses

1: Modified fermentation medium can be developed to increase the biomass content, total lipid and ARA accumulation from the highly productive ARA-producing *M. alpina* wild-

type strain.

2: Random mutagenesis can be successfully applied to *M. alpina* MA2-2 and an effective screening method can be conducted to select beneficial mutants with high biomass content, total lipids and ARA accumulation.

3: High-temperature ALE strategies can be successfully developed for oleaginous filamentous fungi to improve thermotolerance and reduce temperature sensitivity.

4: After media design and strain improvements, the target parameters of 40% (w/w) ARA in total fatty acids and 20% (w/w) oil accumulation in biomass can be achieved.

Chapter 3: Literature Review

3.1 Microalgal lipids, PUFA and ARA

3.1.1 Microalgal Lipids

Microalgae produce a large number of lipid-like compounds such as glycerolipids, sterols, hydrocarbons and waxes. Glycerolipids are the most abundant microalgal lipids. These lipids are characterized by the attachment of one, two or three fatty acid (FA) groups to the glycerol backbone (Morales et al., 2021). The total oil and FAs in microalgae ranges from about 1 to 70% of ash-free dry weight (Borowitzka, 2010).

Glycerolipids can be divided into two categories: storage lipids and structural lipids. Among the structural lipids, membrane lipids are essential for cell and organelle membranes, and they usually contain two FA groups with a polar group bound to the glycerol structure. Phospholipids and glycolipids are the main representatives of polar lipids, while triacylglycerols (TAGs) are the main form of storage lipids with three FA groups attached (Morales et al., 2021).

Microalgae usually have FAs with 12, 16 or 18 carbon atoms as their chain length, while some species also produce FAs with chain length of up to 22 carbon atoms (Montone et al., 2021). TAGs mainly contain saturated and monounsaturated fatty acids (SFAs and MUFAs, respectively), such as C14:0 (myristic acid), C16:0 (palmitic acid), C16:1 (palmitoleic acid), C18:0 (stearic acid) and C18:1 (oleic acid), but PUFAs can be also present (Tababa et al., 2012; Montone et al., 2021; Morales et al., 2021).

3.1.2 PUFA

The production of oleaginous microorganisms rich in MUFAs and SFAs can be used for biodiesel production, while strains rich in PUFAs are more suitable for nutritional and pharmaceutical products. This is due to the fact that lipids with higher content of PUFAs with more than two double bonds are susceptible to auto-oxidation. Therefore, PUFA-rich

lipids are more unstable and technically unsuitable for biodiesel production (Mhlongo et al., 2021).

The reason that PUFAs are mainly produced for use in food commodities and nutritional products is due to two main functions of their essential fatty acids (EFAs). The first is their role in membrane structure, where EFAs confer membrane fluidity and flexibility and regulate the behavior of certain membrane-bound proteins. The second is their role as precursors of various metabolites (e.g. prostaglandins, leukotrienes and hydroxy fatty acids) that regulate critical biological processes, which are essential for nutritional intake in mammals (Certik, 1998; Sakuradani et al., 2010).

Mammals lack the ability to endogenously synthesize most PUFAs because they cannot insert a double bond between the ninth carbon from the carboxyl terminus to the terminal methyl group (Certik, 1998; Shanab et al., 2018). For humans, EFAs are C18:2 (linoleic acid) and C18:3 (α-linolenic acid), which must be obtained from oils of plant and animal origin in the daily diet. Other long-chain PUFAs (LC-PUFAs) including C18:3n-6 (gamma-linolenic acid), C20:4 (ARA), C20:5 (EPA), and C22:6 (DHA) are also of interest for their health benefits. Among the aforementioned dietary PUFAs, n-6 linoleic acid and ARA, n-3 α-linolenic acid and DHA are often added in infant formulas, and research interest has focused on their optimal ratios and amounts in the daily diet (Chang et al., 2022).

However, higher plants cannot synthesize PUFAs in large amounts above C18 due to the lack of necessary enzymes. Fish oil, fungi, marine bacteria or algae are potential sources of C20 PUFAs. Some important PUFAs such as ARA and C20:3n-6 (dihomo-γ-linolenic acid) are now commercially produced through the use of the oily filamentous fungus *Mortierella* (Certik, 1998; Sakuradani et al., 2010).

3.1.3 Lipid, PUFA, ARA biosynthesis pathways

Lipid synthesis pathways that occur in oleaginous microorganisms mostly include

glycolysis, tricarboxylic acid cycle (TCA cycle), pyruvate/malate cycle, fatty acid synthesis and PUFA synthesis (Liang & Jiang, 2013; Zhang et al., 2021; Chang et al., 2022).

In general, glycolysis begins the process of breaking down saccharides. Citric acid accumulates in the mitochondria and is transported to the cytoplasm via the TCA transport system, where it is finally broken down by citrate lyase into oxaloacetate and acetyl CoA, which are involved in the synthesis of fatty acids. In addition, oxaloacetic acid entering the pyruvate/malate cycle produces large amounts of reduced nicotinamide adenine dinucleotide phosphate (NADPH) required for intracellular fatty acid synthesis. Acetyl-Coenzyme (CoA) is catalyzed by acetyl-CoA carboxylase (ACC) to produce malonyl-CoA. Malonyl-CoA and acetyl-CoA are then catalyzed by the fatty acid synthase complex to produce palmitoyl-acid phosphatase (ACP) through sequential polymerization reactions of condensation, reduction, and dehydration, in which two carbons are added per cycle. Subsequently, palmitoyl-ACP undergoes carbon chain elongation and desaturation reactions catalyzed by fatty acid desaturases and fatty acid elongases to produce ARA (Figure 3.1) (Ji et al., 2014; Zhang et al., 2021).

In oleaginous microorganisms, NADPH is critical for fatty acid synthesis and is primarily generated from three main glucose metabolism pathways: (i) the pentose phosphate pathway, with glucose 6-phosphate dehydrogenase and 6-phosphogluconate dehydrogenase, (ii) the pyruvate/oxaloacetate/malate cycle, through nicotinamide adenine dinucleotide phosphate (NADP) with dependent malic enzyme (ME), or (iii) the TCA cycle via NADP with dependent isocitrate dehydrogenase (Hao et al., 2015; Mhlongo et al., 2021). ME is the main source for the production of abundant NADPH for lipid biosynthesis and desaturation, even in the absence of other NADPH-generating enzymes, indicating that NADPH production is highly dependent on ME activity. To achieve efficient PUFA accumulation, two conditions should be met simultaneously. One is a direct and continuous supply of acetyl-CoA at the cell membrane as a necessary precursor for fatty acid synthase and the other is an adequate supply of NADPH as a necessary reductant for fatty acid

biosynthesis (Zeng et al., 2012).

The biosynthesis of TAGs is an important metabolic pathway for oleaginous species that are used for the accumulation of intracellular oils. TAGs are used by organisms for membrane development or for cellular metabolite synthesis during cell growth. It has been demonstrated that TAG formation begins with the synthesis of fatty acids, followed by acyl chain elongation and then TAG biosynthesis in specialized organelles, namely the endoplasmic reticulum and liposomes also known as "lipid droplets". This process produces neutral lipids in the form of TAGs to store fatty acids and thus generate energy (Ji et al., 2014).

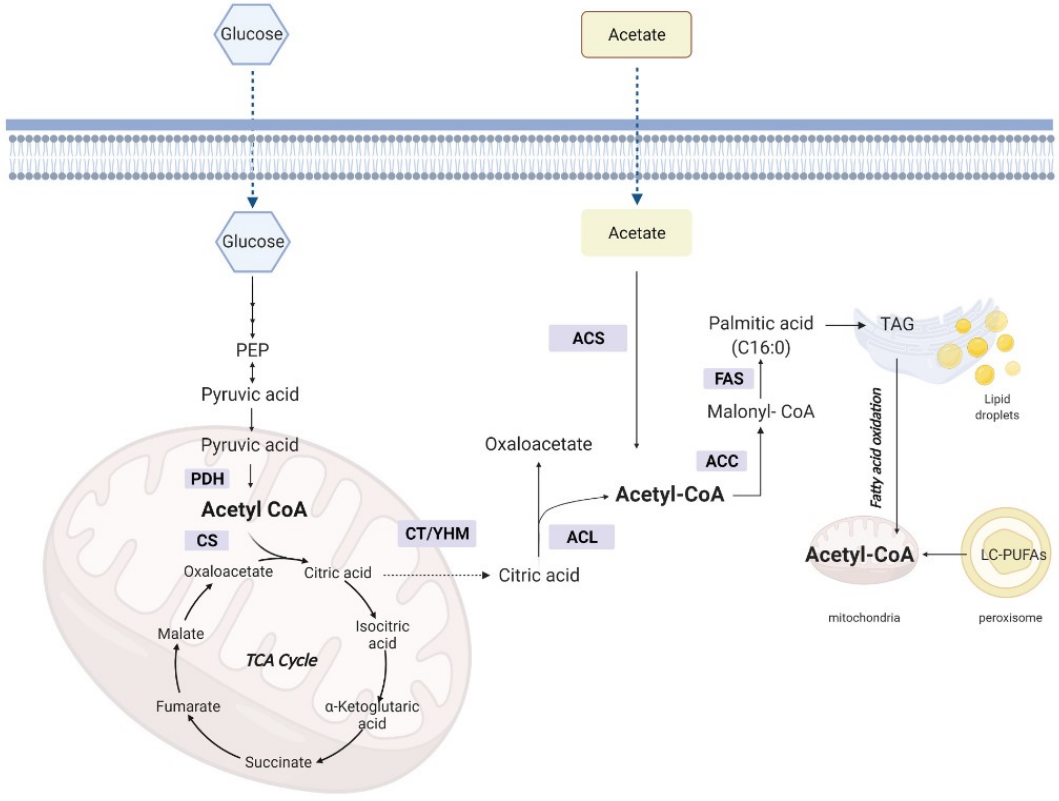

Figure 3.1: Key enzymes and biochemical processes related to acetyl-CoA generation and metabolism in oleaginous fungi. Image with permission from (Chang et al., 2022).

Two types of PUFA biosynthetic pathways exist in the microorganisms. One pathway is the classic desaturation and elongation process, and another is the polyketide synthase (PKS)-like process (Ji et al., 2014). In the former pathway, specific fatty acid desaturases

(Δ12, Δ9, Δ6 and Δ5) and elongases (EL1, EL2) catalyze individual desaturation and elongation steps to synthesize PUFAs. In the latter pathway, PUFA synthases composed of multiply enzyme complexes, with multiple catalytic domains, synthesize PUFA (Hayashi et al., 2019). Oxygen supply and fatty acid desaturase/elongase are crucial for PUFA-rich lipid accumulation. PUFA synthesis in *M. alpina* is catalysed by the aerobic fatty acid desaturase/elongase pathway (Figure 3.2), where adequate dissolved oxygen (DO) plays an important role in enhancing its fatty acid unsaturation (Chang et al., 2021).

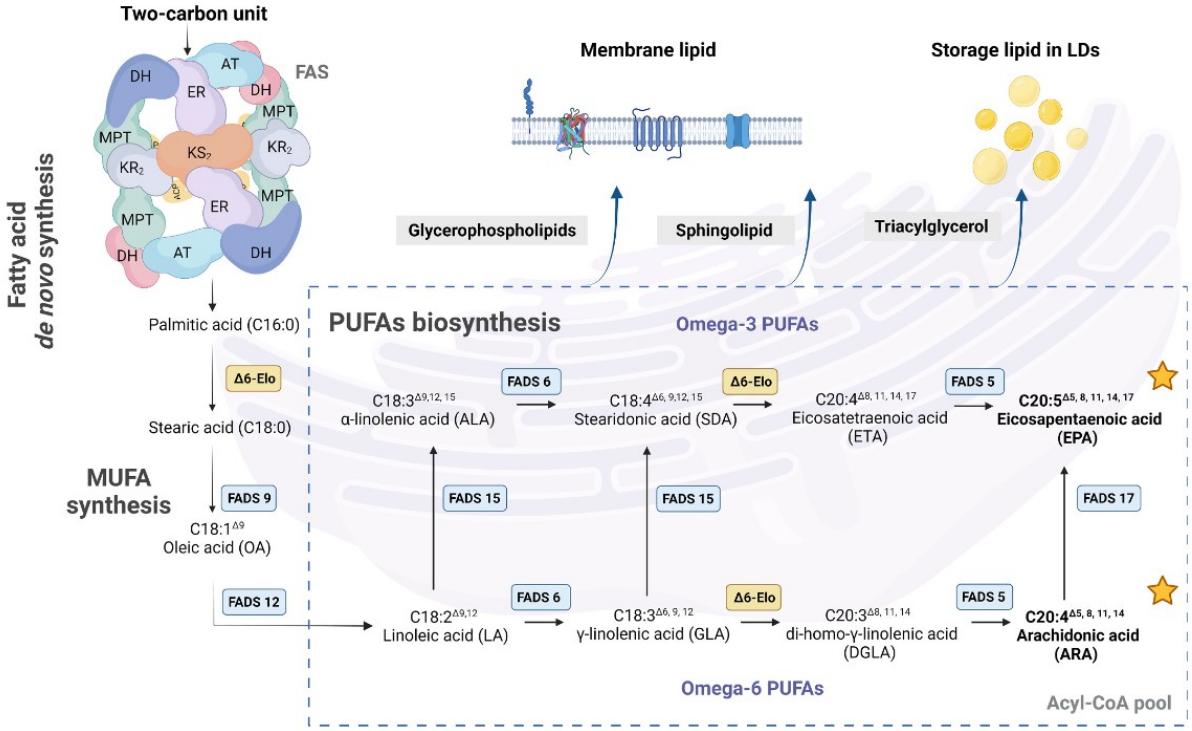

Figure 3.2: Polyunsaturated fatty acid synthetic pathways in *M. alpina.* Image with permission from (Chang et al., 2022).

ARA biosynthesis in fungi uses the desaturation and elongation process starting from the saturated C16:0 from the FA synthesis pathway (Ji et al., 2014). Similar to other n-6 PUFA pathways, the primary substrate C16:0 is converted to ARA in sequential steps catalyzed by elongase 1 (MALCE1), Δ9 desaturase, Δ12 desaturase, Δ6 desaturase, elongase 2 (GLELO), and Δ5 desaturase, respectively (Figure 3.2) (Streekstra, 2010;

Sakuradani et al., 2013; Kikukawa et al., 2018).

3.1.4 ARA Structure

Arachidonic acid (ARA; 20:4n-6) is a long-chain polyunsaturated fatty acid (LCPUFA) with twenty carbon atoms and four double bonds (Figure 3.3) (Streekstra, 2010). ARA belongs to the omega-6 (n-6) PUFAs, and is designated as 20:4n-6, with a biochemical nomenclature of all-cis-5,8,11,14-eicosatetraenoic acid, and usually assumes a hairpin configuration (Tallima & El Ridi, 2018).

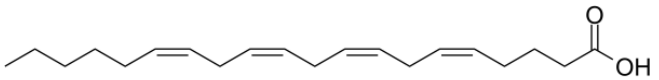

Figure 3.3: Arachidonic acid structure showing linear and hairpin configuration.

ARA is an important structural component of lipids in the central nervous system, including those in the brain. Currently, the commercial demand for ARA is mainly for its use in infant formula. Human milk contains significant amounts of two LCPUFAs: ARA and DHA. There is substantial evidence that the neurodevelopment of growing infants is facilitated by breastfeeding or by the inclusion of these fatty acids in infant formula (Streekstra, 2010).

3.1.5 Safety and dietary requirement of ARA

The brain has the second highest concentration of lipids in the body, after adipose tissue, with 36-60% of the nervous tissue being lipids (Sinclair & Jayasooriya, 2010). Brain glycerophospholipids contain a high proportion of LCPUFA— mainly DHA, ARA, which together account for 20% of the human brain (dry weight), concentrated in the neuron's outer membrane and in the myelin sheath (Tallima & El Ridi, 2018). In rapidly growing infants, there is a high demand for complex lipids that form important cell membrane

structures; therefore, the availability of pre-formed substrates, such as DHA and ARA, as components of intact neural membranes is critical (Hoffman et al., 2009). Blood levels of DHA and ARA are lower in infants fed standard formula than in breast-fed infants. Formula containing LCPUFA can increase these levels to approach those found in breast-fed infants (Sinclair & Jayasooriya, 2010).

ARA-rich Single Cell Oil (ARASCO) are microbial-derived triglyceride oils that are rich in the LCPUFAs known as ARA. The extracted oils, ARASCO, contain between 40 and 55 % ARA (Food Standards Australia New Zealand, 2003). ARASCO and DHA-rich Single Cell Oil (DHASCO) are free flowing triglyceride oils with a fatty acid structure comparable to some other edible oils. Unusual fatty acids are not present in these two oils and there are no detectable (< 1.0%) cyclic or trans fatty acids present. The oils also contain no or only very low levels of EPA, which has been associated with reduced growth in infants (Food Standards Australia New Zealand, 2003; Salem & Van Dael, 2020). ARASCO is commercially produced through a fermentation process that uses the common soil fungus *M. alpina*, which has been extensively studied, is not pathogenic to humans and does not produce mycotoxins harmful to humans or animals (Ryan et al., 2010).

In the United States, almost all preterm and 90% of full-term infants are fed infant formula containing SCOs (Ryan et al., 2010). Some commercially available infant formulas contain about 70 mg of ARASCO per 100 kcal. While at least in advanced countries, the recommended ARA intake for normal healthy adults is 100-250 mg/day (Kawashima, 2019; Salem & Van Dael, 2020). These SCOs are considered by the Food and Drug Administration (FDA) to be highly refined oils that do not cause allergic reactions. In Canada, DHASCO and ARASCO (from *M. alpina*) are used as sources of the nutrients DHA and ARA, respectively, in human milk substitutes. In Australia and New Zealand, DHASCO and ARASCO have been added to infant formula products since about 1998 (Food Standards Australia New Zealand, 2003; Ryan et al., 2010).

3.1.6 Market Overview

Single-cell oils are highly valued products. The first companies to produce ARA by fermentation were Gist-brocades Co. (now DSM) and Suntory Ltd., where DSM had the exclusive rights to the ARA-rich oil produced by Martek Biosciences (Kyle, 2010). Until 2011, Martek Biosciences earned USD $450 million of ARA oil sales annually (Ratledge & Hopkins, 2006).

The price of the oil can vary from USD $65 kg^{-1} to over $500 kg^{-1} or even more if it is composed of pure, specific, fatty acids (Gunstone, 2001). In 2003, the total production of ARA was around 560 tons, which was mostly used in infant formulas, and was much higher than the production in the period of 1985-2002 (690 tons total). In 2006, the global production of infant milk formula was 1.8 million tons, including about 400,000 tons of oil and fat ingredients containing ARA and DHA (Mamani et al., 2019). The overall production of SCO in 2008 is estimated to be about 3,500 tons, of which about 60% was ARASCO and 30% was DHASCO (Kyle, 2010).

According to the Global Arachidonic Acid Market - Industry Trends and Forecast from 2021 to 2028, the ARA market is expected to grow at a rate of 5.80% and is expected to reach USD $0.43 billion by 2028. North America dominates the arachidonic acid market because of the presence of prominent companies and high spending capacity of consumers within the region. The Asia-Pacific region is expected to witness significant growth during 2021 to 2028 due to rapid urbanization, emerging middle-class population and availability of low-cost raw materials and labor in the region (Data Bridge Market Research, 2021).

3.2 *Mortierella* species

3.2.1 Taxonomy

Mortierella is a genus of filamentous fungi within the *Zygomycetes* and belongs to the order of *Mortierellales*, which is characterized as having a sexual cycle that incorporates

zygospores and specific pheromones, and also an asexual sporulation cycle (Streekstra, 2010; Chang et al., 2022). The taxonomy of *M. alpina* is presented below (Nisha, 2009; Rayaroth et al., 2017),

Kingdom: Fungi

Division: Zygomycota

Class: Zygomycetes

Order: Mortierellales

Family: Mortierellaceae

Genus: *Mortierella*

Species: *Mortierella alpina*

3.2.2 Overview of *M. alpina*

Filamentous fungi are heterotrophic, non-photosynthetic organisms, which require organic compounds as a source of carbon and energy for growth (Papagianni, 2004). Filamentous fungi are typically saprophytic microorganisms which produce a large number of enzymes involved in the decomposition and recycling of complex biopolymers from plant and animal tissues (El-Enshasy, 2007).

Most of these oil-producing fungi can accumulate microbial lipids, or SCOs, to 20%–90% (w/w) of their dry cell biomass (Zhu et al., 2021). For example, the *M. alpina* (*Mortierella alpina*) 1s-4 strain was identified as the first high-quality producer able to accumulate high concentrations of ARA as well as other PUFAs (Higashiyama et al., 1998a, 1998b, 1999; Takeno et al., 2005; Sakuradani et al., 2013; Kikukawa et al., 2018). *M. alpina* is chosen to commercially produce ARASCO because it produces an oil that is not only ARA-rich, but also free of EPA and other unwanted components. The ARA-rich oil that is produced is a free-flowing liquid oil with a slightly yellow color (Food Standards Australia New Zealand, 2003; Kyle, 2010). *M. alpina* is considered a high oil-producing strain in which the total lipids constitute more than 50% of its dry cell weight, and it is also

a natural producer of high-value LC-PUFAs. As reported, the predominant fatty acids in *M. alpina* (Figure 3.2) include C16:0, C18:0, C18:1, C18:2, C18:3, C20:3 and a large amount of C20:4 (ARA). Another indispensable essential LC-PUFA C20:5 (EPA) is usually present in trace amounts in *M. alpina* at low temperatures usually below 12℃ (El-Enshasy, 2007; Sakuradani, 2010; Streekstra, 2010; Zhu et al., 2021; Chang et al., 2022).

3.2.3 Distribution and Morphological characterization

M. alpina is a saprophytic and psychrophilic soil fungus that has a varied distribution pattern with strains being isolated from diverse geographic locations around the world. The isolated terrain includes grass lands, pastures, forest lands, agricultural soils, loam, scrubland, pasture soils, from plants as endophytes and even in pond habitats (Rayaroth et al., 2017). It has been found throughout Australia, Canada, China, Corsica, Cyprus, Gibraltar, Hungary, India, Japan, Mexico, Netherlands, New Zealand, Pakistan, Spain, Sweden, UK, former USSR and USA (Nisha, 2009). Species of *Mortierella*, especially *M. alpina, M. elongata, M. parvispora* are often reported from wet alpine and tundra habitats (Onipchenko, 2004).

The colonies formed by *Mortierella* species are usually described as pale white, milky-white zonate, forming a typical rosette pattern (Figure 3.4). The adaxial side of the colony is white, and the center is often dark white. Over time, the reverse side of the colonies may become yellowish and narrowly banded. Extensive aerial mycelium occur in the center of the colony and form many irregular bead-like hyphal swellings. The cottony aerial hyphae of *Mortierella* species form sporangia which are pigmented or colorless. Sporulation is abundant and the mycelium has a garlic-like odor (Yadav et al., 2015; Ozimek & Hanaka, 2020). Mycelia is septate and symbiotic with complex branching. Sporangiophores are hyaline and erect, produced from the mycelial substrate with size of 60~110 μm, and unbranched with terminal sporangia. Sporangia are hyaline, obovoid when young and spherical when mature, 12~35 μm in diameter, and multispored with a deliquescent wall,

wrinkled, and non-columellate. The sporangiospores are hyaline, ellipsoidal or cylindrical, single-celled, with 4~10 μm in size, and sometimes curved to irregular shape (Yadav et al., 2014).

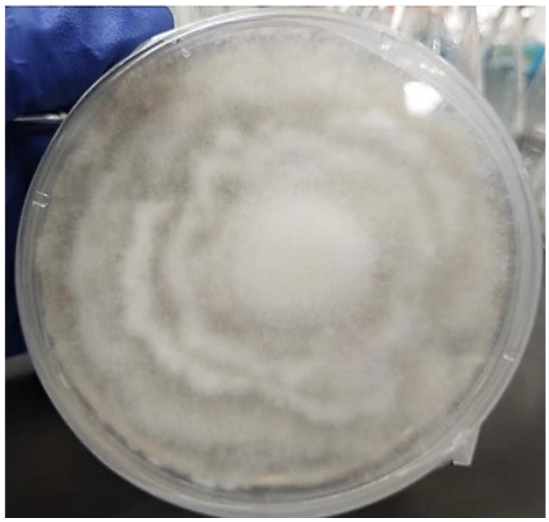

Figure 3.4: *M. alpina* MA2-2 on potato dextrose agar (PDA) plate.

3.2.4 Life cycle

The micromorphological life cycle of filamentous fungi includes the progress of spore swelling, germination, and germ tube elongation and branching (El-Enshasy, 2007) (Figure 3.5). Pellets or filamentous forms are the main macro-morphological growth in such fungi (Streekstra, 2010). In general, a short germination phase is desired in biotechnological processes in order to decrease the cultivation time (El-Enshasy, 2007). The type of sporulation and the morphology of the spores and spore-bearing structures are key characteristics in fungus identification. The fungal spore is considered as the beginning and the end of the fungi life cycle. In mycelial fungi, tip extention occurs when hyphae is extended by a highly polarized process of cell extension. This forms periodic branches at or near the apex of the tip. Spore germination results in the formation of a germ tube, which contributes to the biosynthesis and extension by uptake and metabolism of nutrients from the medium (Papagianni, 2004).

The mycelia of *Mortierella* fungi do not contain septated cells as they are in the form

of a tube comprised of sections composed of a cytoplasm-filled portion and an empty section. The cytoplasm contains multiple nuclei, even in asexual spores, and there is no uninucleate stage in the life cycle. Hence, this multi-cellular microorganism complicates the selection and maintenance of strains, because even a single cell is a population and not a true individual. Such characteristics complicates the development of high-producing industrial strains, for instance, by mutagenesis and selection (Streekstra, 2010).

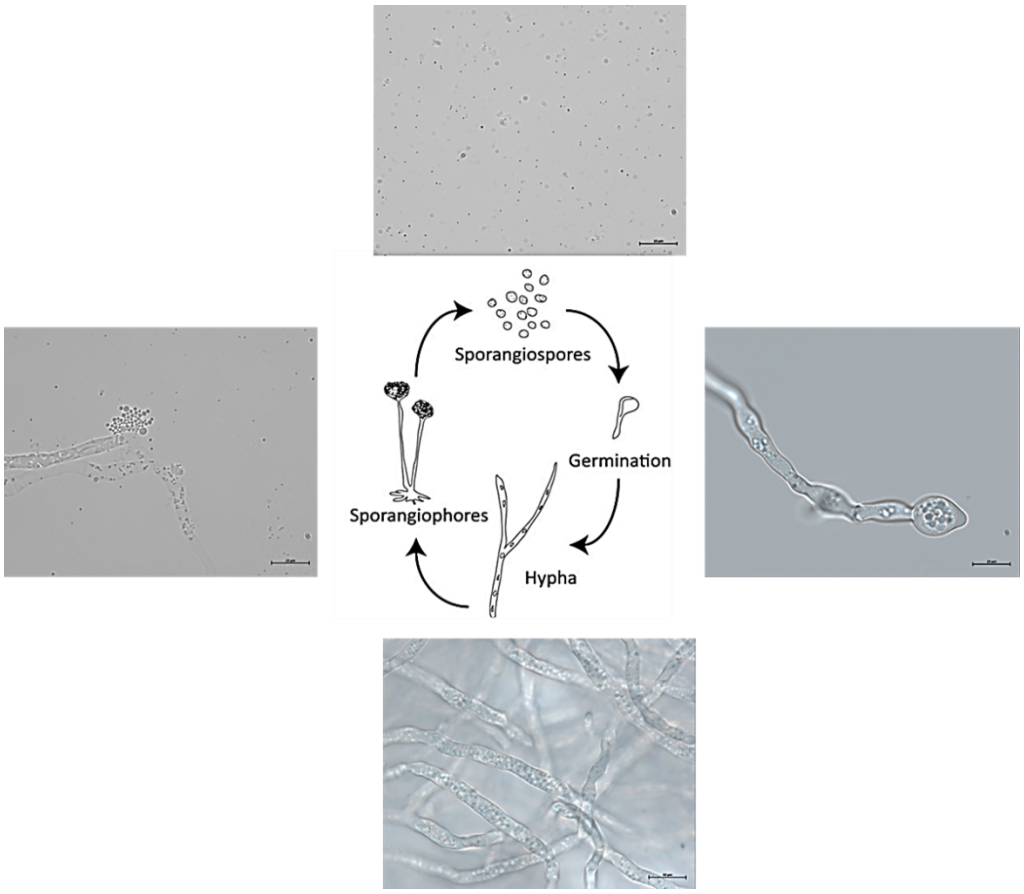

Figure 3.5: Asexual lifecycle of the fungus. Haploid cells form sporangiophores, and sporangiospores germinate to hypha. Image reproduced with permission from (Wang et al., 2011), and micro-pictures of *M. alpina* MA2-2 strain in each lifecycle (scale bars: 10µm).

3.2.5 Fermentation of *Mortierella*

For most oleaginous microorganisms, the fermentation process is divided into two phases: the biomass growth phase and the lipid accumulation phase (Chang et al., 2021).

For most oleaginous microorganisms, the initial growth phase is characterized by rapid cell multiplication that continues until a critical nutrient, usually nitrogen, becomes a limiting factor for growth. The second phase of growth begins as lipid synthesis predominates, leading to the accumulation of storage lipids (Malaiwong et al., 2016). Cell growth occurs mainly in the early fermentation phase, while the ARA content in the lipids starts to increase during the stationary growth phase and continues to increase after glucose depletion in the medium, due to the turnover of intracellular fatty acids (Peng et al., 2010). Researchers have reported that in *M. alpina* fermentation, cell growth led to a continual increase in biomass during the first 5 days, and then reached a stationary growth phase. The maximum accumulation of ARA then occurred on the 6^{th} or 7^{th} day, after which no further improvement in ARA production was observed (Yuan et al., 2002; Nisha & Venkateswaran, 2011).

Lipid production is determined as the lipid content in biomass, and it is important that strains selected for industrial use have high levels of lipid and biomass production (Fang et al., 2018). This means that the media used in submerged industrial fermentations should favor both growth and product formation at high yields (Papagianni, 2004). In addition, the strains should produce a suitable fatty acid profile with high ARA content. Moreover, the biological and physical attributes of the strains, including temperature tolerance, oxygen sensitivity, salinity range and shear sensitivity, as well as suitability for scale-up in culture systems, need to be equally considered when attempting to achieve reliably high ARA productivity (Borowitzka, 2010; Cohen & Khozin-Goldberg, 2010).

3.2.5.1 Effects of Carbon to Nitrogen (C:N) Ratio

Lipid accumulation is only favored by a fixed range of carbon to nitrogen ratio, and C:N ratio also influences ARA production in the culture of *M. alpina* (Lu et al., 2011). Studying the optimal C:N ratio is an important step before optimizing the nitrogen source. Carbon (C) and nitrogen (N) sources present in the fermentation medium may initiate the

biosynthesis of precursors that regulate the metabolism and influence the end product synthesis (Singh et al., 2017). In the lipogenic phase, excess carbon and nitrogen, as the most common growth limiting factor, can result in the accumulation of lipids.

Increasing the C:N ratio can result in the accumulation of FAs following nitrogen starvation. Thus, increasing the carbon source can serve to enhance FAs accumulation and also induce lipid accumulation (Cohen & Khozin-Goldberg, 2010; Bicas et al., 2016). The C:N ratio affects the cellular composition and the typical C:N ratio can range from 5-20, while the optimum ratio is about 15 to 20 (v/v). Nitrogen is essential for protein synthesis, and while the depletion of nitrogen during cultivation is a prerequisite for FA accumulation, it is not favorable for biomass growth (Mamani et al., 2019).

3.2.5.2 Effect of C source

Carbon is the most important medium component, as it is an energy source for many microorganisms and plays an important role in the growth as well as in the production of primary and secondary metabolites (Singh et al., 2017). Glucose is the most preferred carbon source, with a high synthesis efficiency for fatty acids and is frequently used for scientific research and industrial production. Moreover, *Mortierella* strains are saprophytic and prefer to grow rapidly and proliferate extensively on simple sugars (monosaccharides) compared to complex molecules (Nisha & Venkateswaran, 2011; Chang et al., 2021). Chang et al (2021) also indicated that soluble starch or corn flour can be optimal carbon sources, as they found that the total biomass of *M. alpina* TSM-3 was significantly improved by more than 30% compared to when glucose was used, thereby improving the final lipid yield and target PUFAs. Some oleaginous microorganisms can grow with glycerol as the sole carbon source to accumulate PUFAs. However, the main issue with this has been the relatively low assimilation efficiency that limits downstream metabolic processes, due to the insufficient coordination of the enzymes involved in the primary metabolic steps of glycerol assimilation (Hao et al., 2015). Nisha & Venkateswaran (2011)

reported that when oils were used as the carbon source this led to a significant decrease in biomass and ARA production in the *Mortierella* strain studied.

The optimum glucose concentration for fungal ARA-rich oil production has been found to be 20–40 g L^{-1} and a high glucose concentration can inhibit the growth of *M. alpina* and induce the formation of filamentous morphology (Ji et al., 2014). The lipid content in dry biomass has been found to increase with increasing glucose concentration, while dry biomass is low at low glucose concentrations. However, glucose concentrations exceeding 100 g L^{-1} can harm the cell growth and drastically decrease the biomass yield (Zhu et al., 2003; Nisha & Venkateswaran, 2011). High concentrations of glucose can cause excessive osmotic pressure in fermentation broth, which can lead to leakage of intracellular water molecules, further affecting the mycelial growth (Nisha, 2009; Fang et al., 2018; Smith, 2020).

3.2.5.3 Effect of N source

Nitrogen is also an important component of cultivation media and it essential for the production of ARA because it maintains the high activity of the malic enzyme, which plays an important role in the provision of NADPH into the condensation reaction of Acetyl-CoA carboxylase to yield fatty acids in *M. alpina* (Certik, 1998; Wynn et al., 1999; Jin et al., 2009; Malaiwong et al., 2016). Although ARA does not have any nitrogen in its structure, nitrogen plays a critical role in ARA production and the formation of cellular components via the catalytic system. Therefore, nitrogen indirectly affects ARA production (Cao et al., 2015).

The type of nitrogen source has an important effect on the accumulation of microbial lipids (Fang et al., 2018). During a fermentation, nitrogen depletion in the medium is a transition point in cell growth, leading to a significant accumulation of TAG within the lipid droplets of cells (Borowitzka, 2010; Mamani et al., 2019). PUFAs are accumulated due to a metabolic shift in the Kreb's cycle caused by activation of adenosine triphosphate

dependent citrate lyase. Therefore a very important prerequisite for lipid overproduction is the metabolic shift caused by nitrogen depletion (Nisha et al., 2011). Conversely, higher concentrations of nitrogen generally result in higher biomass and inhibit lipid production as nitrogen surplus media can result in an increase in cell division thereby reducing the lipid yield (Chang et al., 2021). Most microorganisms can utilize both inorganic and/or organic sources of nitrogen. In certain instances, the use of specific amino acids as organic nitrogen sources can enhance productivity, while unsuitable amino acids may have an inhibitory effect on the synthesis of secondary metabolites (Singh et al., 2017). Biomass production has been found to decrease in a fermentation medium comprising ammonium nitrate, sodium nitrate, or ammonium sulfate as the nitrogen source, suggesting that *M. alpina* being a saprophyte hardly assimilates inorganic sources of nitrogen and requires amino acid or protein for high biomass buildup (Lu et al., 2011). Organic sources of nitrogen affect lipogenesis regulation and increase acetyl-CoA carboxylase activity (Mamani et al., 2019). Thus, organic nitrogen sources are more effective for *M. alpina* production.

Yeast extract is an excellent nitrogen source for profuse growth of fungi owing to the presence of metal ions and required micronutrients which are vital for fungi growth. Peptone has been found to enhance mycelial growth as well as improved production of ARA; this has been attributed to urea acting as an inhibitor for delta 5 desaturase, a key enzyme which catalyzes the synthesis to ARA (Nisha, 2009; Nisha & Venkateswaran, 2011). Fang et al (2018) reported that a mixture of peptone and yeast extract (2:1 w/w) induced fluffy pellets and gave the highest biomass and lipid yield, indicating that complex nitrogen sources could provide essential nutrients for cell growth and lipid accumulation. Their study also highlighted that different morphological forms might result in different rheological properties, and therefore affect lipid production as well. In addition, beet or cane molasses, corn-steep liquor, whey powder, soy flour, yeast extract and others have also been used as industrial raw materials rich in nitrogen (Papagianni, 2004). It is

important that the concentration of the nitrogen source is controlled at a relatively low level as a high concentration of the nitrogen source directs the flux of carbon to the citric acid cycle with little carbon used for synthesis of lipids (Jin et al., 2009).

3.2.5.4 Effects of Minerals

Numerous elements are essential for growth, for instance, the essential macronutrients include oxygen, carbon, hydrogen, nitrogen, phosphorus, potassium, sulfur, magnesium, and micronutrients such as phosphorus, potassium, sulfur, calcium, sodium, iron and magnesium (Papagianni, 2004). Phosphorus, potassium and sulfur are essential for cell growth, and iron promotes lipid synthesis. A low level concentration of magnesium is beneficial for ARA, but high concentration represses lipid accumulation (Higashiyama et al., 2002). Zinc, or heavy metals and alkaline metals have been shown to affect both fungal morphology and citric acid production (Papagianni, 2004).

3.2.5.5 Effects of Temperature

In most plants and microorganisms, due to the influence of PUFAs on membrane stability, the degree of unsaturation increases with decreasing temperature due to the stress caused by colder conditions (Cohen & Khozin-Goldberg, 2010; Mamani et al., 2019). Lower temperature leads to a higher proportion of ARA in the lipid fraction (Streekstra, 2010). For ARA-rich oil production, it has been found that activities of Δ6 and Δ5 desaturases involved in ARA synthesis increase at lower temperatures, and therefore, the cultivation of fungi at low temperatures is desirable to enhance the ARA accumulation (Ji et al., 2014). Another possible explanation is that, at lower temperature, more dissolved oxygen is available in the culture medium for desaturase enzymes that are oxygen dependent thereby resulting in production of more unsaturated fatty acids (Nisha & Venkateswaran, 2011). Additionally, as the temperature decreases, ARA accumulation is higher in phospholipids while not in TAGs as a result of the adaptation mechanisms of the

fungi to maintain membrane fluidity (Nisha & Venkateswaran, 2011; Ji et al., 2014).

However, the actual productivity of ARA at lower temperatures is not much higher due to the lower metabolic rate, both intrinsic and imposed by limitation of the cooling capacity (Streekstra, 2010). ARA regulates membrane fluidity in *M. alpina*, thereby compensating for the decreased functionality of the biomembranes under cold stress conditions (Nisha & Venkateswaran, 2011) and allows the avoidance of sustained high temperatures or conditions that could lead to the oxidation and rancidity of the oils during their extraction. (Streekstra, 2010). However, a relatively high operating temperature may be preferred to reduce the process cooling requirement, which can be significant at a commercial scale.

M. alpina showed high cell growth at 15-25°C, while its cell growth rate decreased at temperatures above 28°C or below 8°C (Yuan et al., 2002; Peng et al., 2010). A study by Chen et al. (1997) indicated the highest ARA yield was obtained at 24°C, which was 30.7 and 66.7% higher than those at 18 and 30°C, respectively (Chen et al., 1997). It was found that a relatively high fermentation temperature was advantageous for cell growth and glucose consumption. However, a moderately low temperature could enhance the ARA accumulation. A temperature shift strategy could be used to solve this problem (Ji et al., 2014). Peng et al. (2010) investigated a 2-stage temeprature shift strategy, by adjusting temperature to 25℃ at an early stage to facilitate optimal cell growth and then to 20℃ until the end of the experiment to obtain high efficiency for ARA accumulation. They concluded that this strategy improved the ARA and total lipid concentration but also shortened the culture time. However, it should be noted that a temperature shift strategy may not optimal in pilot-scale fermentation as the cooling jackets which faciliate temperature may have high energy requirement and the high cost may not be suitable for ARA commercialization.

3.2.5.6 Effects of Oxygen

Oxygen supply is crucial for PUFA-rich lipid accumulation. Synthesis in *M. alpina* is catalysed by the aerobic fatty acid desaturase/elongase pathway, in which oxygen consumption is extremely high, and sufficient DO has been proven to play an important role in improving its degree of fatty acid unsaturation (Chang et al., 2021). The industrial production of various metabolites of filamentous fungi is susceptible to the influence of dissolved oxygen. This is a common feature of fungal metabolism and points to a general role of oxygen in metabolic regulation, where oxygen acts as a direct regulator of citric acid accumulation (Papagianni, 2004).

In addition, agitation speed level is always an important factor in aerobic biological systems, since when the supply of oxygen is limited, both cell growth and product formation can be severely affected. Higher agitation rates result in an increase in oxygen supply for growth, and can lead to an increase in the availability of intracellular molecular oxygen. This ensures optimum activities of the oxygen-dependent enzymes in PUFA biosynthesis (Saelao et al., 2011).

3.2.5.7 Effects of pH

The pH of the medium is very important for growth and metabolite production. This can be possibly due to some media–pH interactions which reduce the efficiency of the strain to utilize the carbon source provided. Most of the fungi require more acidic pH for growth in submerged culture and an increase in initial pH has been found to stimulate the accumulation of metabolites (Nisha & Venkateswaran, 2011). Biomass growth in *M. alpina* strains tend to cease at pH levels outside of the range from 4.5 to 8.0. The optimum pH level for ARA production has been found in the range of 6 - 6.5. The initial pH influences the fungal mycelial morphology, which is a critical factor for metabolite formation and that allows cells to aggregate due to the production of hydrophobic proteins to coordinate the adherence of hyphae (Mamani et al., 2019; Papagianni, 2004).

The composition of the medium can affect the initial pH as well as the degree and direction of pH drift during fungal growth. Poorly buffered media containing ammonium salts may become more acidic during growth, while media containing nitrates may become alkaline. Minimizing pH drift during growth is a desirable goal, but often difficult to achieve (Papagianni, 2004)

3.2.5.8 Effects of Morphology

Morphology has a strong influence on the physical properties of fermentation broth and causes many problems in terms of gas dispersion, mass and heat transfer, and homogenization in the fermenter. Two morphological types, hyphal filaments and pellets, are frequently observed in submerged liquid cultures (Ji et al., 2014; Chen et al., 2022). In submerged cultures, many filamentous microorganisms tend to aggregate and grow as pellets. Pellets are spherical or ellipsoidal masses of hyphae with variable internal structure, ranging from dispersed filaments, ‘‘fluffy’’ pellets, to tightly packed, compact, dense hollow pellets (Papagianni, 2004; Fang et al., 2018). Different nitrogen sources also affect mycelial morphology and the activities and expression of critical enzymes in the nutrient metabolism-related pathways and therefore significantly affect growth and lipid biosynthesis of *M. alpina* (Higashiyama et al., 2002; Chang et al., 2021).

It has been reported that higher growth rate favours the optimal morphology of pellets, which could cause a decrease in the viscosity of the culture (Higashiyama et al., 1998a; Liao et al., 2007; Ji et al., 2014; Fang et al., 2018; Chen et al., 2022). Small pellets can apparently allow sufficient mass transfer and maintain the broth viscosity at an acceptable level (Ji et al., 2014). Hyphal filaments yield the optimal ARA-rich oil production at low cell densities because of the easy access to nutrients and the ease of gas exchange between the hyphae and the medium (Chen et al., 2022). However, dispersed mycelia at high cell densities causes the high viscosity of the culture and can reduce the efficiency of mixing and oxygen supply as well as increased wall growth (Higashiyama et al., 1998a, 1999;

Papagianni, 2004; Ji et al., 2014; Chen et al., 2022). Therefore, fluffy pellet morphology has been suggested to be more suitable for ARA-rich oil production than the smooth pellet morphology (Higashiyama et al., 2002; Ji et al., 2014; Chang et al., 2021; Chen et al., 2022).

3.3 Strain Improvement

3.3.1 Random Mutagenesis

Wild-type microorganisms typically yield small quantities of compounds that may be commercially desirable when initially isolated from the wild (Dragosits & Mattanovich, 2013). Genetic modification methods based on the use of largely empirical whole-cell mutagenesis, coupled with high-throughput screening methods, often result in dramatic one-step improvement (Nisha, 2009). Classical genetics allows the generation of a large number of mutant phenotypes without prior knowledge of the genetics and metabolism of the target organism and without the development of molecular tools, which can be time consuming and expensive (Trovão et al., 2022). In comparison, metabolic engineering focuses on the metabolic pathways that lead to metabolites or biomolecules that are desired fermentation products and can be produced at a high rate and yield from glucose and other affordable carbon sources. Classical strain improvement uses random mutagenesis to accumulate genomic alterations and then screens for phenotypes with desirable characteristics (Yang et al., 2007). Mutation techniques leading to the inhibition or activation of specific fungal desaturases are not only beneficial for the production of tailored PUFAs, but can also be used to study fungal PUFA biosynthesis. Molecular engineering of parental strains and their mutants is a powerful tool for the construction of novel microbial strains for the synthesis of economically valuable fatty acids (Certik, 1998).

Strain improvement by mutagenesis and selection is a highly developed technique and it plays an important role in the commercial development of microbial fermentation processes. Mutagenic procedures can be carried out according to the type of mutagen to obtain mutant types that may be screened for improved activity. Random mutagenesis

accelerates the naturally occurring process by exposing the organism to a powerful physical or chemical mutagen and organisms are screened for the desired phenotype or trait (Yang et al., 2007; Trovão et al., 2022). The use of random mutagenesis provides advantages over genetic engineering techniques as it is not dependent on the host's genetic information, requires simpler and cheaper tools, produces mutant libraries with high genetic diversity and avoids the metabolic burden caused by the targeted incorporation or deletion of foreign genes (Arora & Philippidis, 2021; Arora et al., 2022). Random mutagenesis also eliminates the need for selective agents that can be harmful to the environment and it avoids the lengthy and expensive legal requirements involved in controlling and labeling genetically modified products (Beacham et al., 2015).

However, strain improvement may bring low mutation frequency in the desired gene. Even if mutants with the desired phenotype are isolated, there is no guarantee that the mutation has occurred in the gene of interest (Bhavsar et al., 2013). Random mutagenesis results in the production of hundreds of mutant colonies, though the mutation frequency may be low. Screening for mutants is very time and labour intensive, as only a small fraction of them have the desired phenotype, thus efficient screening methods are required (Li et al., 2015; Zhang et al., 2018; Trovão et al., 2022).

Low temperature (4 - 5°C) was first used as a screening method by Botha et al (1999) for *Mortierella* species isolation. It was found that fungi produced more PUFAs at lower growth temperatures which would have increased the membrane fluidity and was hypothesized to be an adaptive response to a cold environment (Botha et al., 1999). However, using low temperature as a screening tool is time-consuming and it is difficult to manually screen the gene-interest mutants (Yao et al., 2019).

Later, low temperature combined with staining Triphenyltetrazolium Chloride (TTC) was introduced by Zhu et al., (2004). Tetrazolium salts, such as TTC, are a large group of organic compounds that can react to form highly colored products and are sometimes used to detect biological reducing systems (Moussa et al., 2013). TTC is an oxidant that can be

reduced from colourless TTC to red-coloured triphenylformazan (TF). It has been used extensively to assess the viability of plant cells and tissues and the measurement of respiratory activity in bacteria (Zhu et al., 2004). TTC can be absorbed by living cells (Li et al., 2015), where it reacts with hydrogen atoms released by mitochondrial dehydrogenases during cellular respiration to produce the carmine red product, triphenylformazan (Zhu et al., 2004; Nisha, 2009; Shofiul Azam et al., 2015). In the presence of bacteria, TTC is reduced to red formazan which is directly proportional to the viable active cells present. Therefore, the TTC test method is considered as a comparatively fast method for evaluating the antibacterial activity of antimicrobial agents (Moussa et al., 2013).

Zhu et al., (2004) were able to isolate *M. alpina* with TTC stain, and observed that the degree of staining for the mycelia stained with TTC increased when ARA content in mycelia lipids increased. TTC staining of *M. alpina* is based on the presence of Δ5 desaturase, a dehydrogenase enzyme which catalyzes the formation of ARA from dihomo-γ-linolenic acid. Mutants with high levels of the enzyme are hyper stained, whereas negative mutants remain less stained or unstained due to reduced or absent activity of Δ5 desaturase (Nisha, 2009). Only ARA-producing fungus *M. alpina* could be stained red; *Mucor* which do not produce ARA could not be stained red. This suggests that a specific dehydrogenase is only present in the *M. alpina* and not in *Mucor rouxianus* (Zhu et al., 2004; Shofiul Azam et al., 2015). The standard TTC method measured the absorbance of formazan at 480 nm after staining harvested mycelia (Moussa et al., 2013). Li et al. (2015) adapted the method to make it quicker and more convenient for screening by supplementing TTC directly in PDA plates. They found that after mutation, many colonies on the selection plate supplemented with TTC were stained red and the darkest colored mutant colonies were selected for further testing (Li et al., 2015). This method was subsequently used to screen *M. alpina* isolates by Yao et al. (2019) as well. TTC staining has been used as an effective and fast screening method on strain isolation or strain genetic

breeding experiments and has been extensively used in studies on *Mortierella* (Nisha, 2009; Yadav et al., 2014; Li et al., 2015; Shofiul Azam et al., 2015; Yao et al., 2019).

The most frequently used and selective process of screening for mutants with high compound accumulation is the use of pathway inhibitors that specifically target the rate-limiting enzymes for the biosynthesis of the desired compound (Trovão et al., 2022). In addition to TTC staining, FAS inhibitors such as nocodazole, C75, (Shofiul Azam et al., 2015), cerulenin (Li et al., 2015; Shofiul Azam et al., 2015; Yao et al., 2019), and triclosan (Zhang et al., 2018) have been compared and utilized as an effective screening strategy for *Mortierella* strains. Cerulenin, 2,3-epoxy-4-oxo-10-dodecadienamide, is a natural product of the ascomycete fungus *Cephalosporium caerulens*, and originally described as having antifungal properties. Cerulenin is a potent inhibitor of lipid biosynthesis and this response was shown to be associated with its inhibitory effect on the activity of fatty acid synthase (Tapia V et al., 2012). It mainly interferes with both de-novo fatty acid synthesis and chain elongation starting with palmityl-CoA as shown in Figure 3.6 (Arora et al., 2020). Cerulenin has been extensively used to select high lipid producing mutants in the oleaginous microorganisms (Li et al., 2015). It inhibits FAS activity by covalent modification of the active site. Mutants demonstrating normal growth rates at a certain concentration of cerulenin are identified as having relatively high FAS activity and are good candidates for lipid production (Li et al., 2015; Yao et al., 2019).

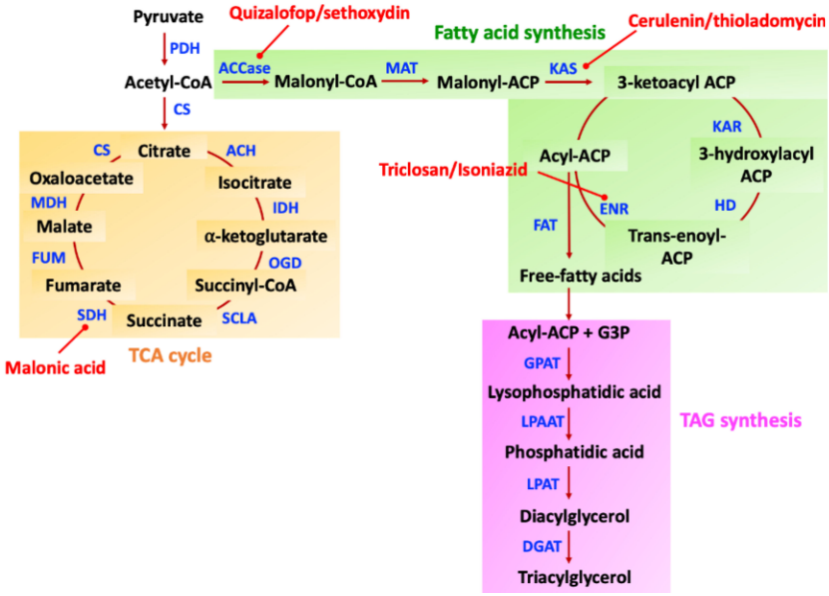

Figure 3.6: Schematic of the lipid biosynthesis pathway in microalgae and yeasts highlighting the action of chemical mutagens on metabolic enzymes. Image with permission from (Arora et al., 2020).

The most simple and common mutagenesis methods are physical mutagenesis using Ultra-violet (UV) light and chemical mutagenesis using chemical agents such as ethyl methane sulphonate (EMS). With UV light, non-ionizing radiation absorbed by Deoxyribonucleic acid (DNA) leads to thymine dimers that cause mispairing during DNA replication, and permanent mutation if not repaired (Hlavova et al., 2015; Trovão et al., 2022). UV radiation (254 nm) can alter the structure of important biomolecules, such as proteins and DNA, affecting growth and cell division in some organisms (Rastogi et al., 2010). UV radiation-mediated mutagenesis is often more appealing than other methods, since it uses UV sterilizing lamps commonly found in flow chambers. In addition, it facilitates the isolation of mutants under sterile conditions, reducing biological contamination (Liu et al., 2015). A major advantage of UV generated mutants is that no additional requirements and regulations are expected for large-scale outdoor cultivation and eventual use in food (de Jaeger et al., 2014). The main advantages of using physical mutagenesis over chemical mutagenesis are accuracy and reproducibility, due to uniform

penetration in the tissue (Oladosu et al., 2016).

EMS is an alkylating agent that induces point mutagenesis (Nisha, 2009; Beacham et al., 2015; Yang et al., 2019). Nisha (2009) investigated the chemical (N-methyl-N'-nitro-N'nitrosoguanidine (NTG) and EMS and UV mutagenesis, screening by low temperature and TTC staining on *M. alpina* CBS 528.72. The results from that study showed that the mutants had a higher ARA% in total lipids than the control (2009). Other mutagenesis methods such as Protoplast Regeneration Mutagenesis (Lina et al., 2011), atmospheric and room temperature plasma and diethyl sulfate treatments (Li et al., 2015), and heavy ion mutagenesis (Zhang et al., 2018) have also been successfully applied to *Mortierella* species.

Other high-throughput screening methods, such as fluorescence microscopy and Fourier transform infrared spectromicroscopy provide spatial resolution of the intracellular biochemical composition of filamentous fungi. Measurement of the carbon dioxide evolution rate, multi-wavelength fluorescence spectroscopy, turbidity measurement, and near-infrared spectroscopy are also used (Posch et al., 2013). In addition, fluorescence-activated cell sorting (FACS), applies multi-dimensional selection to a strain engineered with a biosensor for valine-induced fluorescence on other oleaginous microalgae (Sandberg et al., 2019; Lee & Kim, 2020). Biosensors provide a powerful way to associate otherwise inconspicuous intracellular states with screenable output by screening and continuously propagating only the most highly fluorescent cells (Sandberg et al., 2019). However, FACS has been extensively used on unicellular microorganisms to perform the single sorting technique, while it is not possible to do so on filamentous fungi due to their multi-cellular characteristics (Chang et al., 2022).

3.3.2 Adaptive Laboratory Evolution (ALE)

Natural evolution is when species undergo mutations and recombination that are either environmentally dependent or heritable, followed by natural selection in which the most beneficial phenotypes are adapted, survive and reproduce in their particular environment.

This whole process is also known as adaptive evolution (Mavrommati et al., 2022). ALE is a process in which the principles of natural evolution are implemented in the laboratory to specific populations under controlled conditions for a long period of time. In ALE, natural selection is directed to a selected environment with ideal conditions for a population to achieve better adaptation (Dragosits & Mattanovich, 2013; Lee & Kim, 2020; Mavrommati et al., 2022). Under these artificial stress conditions, the metabolic pathways of the organism are varied so that the mutations may adapt by exhibiting a faster growth rate resulting in higher product yields (Conrad et al., 2011).

Given the complexity of strain improvement which requires comprehensive metabolic knowledge, and general societal concerns surrounding the use of genetically modified organisms (GMOs), ALE has been proposed as an alternative strategy to improve the stress resistance and growth rate without requiring *a priori* knowledge to produce commercially viable strains (Sun et al., 2016; Lee & Kim, 2020). ALE experiments in microbial systems are easier to perform because of the short generation time, simple experimental setup, and tight control of experimental variables (Sun et al., 2018). ALE experiments in microalgae are less common and often focus on acclimation mechanisms, rather than adaptation. The former mechanism occurs without genetic changes over a shorter period of time, whereas adaptation involves the accumulation of beneficial genetic mutations, which leads to new genotypes more suitable for the applied stress (LaPanse et al., 2021).

Mutations that appear in populations are generally classified as beneficial, neutral, deleterious, or lethal. In most environments, most new mutations appear to be neutral, while deleterious mutations occur at a much higher rate than beneficial mutations (Charlesworth, 2012). In ALE experiments, beneficial mutations should be retained as new populations, not deleterious mutations (Dragosits & Mattanovich, 2013; Lee & Kim, 2020; Mavrommati et al., 2022). In fact, multiple beneficial mutations appear simultaneously in different cell lines, and they compete with each other, leading to a slower accumulation of any of these mutations toward new populations, a phenomenon known as "clonal

interference" (Buckling et al., 2009; Winkler & Kao, 2014). Weak selection allows more genetic diversity and permits the exploration of more mutational pathways whereas strong selection results in the survival of rare mutations leading to the generation of unique phenotypes (Mavrommati et al., 2022).

Culture propagation methods have been successfully used for ALE including serial transfer in batch cultures, continuous cultures in a chemostat, streaking cells onto solid media for mutation analysis, emulsion cultures, microfluidics, and evolution of microorganisms inside an alternative host (McDonald, 2019). Serial transfer in shake-flasks is the most common ALE method used for microalgae to improve growth rate, inhibitor tolerance, high salinity, oxidative pressure, high-lipid productivity and result in other beneficial phenotypes (LaPanse et al., 2021). However, serial propagation of colonies streaked onto plates without secondary screening measures for the transfer process is not a form of "adaptive" evolution, but can be used for mutation accumulation studies (Sandberg et al., 2019).

An important factor affecting the outcome of evolution is the passage volume, which determines how many populations are allowed to propagate to each subsequent batch culture. Usually, smaller passage sizes can reduce the rate of evolution. When the change of passage size only affects the duration of the growth and stationary phase, it is easier to perform a serially passaged batch culture ALE under alternating environments (LaCroix et al., 2017). However, this is a prerequisite to avoid stationary phase adaptation in serial transfer. Thus, it is preferable for microbial cells to be transferred in exponential cultures (Dragosits & Mattanovich, 2013). Typically, the time between passaging cannot be shorter than 12 hours. Consequently, as the culture adapts and begins to grow rapidly, the passage size must be decreased (LaCroix et al., 2017).

Another critical parameter is the length of time for which populations of strains are evolved. The time span of a typical ALE experiment is performed between 100 and 2000 generations and usually takes a few weeks up to a few months. It has been estimated that

within 100 to 500 generations, which corresponds to up to 2 months of selection for a typical *E. coli* or *S. cerevisiae* culture, an increase in fitness of up to 50-100% can be achieved (Dragosits & Mattanovich, 2013; Sandberg et al., 2019).

The main challenge with ALE is that the population density varies from flask to flask, and since cell density varies depending on the amount of nutrients remaining, the fluidity of the physicochemical environment, including pH and dissolved oxygen, is difficult to keep constant. This can lead to erroneous evolutionary stresses, resulting in undesired phenotypes and making the relationship between genotype and phenotype difficult to determine (Lee & Kim, 2020; LaPanse et al., 2021). ALE can also be used to increase tolerance under multiple stresses, however, the tolerance to one stress is often accompanied by trade-offs in separate growth environments, which depends on the specific adaptive mutation acquired (Sandberg et al., 2019). In this case, the best phenotype as far as biotechnology is concerned is not necessarily the one with the highest fitness in a given condition, but rather one that exhibits higher performance and minimal trade-offs in other environmental conditions (Dragosits & Mattanovich, 2013; Sandberg et al., 2019).

The key stressors controlling such ALE experiments are environmental factors including temperature, pH, salinity, oxidative stress; nutrient or substrate stress; sampled mutations such as the intrinsic mutation rate; and growth parameters/selection pressures that include exponential growth, biomass production, stationary period or lag period (Winkler & Kao, 2014; Sandberg et al., 2019; Lee & Kim, 2020; LaPanse et al., 2021; Mavrommati et al., 2022). To minimize energy consumption and emissions during biofuel production, it can be advantageous to develop industrial strains with high temperature tolerance as this can significantly reduce the cooling costs and help prevent contamination (Xu et al., 2018; Barten et al., 2022). According to energy consumption and cost analysis, Xu et al. (2018) reported that increasing every 2°C of fermentation temperature reduced the energy consumption of distillation by 1%. In another study by Barten et al. (2022), they showed that maximal productivity rate under daily temperatures ranging from 30°C

to 45°C would cause a cost reduction of 31% and Hu et al. (2021) reported that if the fermentation temperature was increased by 5°C, the cost of cooling water and cooling power would be reduced by 15% and 10% respectively per year. Therefore, temperature is one of the most important environment parameters affecting cell growth and product formation (Peng et al., 2010; Cao et al., 2015), and improving the thermotolerance of strains can greatly reduce energy consumption and fermentation cost.

Chapter 4: Methods and Materials

4.1 Overview of Project Methodology

Figure 4.1 represents a flow diagram of the project methodology, which shows the experimental approach taken to develop beneficial mutants by fermentation media optimization followed by strain improvement. In the fermentation media optimization part, micronutrients were screened and optimized by Plackett-Burman (PB) and Response Surface Methodology (RSM) methods, followed by screening for C:N and optimization of nitrogen sources to investigate macronutrients. Finally, a modified medium was formed. The modified medium was used as a working medium for strain improvement by random mutagenesis and ALE experiments.

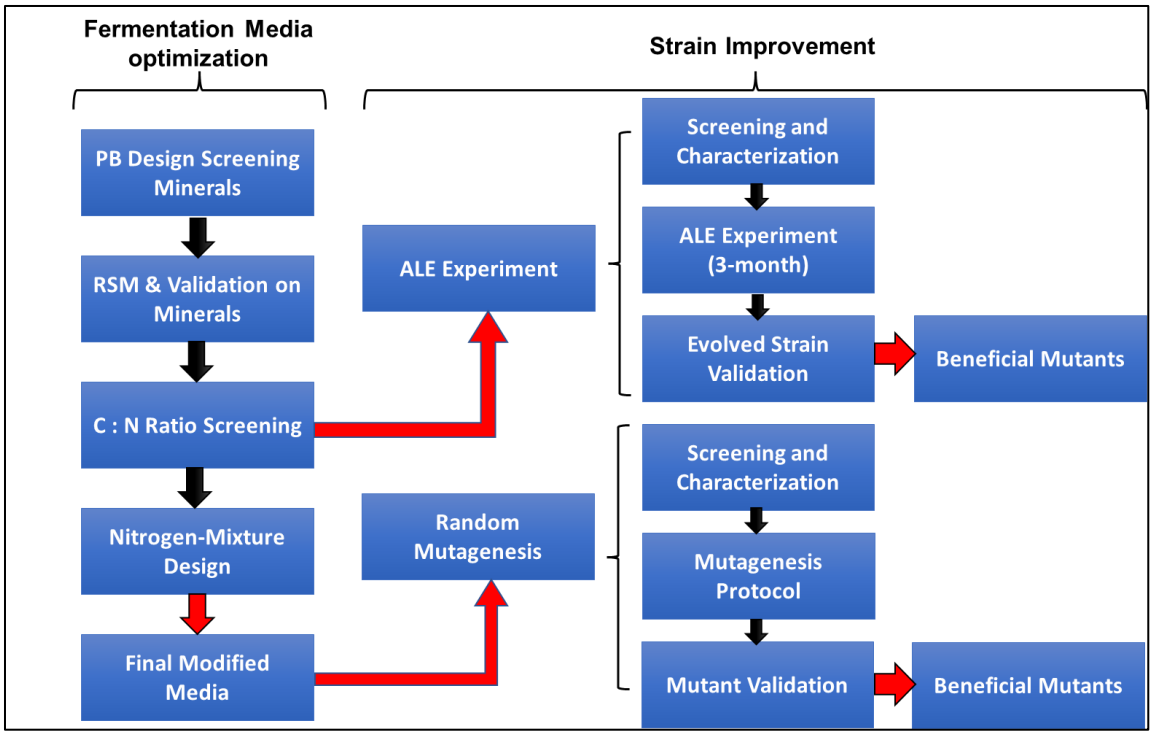

Figure 4.1: Flow Diagram of Overall Project Methodology

4.2 Microorganism, inoculum preparation and general culture conditions

The ARA-producing strain *M. alpina* MA2-2, supplied by Mara (*M. alpina* isolates came from DAOM 220666, CCoFC), was maintained on PDA plates and sub-cultured every 1 month. This strain was preserved in either deionized water stored at 3 ± 1°C or 10% (v/v) glycerol at -80°C.

For cultivation experiments, the *M. alpina* culture was initially grown on PDA plates until the mycelium were observed spreading on the plate for 7-15 days at 25°C. Then MA2-2 strain was cultivated in 250 mL baffled shake-flasks covered with aluminum foil containing 60 mL of medium at a control temperature of 28°C, under constant orbital shaking at 200 rpm. The culture was inoculated by adding 3 pieces of mycelia-covered agar (~0.5 cm^2 each).

4.3 Plackett-Burman and Response Surface Methodology Experimental Designs on Micronutrients

To improve the productivity of ARA in the MA2-2 strain, the focus was on using PB screening and RSM optimization aimed at maintaining a constant basal medium of glucose and yeast extract, while testing various minerals, vitamins and trace elements to create a blend of micronutrients that could enhance ARA production.

4.3.1 Culture conditions

The strain was first cultivated and grown on flask cultures using a standard fermentation basal medium. Here, sole carbon (glucose, 20 g L^{-1}) and nitrogen (yeast extract, 11 g L^{-1}) sources were used for the basal fermentation media for ARA production (Aki et al., 2001; Nisha & Venkateswaran, 2011). The initial pH for the basal medium was adjusted to 6.0 with 1 M sodium hydroxide (NaOH) or hydrogen chloride (HCl) prior to autoclaving. Selected inorganic salts were added to the basal medium post-autoclave to avoid precipitation.

4.3.2 Plackett-Burman Media Screening

For the first step in optimizing fermentation conditions, PB experimental design was used to develop an orthogonal array for screening micronutrients, and unbiased estimates of all main effects were obtained in the minimal design (Vanaja & Shobha Rani, 2007). PB design is useful for detecting significant main effects in an economic manner, assuming all interactions are negligible compared with the few critical main effects (Guthrie, 2020). Biomass dry cell weight (DCW) (g L^{-1}), Total Fatty Acid (TFA) or total lipid content w/w% in biomass, ARA w/w% in TFA and ARA concentration (mg L^{-1}) were used as response variables.

In the PB design, eight nutritional factors including mineral ions, vitamins and trace elements were tested at high (+) and low (-) levels (Rocky-Salimi et al., 2011). Here, the high level of addition was determined from literature on ARA producing strains, while the low level meant no addition of the nutrient (Table 4.1). In total, 12 random runs were performed in duplicate to reduce the experimental bias. The average of the duplicate results was used for statistical analysis to identify variables with significant effects on the response (Table 5.1) (Malaiwong et al., 2016).

The PB experimental design is based on the first order model:

$$Y = \alpha_0 + \sum \alpha_1 X_i \quad (1)$$

where Y is the response (here referred to DCW (g L^{-1}), TFA%, ARA% or ARA concentration (mg L^{-1}), α_0 is the model intercept, α_1 is the linear coefficient and X_i is the level of independent variable (Ademakinwa et al., 2017).

Table 4.1: Plackett-Burman low/high levels table.

Composition:	Name	Unit	Coded Levels		Source
			-1 (low level)	+1 (High Level)	
KH_2PO4	Potassium Dihydrogen Phosphate	g L^{-1}	0	7.5	Liu et al., 2012
NaCl	Sodium Chloride	g L^{-1}	0	15	Saelao et al., 2011
$MgSO_4.7H_20$	Magnesium Sulfate Heptahydrate	g L^{-1}	0	2.7	Saelao et al., 2011
$CaCl_2.2H_20$	Calcium Chloride Dihydrate	g L^{-1}	0	0.5	Higashiyama et al., 1998a; Saelao et al., 2011
$MgCl_2.6H_20$	Magnesium Chloride Hexahydrate	g L^{-1}	0	5.4	Saelao et al., 2011
Sodium Citrate		g L^{-1}	0	2	Sun et al., 2015
Trace Mineral Solution (TMS) (g L^{-1}):					
$MnCl_2.4H_20$ 0.3	Manganese(II) Chloride Tetrahydrate				
$ZnSO_4.7H_20$ 0.3	Zinc Sulfate Heptahydrate	mL L^{-1}	0	24	Mara
$CoCl_2.6H_20$ 0.004	Cobalt(II) Chloride Hexahydrate				
$CuSO_4.5H_20$ 0.2	Copper Sulfate Pentahydrate				
$NiSO_4.6H_20$ 0.2	Nickel Sulfate Hexahydrate				
$FeSo_4.7H_20$ 1	Iron(II) Sulfate Heptahydrate				
Vitamin Solution (g L^{-1}):					
Thiamin B1 0.05					
Nicotinamide B3 0.15		mL L^{-1}	0	10	Zeng et al., 2012
D-pantothenate B5 0.2					
Pyridoxine B6 0.1					

4.3.3 RSM Experimental Design and Data Analysis

RSM is a technique that is used to estimate interaction and quadratic effects and can determine the shape of the response surface of interest (Malaiwong et al., 2016; Guthrie, 2020). Here, *M. alpina* MA2-2 strain was selected for RSM analysis.

Based on the results of the PB design, a 2^3 factorial central composite design (CCD) was studied at five coded levels (−1.683, −1, 0, +1, +1.683) with 8 points, 6 quadrant or edge points (α) and 6 replicates at the center points leading to a table of 20 sets of experiments. These were performed in duplicate and the data was calculated as the mean ± standard deviation (SD) (n = 2). All the variables were taken at a central coded value (considered as zero). The variables include KH_2PO_4, $CaCl_2.2H_20$ and $MgSO_4.7H_20$ for RSM design on study the responses to high biomass, total TFA% and ARA production (Table 4.2). Biomass DCW (g L^{-1}), TFA or total oil content w/w% in biomass, ARA w/w% in TFA and ARA concentration (mg L^{-1}) were used as response variables. The relationship of the independent variables and the responses were calculated by the second-order polynomial equation:

$$Y = \beta_0 + \sum_{i=1}^{k} \beta_i x_i + \sum_{i=1}^{k} \beta_{ii} x_i^2 + \sum_{i=1}^{k} \beta_{ii} x_i x_j \qquad (2)$$

where Y is the predicted response, β_0 is the model constant, β_i is the linear coefficient, β_{ii} is the quadratic coefficient, β_{ij} is the interaction coefficient, and k is number of factors. The analysis of variance (ANOVA) for the experimental data and the model coefficients were calculated using the statistical software package, Minitab 19.2020.1. In addition, response surface and two-dimensional contour plots were constructed to visualize the trend of the maximum response and the interaction effects of important variables on the response (Jin et al., 2009; Nisha et al., 2011).

Table 4.2: Experimental variables at different levels used for the RSM approach.

Composition:	Unit	Coded Levels				
		$-\alpha$ (-1.683)	-1	0	+1	$+\alpha$ (+1.683)
KH_2PO4	g L^{-1}	0	0.5	4	7.5	9.886
$MgSO_4.7H_20$	g L^{-1}	0	0.5	2.75	5	6.534
$CaCl_2.2H_20$	g L^{-1}	0	0.05	1.025	2	2.665

The ANOVA of the quadratic regression models can be confirmed the significance by Fisher's test (F test). The coefficient of determination R^2 represents the quality of the fit of the second order equation model (Jin et al., 2009; Nisha et al., 2011; Rocky-Salimi et al., 2011). The significance of each variable was determined using the student's t test. The variables at or above the 95.0 % confidence level ($p \leq 0.05$) were considered to have significant effects on the responses (Nisha et al., 2011; Rocky-Salimi et al., 2011; Saelao et al., 2011; Malaiwong et al., 2016; Guthrie, 2020). Lack of fit measured the failure of the model at points in the experimental domain that were not included in the regression where a nonsignificant lack of fit would be considered a suitable fit for the model (Yang et al., 2006; Ademakinwa et al., 2017). The fitted polynomial equation was then expressed in the form of contour plots in order to illustrate the relationship between the responses and the experimental levels of variables in this study (Rocky-Salimi et al., 2011). The statistical software package, Minitab 19.2020.1, was used for the regression analysis of the experimental data of PB and RSM design.

4.4 Mixture Experimental Design on Macronutrients

Section 4.4 studied the macronutrients consisting of carbon to nitrogen ratios and to optimize mixing of nitrogen source combinations.

4.4.1 Culture Conditions

The strain was first cultured in shake flasks, using a basal medium containing mineral optimized from the previous RSM design, and grown at 28°C until glucose depletion. Here,

minerals included KH_2PO_4 5.023 g L^{-1}, $MgSO_4.7H_20$ 0.796 g L^{-1} and $CaCl_2.2H_20$ 0.318 g L^{-1} were added to the fermentation medium as basal micronutrients. Glucose 20 g L^{-1} and yeast extract 11 g L^{-1} were used as the main carbon and nitrogen sources in the basal medium to form a C:N ratio of 7.2 for ARA production (Aki et al., 2001; Nisha & Venkateswaran, 2011). The latter experiments were adjusted to the current composition of the carbon and/or nitrogen sources. The pH of each medium was adjusted to 6.0 with 1 M NaOH or HCl prior to autoclaving. $MgSO_4.7H_20$ and $CaCl_2.2H_20$ were added post-autoclave to prevent precipitates from forming.

4.4.2 Evaluation of Suitable Carbon to Nitrogen (C:N) Ratio

Since the nitrogen content of the medium is a determining factor for the production of secondary metabolites, the appropriate ratio of carbon to nitrogen in the medium should be evaluated (Shariati et al., 2019). Four different C:N ratios including 7.2 (initial basal C:N ratio shown in Eq. 3), 10, 15 and 20 were calculated in two ways, one by decreasing the concentration of the nitrogen source i.e., yeast extract, while keeping the concentration of glucose fixed at 20 g L^{-1}, containing total carbon of 8 g L^{-1} (Eq. 3, 4 and 5); and the other by the opposite, increasing the concentration of glucose while keeping the concentration of yeast extract fixed at 11 g L^{-1}, containing 1.1 g L^{-1} of total nitrogen (Eq. 6). The C:N ratios used in this study are shown in Table 4.3. The optimal C:N ratio was then kept constant in subsequent nitrogen optimization experiments.

Table 4.3: Experimental deign for screening of carbon to nitrogen ratio.

C:N ratio	Fixed Glucose [b] g L^{-1}	Fixed Total Carbon [c] g L^{-1}	Yeast Extract g L^{-1}
7.273 [a]	20	8	11.00
10			8.00
15			5.33
20			4.00
C:N ratio	Fixed Yeast extract g L^{-1}	Fixed Total Nitrogen [d] g L^{-1}	Glucose g L^{-1}
7.273	11	1.1	20.00 [d]
10			27.50
15			41.25
20			55.00

[a] Control C:N ratio was when glucose and yeast extract maintained at 20 g L^{-1} and 11 g L^{-1}.

$$\text{Control C: N} = \frac{20\ \text{g L}^{-1}\text{glucose} \times 40.0\%\ \text{C}}{11\ \text{g L}^{-1}\text{yeast extract} \times 10.0\%\ \text{N}} = 7.273 \quad (3)$$

[b] Glucose $C_6H_{12}O_6$

$$\%\ \text{composition of carbon} = \frac{6\ \text{mol C}}{1\ \text{mol } C_6H_{12}O_6} = \frac{6(12.01\ \text{g mol}^{-1})}{180.16\ \text{g mol}^{-1}} \times 100 = 40.0\% \quad (4)$$

[c] $\text{Total Carbon (g L}^{-1}) = 20\ \text{g L}^{-1}\text{glucose} \times 40.0\%\ \text{C} = 8\ \text{g L}^{-1}\text{C}$ (5)

[d] $\text{Total Nitrogen (g L}^{-1}) = 11\ \text{g L}^{-1}\text{Yeast Extract} \times 10.0\%\ \text{N} = 1.1\ \text{g L}^{-1}\text{N}$ (6)

4.4.3 Pre-screening of Different Nitrogen Sources

Three inorganic and three organic components were selected for pre-screening of different sources of nitrogen, including sodium nitrate ($NaNO_3$), monosodium glutamate (MSG), ammonia sulfate $(NH_4)_2SO_4$, yeast extract, peptone and urea. For the inorganic components, the percentage of total nitrogen was calculated according to molecular weight, and for the organic nitrogen sources, it was based on information from the manufacturers (Shariati et al., 2019), shown in Table 4.4.

The purpose of the nitrogen pre-screening was to examine all potential inorganic and organic nitrogen sources at a constant C:N ratio of 7.2 (initial basal C:N ratio) prior to nitrogen mixture design experiments. This was done to eliminate some nitrogen sources with minimal effects as only three to four nitrogen sources could be selected for mixture design to avoid large experimental runs. As other nitrogen sources were never used as the sole nitrogen source for the strain MA2-2, to evaluate the performance of each nitrogen

source, yeast extract was added at 10% of the total nitrogen content, combined with 90% from the other nitrogen source.

Table 4.4: Experimental design of pre-screening nitrogen sources

Nitrogen source	% of nitrogen	PH	10% total nitrogen [a]	90% total nitrogen [b]	reference
Yeast extract	10	6-6.5	1.1		Sigma-Aldrich, 2020
Peptone	10.4	7.2		9.52	HiMedia Laboratories, 2018
Sodium nitrate ($NaNO_3$)	16.47	7		6.01	National Center for Biotechnology Information, 2023a
Urea	46.6	4-8		2.12	Sigma-Aldrich, 2022
Monosodium glutamate (MSG)	8.29	6.7-7.2		11.94	National Center for Biotechnology Information, 2023c
Ammonia Sulfate ($(NH_4)2SO_4$)	21	5.5		4.71	National Center for Biotechnology Information, 2023b

[a] Represents the coded concentration of yeast extract in each medium accounted for a 10% total nitrogen content.

[b] Represents the coded concentrations of other nitrogen sources accounted for a 90% total nitrogen content.

4.4.4 Mixture Experimental Design on Pre-screened Nitrogen Sources

Mixture analysis design is an alternative method for screening and optimizing of components in culture media by studying the interactions of factors (Rispoli & Shah, 2009). It is a suitable method to simultaneously evaluate the proportion of different nitrogen sources in culture media, while keeping the final concentration of total nitrogen constant to maintain a constant C:N ratio. The other advantage of the mixture analysis method is that it is able to eliminate both neutral- and negative-factors (Shariati et al., 2019).

In the mixture experiment, the different nitrogen sources were used as independent factors in a blend so that the sum of the proportions of all substrates in each mixture totaled 100% (Sathish et al., 2008). Optimization of the mixture with the different nitrogen sources was carried out using a triangular surface response (Figure 4.2) (Moldes et al., 2007). The

mixture design strategy was used to obtain the maximum ARA production and to investigate the presence of either synergistic or antagonistic effects in a blend of components.

The prediction equation (Eq. 7) of the response variables is given below (Rispoli & Shah, 2009):

$$Y = \sum_{i=1}^{k} \beta_i X_i + \sum_{i<j} \sum^{k} \beta_{ij} X_i X_j \quad (7)$$

where Y is the predicted response, β_i is the linear coefficient, β_{ij} is the interaction coefficient, and k is number of factors.

A four-component augmented simplex-centroid design with center point and axial points was used in which each component was studied at five levels, namely 0%, 25%, 33%, 50%, 62.8%, 100% (de Castro & Sato, 2013). Four nitrogen sources, namely yeast extract, peptone, $NaNO_3$ and MSG, were selected from the previous nitrogen pre-screening experiments (Appendix B – Table B.1).

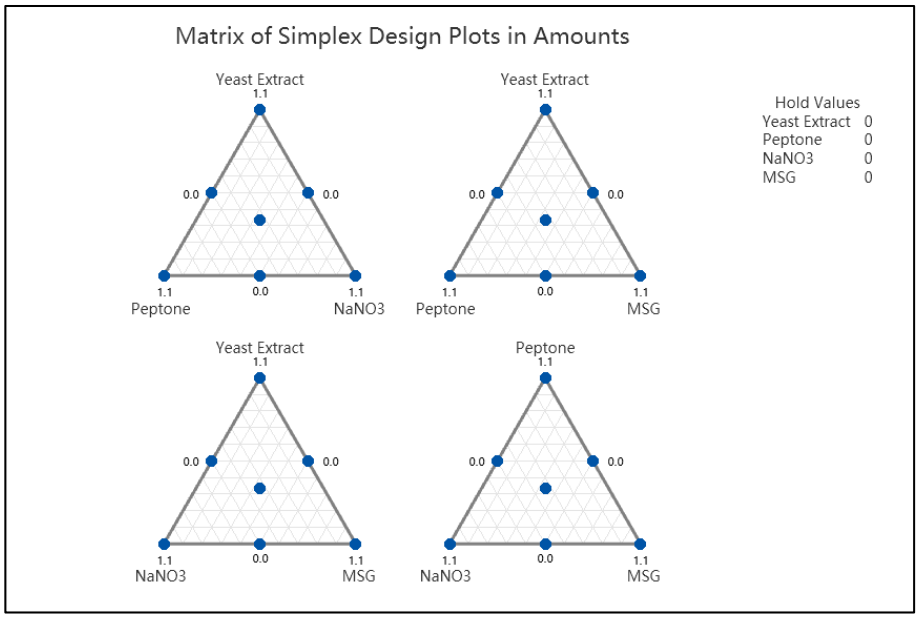

Figure 4.2: Experimental matrix of Simplex Design plots for optimization of nitrogen sources.

In each trial the C:N ratio was constant at 15 obtained from previous C:N ratio screening and each nitrogen source was investigated in the presence of other nitrogen sources in culture medium, while the final concentration of total nitrogen in culture medium was constant. This design aimed to evaluate the effect of the interaction of different nitrogen sources in the mixture. Biomass DCW (g L^{-1}), TFA or total oil content w/w% in biomass, ARA w/w% in TFA and ARA concentration (mg L^{-1}) were used as response variables.

The significance of each variable was determined using the student's t test. The variables at or above the 95.0 % confidence level ($p \leq 0.05$) were considered to have significant effects on the responses (Malaiwong et al., 2016; Guthrie, 2020). The statistical software package, Minitab 19.2020.1, was used for the regression analysis of the experimental data.

4.5 Strain Improvement: Random Mutagenesis

4.5.1 Flask Culture Conditions

The mutagenesis working medium was the previous modified medium, containing glucose 41.25 g L^{-1}, yeast extract 7 g L^{-1}, $NaNO_3$ 2.429 g L^{-1}, KH_2PO_4 5.023 g L^{-1}, $MgSO_4.7H_20$ 0.796 g L^{-1}, $CaCl_2.2H_20$ 0.318 g L^{-1}, adjusted initial pH to 6 using 1 M NaOH or HCl, prior to autoclaving at 121℃. $MgSO_4.7H_20$ and $CaCl_2.2H_20$ were added post-autoclave to prevent precipitates from forming.

4.5.2 Random Mutagenesis Strategies Along with High-throughput Screening

A physical mutagenesis strategy, namely ultraviolet (UV) mutagenesis, coupled with a high-throughput screening approach, i.e. supplementation with the FA synthesis inhibitor cerulenin and the tetrazolium dye TTC, was performed on a wild-type ARA-producing strain (MA2-2) to effectively screen for beneficial mutants with high potential to synthesize PUFA, especially ARA. The screened beneficial mutants were used in shake flask

experiments to verify the stability of their fatty acid profile. Figure 4.3 shows a schematic of the mutagenesis experimental protocol.

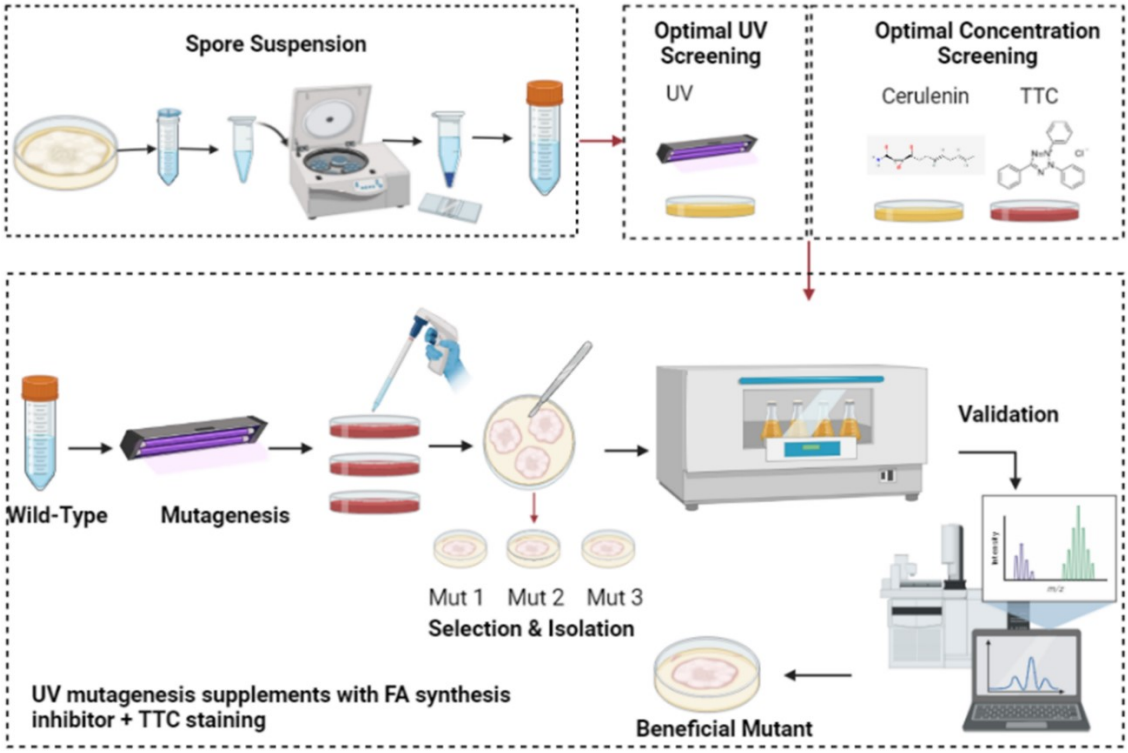

Figure 4.3: Schematic of the mutagenesis experimental protocol with high-throughput screening. Drawn with Biorender.ca

4.5.2.1 Culture Conditions: Spore Suspension Preparation

Spores of MA2-2 grown on PDA plates rinsed with sterile 1x phosphate buffer solution (PBS) containing 0.1% (v/v) Tween 20 (Shofiul Azam et al., 2015; Yao et al., 2019) and filtered through 30 µm Whatman filter paper or 8 layers of cheese cloth. The spore suspension was centrifuged at 12,000×g for 10 min (Li et al., 2015) and diluted with sterile water to a concentration of 10^8 spores mL^{-1}, enumerated using a hemocytometer. The spore suspension was kept in liquid medium at 4°C at a density of approximately ~10^8 spores mL^{-1}.

4.5.2.2 Mutagenesis Characterization – UV Screening and Treatment

Cells were exposed to UV radiation using the UVP CL-1000 UV Crosslinker, with a short wave UV source (254 nm) (Nisha, 2009; Beacham et al., 2015). UV irradiation was performed inside a dark box of 51 cm × 22 cm × 24.5 cm (length × width × height) containing two UV lamps of 15 W each, positioned inside the box top. The default energy emission was estimated as 120,000 μJ × cm^{-2} (Artisan Technology Group, n.d.; Tapia V et al., 2012). Two modes existed in the UV chamber, namely 'Preset UV Energy Exposure' and 'Preset UV Time Exposure'. 'Preset UV Energy Exposure' provided a measured dose of UV exposure to the sample, whereas 'Preset UV Time Exposure' measured the exposure time (Artisan Technology Group, n.d.)

The spore-suspension (10^8 spores mL^{-1}) was transferred into sterile petri dish and irradiated for different time intervals (0, 1, 5, 15, 25, 35 and 45 minutes (min)) with petri dish lid-on condition. Subsequently, a 2^{nd} screening was performed by irradiation (0, 0.1, 0.5, 1, 3, and 7.5 min) with petri dish lid-off condition. The plate containing the culture was manually agitated every 10 minutes for cell resuspension (Tapia V et al., 2012). Additionally, the spore-suspension was irradiated for different energy intensities (4000, 6000, 8000, 10,000, 12,000 μJ × cm^{-2}). Sampling was performed at regular intervals and maintained in darkness overnight to avoid photo reactivation (Nisha, 2009; Tapia V et al., 2012).

Suspensions were suitably diluted, and appropriate dilutions were plated. Then 100-200 μL aliquots were collected, properly diluted and plated by spreading on the PDA agar plates at room temperature for 2-3 days and the mortality rate was calculated using the untreated spore suspension as a control. Spores unexposed to radiation were taken as the control and the percentage of survivors was calculated by considering the colonies developed on control plates as 100% (Nisha, 2009; Zhang et al., 2018).

4.5.2.3 Mutagenesis Characterization –TTC Screening and Treatment

TTC powder was dissolved in sterile distilled water at an initial stock concentration

of 5 mg mL^{-1} or 15 mM at room temperature, then filtered through 0.22 μm filter paper and stored at −20°C until used (Moussa et al., 2013; Shofiul Azam et al., 2015). To determine the optimal TTC concentration for mutagenesis, the MA2-2 spore suspension was inoculated on PDA plates supplemented with various TTC concentrations (0, 0.15, 0.3, 1.5, 3 mM), followed by incubation at 25 °C for 2-3 days (Moussa et al., 2013). The proper concentration of TTC was also identified through the observation of growth status of the colonies (Yao et al., 2019). Single colonies with a deep color were selected as preferable ARA producers for further study (Li et al., 2015).

4.5.2.4 Mutagenesis Characterization – FA Inhibitor Cerulenin Screening

Cerulenin was dissolved in sterile distilled water at an initial stock concentration of 0.05 mg mL^{-1} or 0.224 mM at room temperature, then filtered through 0.22 μm filter paper and stored at −20°C until used. MA2-2 spore-suspension (10^8 spores mL^{-1}) was inoculated on PDA plates supplemented with various cerulenin concentrations (0, 0.1, 0.6, 1 and 4.5 μM), then incubated at 25 °C for 2-3 days (Yao et al., 2019). The growth status of colonies was monitored to achieve the proper concentration of cerulenin for preliminary screening and selection by estimating the mortality rate, shown in Eq. 8 (Li et al., 2015).

$$\text{Lethality rate } \% = \frac{\text{control colonies} - \text{survival colonies}}{\text{control colonies}} \times 100\% \quad (8)$$

4.5.2.5 UV Mutagenesis Supplemented with Cerulenin and TTC

After determining the optimal energy intensity of the UV mutagen, and the optimal concentrations of cerulenin and TTC. Wild-type MA2-2 spore suspensions were exposed to selected UV light for mutagenesis and mutated spores were grown on PDA agar plate medium supplemented with cerulenin and TTC for 2-3 days at 25°C (Li et al., 2015). The growth status of the colonies was monitored for mutant screening.

Relatively large, fast-growing colonies that were stained red were identified and selected as having high potential for FA production, particularly ARA. Selected mutants were isolated onto new PDA agar plates for long-term storage. Subsequently, all isolates were inoculated into modified fermentation medium (Section 4.5.1) with mycelium-agar pieces (described in Section 4.2) to verify the fatty acid profile. The stability of four or five mutant isolates screened from the above flask experiments was tested by repeating the experiment in triplicate. The mutants with the least variation showed consistency (Zhang et al., 2018).

4.6 Strain Improvement: High-Temperature ALE

Improving the thermotolerance of the strain can be advantageous in reducing energy consumption and production cost. The purpose of this high-temperature adaptive laboratory evolution strategy was to enhance the tolerance of strain in high temperature environment.

4.6.1 Culture Conditions

To prepare the seed culture, the wild-type MA2-2 strain was initially grown under the general culture conditions described in section 4.2. For long-term passage at high temperature ALE, seed cultures were inoculated with a 10% (v/v) mycelial suspension into 125 mL baffle flasks containing 30 mL of medium at the high temperature under constant orbital shaking at 200 rpm. Each 10% (v/v) of the mycelial suspension was passaged into a new medium, described as a new generation (Hu et al., 2021). The working medium for the whole ALE experiments was the C: N screened modified medium obtained from the section 4.4.2, containing glucose 41.25 g L^{-1}, yeast extract 11 g L^{-1}, KH_2PO_4 5.023 g L^{-1}, $MgSO_4.7H_20$ 0.796 g L^{-1}, $CaCl_2.2H_20$ 0.318 g L^{-1}, adjusted initial pH to 6 using 1 M NaOH or HCl, prior to autoclaving at 121℃. $MgSO_4.7H_20$ and $CaCl_2.2H_20$ were added post-

autoclave to prevent precipitation.

When the long-term ALE generation was completed, the MA2-2 final modified medium was also used to compare ARA performance with evolved strains cultured in ALE working medium. The final modified media, containing glucose 41.25 g L^{-1}, yeast extract 7 g L^{-1}, $NaNO_3$ 2.429 g L^{-1}, KH_2PO4 5.023 g L^{-1}, $MgSO_4.7H_20$ 0.796 g L^{-1}, $CaCl_2.2H_20$ 0.318 g L^{-1}, adjusted initial pH to 6 using 1 M NaOH or HCl, prior to autoclaving at 121°C. $MgSO_4.7H_20$ and $CaCl_2.2H_20$ were added post-autoclave to prevent precipitation.

4.6.2 Schematic Review of Adaptative Laboratory Evolution

An overview of the ALE experimental approach is shown in Figure 4.4.

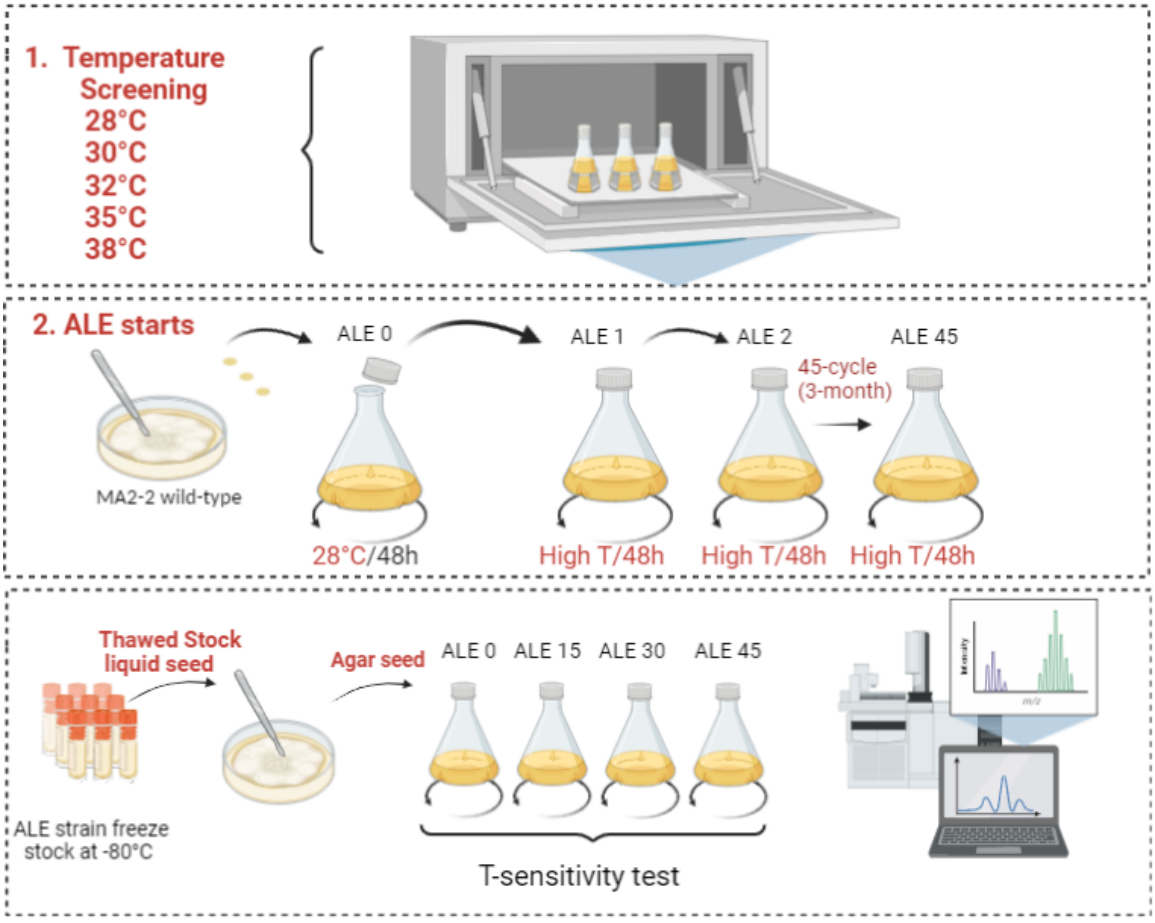

Figure 4.4: High-temperature adaption laboratory evolution schematic review. Drawn with Biorender.ca

4.6.2.1 Temperature Pre-screening

The effect of various temperatures (28℃ (control), 30℃, 32℃, 35℃, 38℃) on the growth of *M. alpina* MA2-2 were investigated by comparing daily glucose consumption and biomass DCW. The fatty acid profiles of the surviving strains were further studied to investigate their PUFA synthesis capacity. A suitable high stress temperature was chosen for the ALE study, where cells exhibited severe inhibition but were still able to survive.

4.6.2.2 ALE Adaption Cycles

An adaptive laboratory evolution experiment was based on a long-term serial transfer procedure at a high temperature of 32.5℃ as the stress inducer. Cells were cultivated in the seed medium for 48 h which was defined as one cycle. The high-temperature ALE experiment was repeated for a total three-month period (90 days). After 5 cycle periods, the evolved ALE strains were named ALE5, ALE10, until ALE45 was treated as the endpoint strain. The evolved strains after every five cycles were stored frozen in 10% glycerol at −80℃. High-temperature ALE experiments were performed in triplicate.

4.6.2.3 Temperature Sensitivity Test After Adaption

A temperature sensitivity test was performed to compare the temperature sensitivity of the starting strain and evolved strains, where the strains were cultivated in the C: N screened modified medium (section 4.6.1) at 28℃ (control) and 32.5℃ (stress). After partial thawing of the frozen strain, a loop of mycelium was placed on a PDA agar plate for recovery and growth for approximately 10 days. The culture was inoculated by adding pieces of mycelia covered agar in the C: N screened modified medium (section 4.6.1). Cell growth, lipid accumulation, fatty acid profile were determined to calculate parameters to assess temperature sensitivity. The reduction ratio was used to determine the effects on cell performance. The reduction ratio was calculated using Eq. 9:

$$\Delta(T_1 \sim T_2) = \frac{X_2 - X_1}{X_1} \quad (9)$$

where X_1 and X_2 refer to cell performance, including biomass DCW (g L^{-1}), total oil%, ARA%, ARA concentration (mg L^{-1}) and ARA productivity (g $L^{-1}d^{-1}$) at temperature T_1 (control temperature at 28℃) and T_2 (high temperature at 32.5℃), respectively.

4.6.2.4 Comparison of cell performance between modified medium and ALE medium

To investigate whether the adapted strain increased ARA production in the previous modified medium, the starting strain and the evolved strain every 15 cycles were cultured in modified and ALE fermentation medium (control) at 28°C. Response variables including biomass DCW (g L^{-1}), total oil%, ARA%, ARA concentration (mg L^{-1}) were compared.

4.7 Biomass Harvest and Fatty Acid Methyl Esters Analysis

The fungal biomass was harvested at the glucose exhaustion or end of 14 days of incubation. Daily glucose depletion was monitored using the YSI 2500 Glucose/Lactate Analyzer. The 300 µL of the supernatant was taken for a glucose-level reading with the YSI, and the remaining supernatant was decanted. All fungal biomass was harvested by centrifugation (Eppendorf 5920 R centrifuge: catalogue number 2231010061) at 4,200 rpm for 20 minutes at 4°C. The biomass was washed two times with deionized water and vortexed for 10 seconds until all mycelia were harvested. The tubes were then centrifuged a third time and the supernatant was again discarded. The fresh cells were then stored at -80°C freezer for overnight, then moved to a Labconco freeze-dryer (catalogue number 7755040) for 3 days. The freeze-dried biomass was weighed to obtain the dry cell weight by subtracting the tube weight. Then biomass was crushed finely with a mortar and pestle and stored in capped tubes at -20°C until analysis was carried out.

For analysis, the fatty acids were extracted from the biomass and trans-esterified into fatty acid methyl esters (FAMEs) and then analyzed through gas chromatography (GC)

combined with Flame ionization detector (FID). A 2 mg/mL solution of tritricosanoin (C23:0 triglyceride) was prepared in toluene and sonicated until the lipid was completely dissolved. The weights of both the C23:0 and toluene were recorded as the internal standard solution. For each biomass sample, 45-48 mg of biomass was added in 40 mL glass tube. Then 950 µL of the C23:0 internal standard solution was added to each tube and the mass was recorded in grams. Next, 6 mL of toluene and 6 mL of 12.5% acetyl chloride in methanol solution were added to each tube and which was placed in a hot water bath for 2 hours at 80°C and 60 rpm. Then 10 mL of 6% sodium carbonate solution was added to each tube once cool. The tubes were then vortexed until homogenous and centrifuged for 15 minutes at 1100 rpm and 4°C. The toluene layer was carefully transferred to a 2 mL GC vial for analysis. FAMEs samples were analyzed by GLC-FID using the following GLC operating parameters:

- FID and injector temperature of 250°C
- Carrier flow of 3 mL/min Hydrogen
- Split ratio of 20:1
- Make-up flow of 38.2 mL/min Helium
- Oven temperature of 190°C at 5°C per minute to 240°C and held for 2 minutes

The column used was Restek FAMEwax catalogue number 12498 (30 m x 0.32 mm x 0.25 µm). GLC Reference Standard 566b (Nu-Chek Prep Inc. catalogue number GLC-566B) was run at the beginning of the sequence to determine retention times of FAMEs and GLC Reference Standard 714 (Nu-Chek Prep Inc. catalogue number AC-714) ran at the beginning and end of the sequence to act as an external response factor for selecting fatty acids such as ARA, EPA or DHA. The methyl esters of fatty acids were manually integrated using OpenLab CDS.2x Agilent software, and the area of chromatogram peaks were calculated to determine the mg/g FAME.

Chapter 5: Results

5.1 Micronutrient Studies

In this section, combined DOE were applied for screening and optimizing micronutrients that may affect ARA performance. Subsection 5.1.1 applied the Plackett-Burman method to screen various micronutrients such as mineral ions, trace elements or vitamins, and to select the best performing components for further optimization. Subsection 5.1.2 and 5.1.3 used two Response Surface Methodology approaches to optimize different levels of preselected components and to predict the best solutions to enhance ARA production.

5.1.1 Plackett-Burman Screening of Micronutrients

Experiments were conducted following a PB design that was used to select the most significant factors. The data presented in Appendix B – Table B.2 indicated that there was a wide variation in responses for DCW, TFA %, ARA % and ARA concentration, from 3.61 to 14.87 g L^{-1}, 8.1 to 17.15 %, 19.58 to 31.31 %, and 62 to 760 mg L^{-1}, respectively.

The coefficient values from the regression analysis for the PB design revealed the main effects, associated t-values and significant levels of the variables on biomass DCW (g L^{-1}), TFA %, ARA % and ARA yield (mg L^{-1}) (Table 5.1). The positive/negative effects of the measured variables indicated that the yield of ARA was greater/smaller at higher levels of the measured variables than at lower levels (Ghobadi et al., 2022).

Out of the eight variables shown in the Pareto chart with positive and negative effects (Figure 5.1), KH_2PO_4 and $CaCl_2.2H_20$ positively affected DCW, ARA concentration and ARA % ($p \leq 0.01$) and TFA % ($p \leq 0.05$). This indicated that both variables significantly affected all responses and were therefore selected for further optimization. The positive effect that $MgSO_4.7H_20$ had on DCW ($p \leq 0.05$) was greater at high concentration. By contrast, sodium citrate and NaCl negatively affected TFA% ($p \leq 0.05$),

and NaCl, TMS and vitamin solution negatively affected ARA concentration ($p \leq 0.05$) at low concentrations. Factors such as NaCl, TMS and vitamin solution negatively affected all responses, whether significantly or not, and they were not optimal for improving ARA production. Sodium citrate positively affected DCW and ARA %, and negatively affected TFA % and ARA concentration, whereas $MgSO_4.7H_20$ positively affected all responses, except ARA%. This indicated that sodium citrate had a more negative effect on multiple responses than $MgSO_4.7H_20$. Therefore, the factor of $MgSO_4.7H_20$ concentration was selected for further optimization.

Table 5.1: ANOVA test of MA2-2 strains from PB design

Term	Biomass DCW (g L^{-1})			TFA %			ARA %			ARA (mg L^{-1})		
	Effect	t value	p value	Effect	t value	p value	Effect	t value	p value	Effect	t value	p value
Constant		25.9	0		35.05	0		40.29	0		22.66	0
KH_2PO_4	3.171	3.49	**0.003***	2.094	2.62	**0.019**	1.571	1.38	0.188	178.4	5.1	**0***
NaCl	-1.366	-1.5	0.153	-2.144	-2.69	**0.017**	-1.013	-0.89	0.388	-99.5	-2.85	**0.012**
$MgSO_4.7H_20$	2.002	2.21	**0.043**	0.403	0.5	0.621	-0.239	-0.21	0.836	60.2	1.72	0.105
$CaCl_2.2H_20$	3.634	4	**0.001***	0.821	1.03	0.32	3.923	3.45	**0.004***	197.7	5.65	**0***
$MgCl_2.6H_20$	0.836	0.92	0.372	-1.121	-1.4	0.181	-1.429	-1.26	0.228	-47.2	-1.35	0.197
Sodium Citrate	0.334	0.37	0.718	-1.982	-2.48	**0.025**	0.174	0.15	0.88	-9.8	-0.28	0.782
TMS	-0.249	-0.27	0.787	-1.639	-2.05	0.058	-2.149	-1.89	0.078	-77	-2.2	**0.044**
Vitamin Solution	-0.692	-0.76	0.457	-1.294	-1.62	0.126	-1.654	-1.45	0.167	-85	-2.43	**0.028**

The bold values indicate the significance at or above the 95.0 % confidence level ($p \leq 0.05$). The bold values with * indicate the significance at or above the 99.0 % confidence level ($p \leq 0.01$).

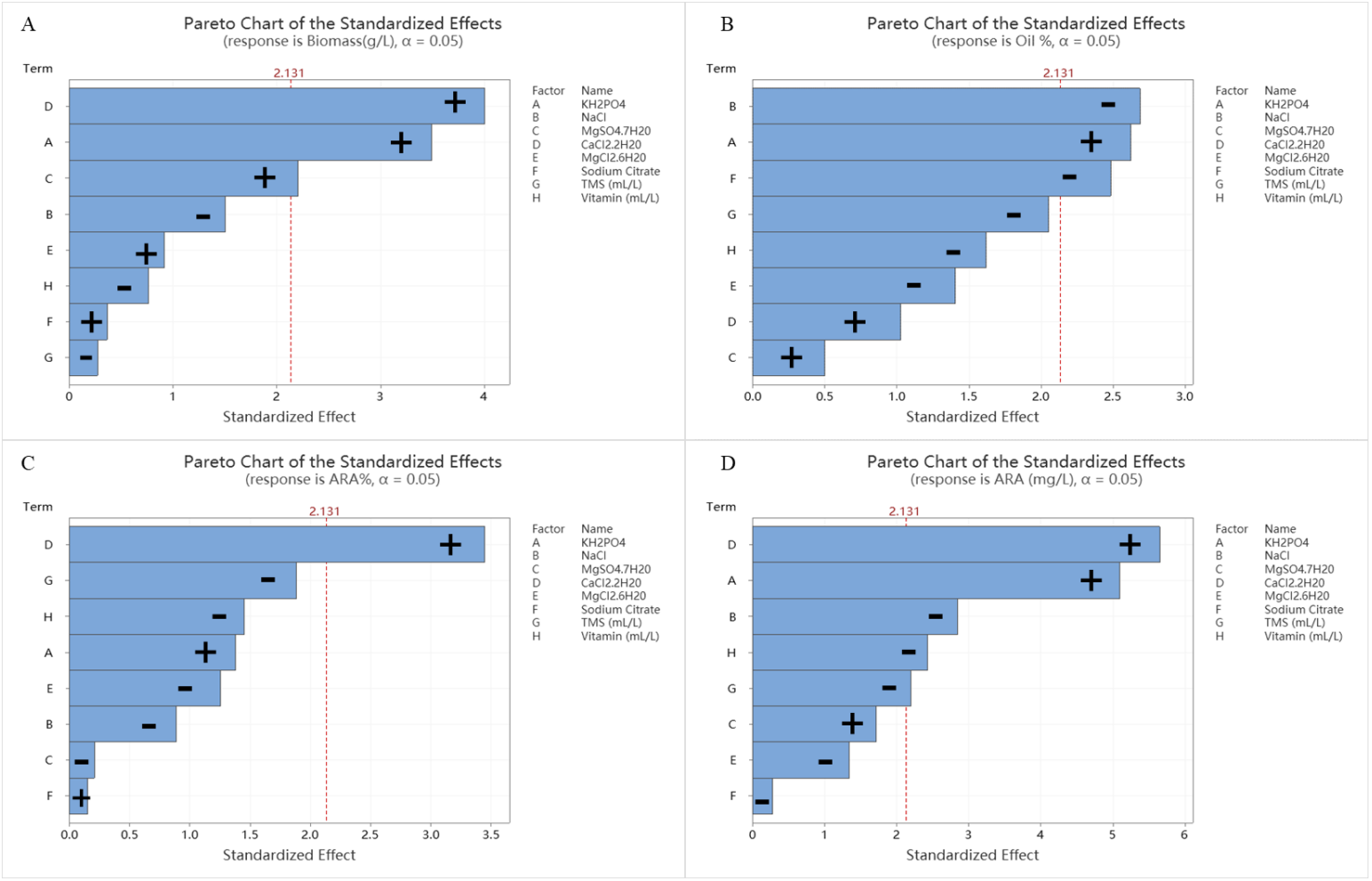

Figure 5.1: Pareto chart showing the positive and negative effects of eight micronutrients (A-H) on responses A) biomass DCW (g L^{-1}), B) TFA %, C) ARA % and D) ARA yield (mg L^{-1}). Bars that cross the dotted red line indicate that the effect is statistically significant (at a 95% level of confidence). The +/- symbols next to each factor row refer to positive or negative effects.

5.1.2 First RSM Optimization on KH_2PO_4, $MgSO_4.7H_20$ and $CaCl_2.2H_20$

5.1.2.1 Experimental Results of the First RSM

Based on the PB screening tests, KH_2PO_4, $MgSO_4.7H_20$ and $CaCl_2.2H_20$ had high impact on biomass, lipid accumulation and ARA production by *M. alpina* MA2-2 strain. The optimum levels of these three significant parameters were determined by CCD and RSM, and their low/high levels are shown in Table 4.2. The observed responses are summarized in Appendix B - Table B.3, and analysis of the results by standard ANOVA are shown in Table 5.2. The maximum responses of DCW, TFA%, ARA%, and ARA yield were 17.3 ± 0.02 g L^{-1}, 18.3 ± 0.22%, 37.2 ± 1.60% and 781 ± 62.2 mg L^{-1} respectively.

5.1.2.2 Diagnostic Checking of the Models

The ANOVA of the quadratic regression models indicated, that with the exception of ARA concentration, there was a significant relationship between the dependent and independent variables ($p < 0.05$) (Table 5.2). Thus, the full quadratic model with $CaCl_2.2H_20$, KH_2PO_4, and $MgSO_4.7H_20$ (as independent variables) significantly affected the responses DCW, oil% or TFA% and ARA% (dependent variable). The ANOVA of the quadratic regression model for ARA concentration indicated the F value was 1.8, which confirmed the lack of significance of the experimental data to this response. Second-order polynomial models from the ANOVA results are given as follows, with respect to growth (Eq. 10), total oil (Eq. 11) and the percentage (Eq. 12) of ARA in the term of significance ($p < 0.05$):

$$Y_{DCW}(g\,L^{-1}) = 12.521 + 0.697\ KH_2PO_4 - 1.208\ CaCl_2.2H_20^2 \quad (10)$$

$$Y_{Oil}(\%) = 18.470 - 0.03\ KH_2PO_4 - 3.634\ CaCl_2.2H_20 + 0.0969\ KH_2PO_4 \times MgSO_4.7H_20 + 0.412\ MgSO_4.7H_20 \times CaCl_2.2H_20 \quad (11)$$

$$Y_{ARA}(\%) = 28.32 - 2.493\ KH_2PO_4 + 0.993\ MgSO_4.7H_20 - 2.76\ CaCl_2.2H_20 + 0.2132\ KH_2PO_4{}^2 \quad (12)$$

5.1.2.3 Determination of Lack of Fit and/or Outlier

The ANOVA table for the oil % and ARA % regression models in this study show an insignificant lack-of-fit (F=0.79 and 4.25; P=0.599 and 0.069) for the models (Table 5.2), which suggest these models are suitable for explaining the data. However, the biomass regression model indicated a significant lack-of-fit (p = 0.00). Although the biomass regression model was significant, the data corresponding to the center points had small variation so that they became close enough to overlap and this triggered the significant lack-of-fit (Kraber, 2022). A potential solution would be to increase the level of factor selection to expand the variation between model points and centroids, reducing overfitting.

5.1.2.4 Plot Analysis (Normality Probability Plot, Residual vs. Fit)

In addition to ANOVA, normal probability plots (Appendix A) are an important visualization method for conducting regression model analysis. The normality plot of the response to ARA% closely aggregated to follow a straight line (Figure A.1 E). The biomass and Oil% represented an approximate straight but with small variations in the scatter (Figure A.1 A and C). The results showed that all three responses formed a normal distribution, but small variations indicated that the prediction terms did not match the experimental results exactly, which was consistent with the previous ANOVA analysis.

Plots of the residuals vs. fitted values are shown in Figure A.1. Compared to biomass and ARA%, Oil% shown a random scatter without an obvious pattern (Figure A.1 D), indicating the residuals were considered independent with normally distributed (Ahmed, N.d.; Olawoye, 2016; ISixSigma, 2022). The plot for biomass showed a few clusters of residuals, which may imply dependence (Figure A.1 B). ARA% showed more clusters of residuals, while the distribution of residuals over the fitted values of x was not homogeneous, indicating dependence and non-constant variance (Figure A.1 F). According to the normal plot, oil % represented the better regression hypothesis, followed by ARA % and biomass, in agreement with the results of the ANOVA regression model.

Table 5.2: Analysis of variance (ANOVA) for response surface quadratic model of biomass DCW, oil%, ARA% and ARA concentration by RSM.

Term	DF[f]	Biomass DCW (g L^{-1}) [b]				Oil % [c]				ARA % [d]				ARA (mg L^{-1}) [e]			
		SS [g]	MS [h]	F- value	p value	SS	MS	F- value	p value	SS	MS	F value	p value	SS	MS	F value	p value
Model	9	36.40	4.04	3.48	**0.032**	38.3	4.3	6.12	**0.005**	286.5	31.8	5.98	**0.005**	107112	11901	1.8	0.186
X_1 [a]	1	18.33	18.33	15.79	**0.003**	7.5	7.5	10.75	**0.008**	93.7	93.7	17.6	**0.002**	6112	6112	0.93	0.359
X_2	1	0.00	0.00	0	0.997	3.1	3.1	4.4	0.062	41.3	41.3	7.76	**0.019**	4264	4264	0.65	0.44
X_3	1	5.20	5.20	4.48	0.06	14.7	14.7	21.13	**0.001**	59.0	59.0	11.07	**0.008**	12123	12123	1.84	0.205
$X_1 \times X_2$	1	0.01	0.01	0.01	0.935	4.7	4.7	6.69	**0.027**	2.9	2.9	0.54	0.477	5555	5556	0.84	0.38
$X_1 \times X_3$	1	0.49	0.49	0.42	0.531	0.2	0.2	0.29	0.603	2.6	2.6	0.49	0.5	11096	11096	1.68	0.224
$X_2 \times X_3$	1	0.16	0.16	0.13	0.721	6.5	6.5	9.39	**0.012**	21.9	21.9	4.11	0.07	46663	46663	7.07	**0.024**
X_1^2	1	3.47	3.47	2.99	0.114	0.1	0.1	0.08	0.781	64.7	64.7	12.15	**0.006**	8177	8177	1.24	0.292
X_2^2	1	0.11	0.11	0.1	0.76	0.6	0.6	0.92	0.36	3.3	3.3	0.61	0.452	9793	9793	1.48	0.251
X_3^2	1	11.97	11.97	10.31	**0.009**	2.4	2.4	3.51	0.091	11.4	11.4	2.14	0.175	4	4	0	0.981
Error	10	11.61	1.16			7.0	0.7			53.3	5.3			65990	6599		
Lack-of-fit	5	11.41	2.28	57.49	**0**	3.1	0.6	0.79	0.599	43.1	8.6	4.25	0.069	49148	9830	2.92	0.132
Pure Error	5	0.20	0.04			3.9	0.8			10.1	2.0			16842	3368		
Total	19	48.00				45.3				339.8				173101			

The bold values indicate the significance at or above the 95.0% confidence level [f] DF degree of freedom [g] SE sum of square [h] MS mean of square

[a] $X_1 = KH_2PO_4$ (g L^{-1}); $X_2 = MgSO_4.7H_20$ (g L^{-1}); $X_3 = CaCl_2.2H_20$ (g L^{-1})

[b] Biomass DCW production (g L^{-1}) note: $R^2 = 0.7582$; Adj. $R^2 = 0.5406$; Pred. $R^2 = 0$

[c] Oil content (%) note: $R^2 = 0.8463$; Adj. $R^2 = 0.7079$; Pred. $R^2 = 0.4261$

[d] ARA content (%) note: $R^2 = 0.8433$; Adj. $R^2 = 0.7022$; Pred. $R^2 = 0.027$

[e] ARA production (mg L^{-1}) note: $R^2 = 0.6188$; Adj. $R^2 = 0.2757$; Pred. $R^2 = 0$

5.1.2.5 Evaluation of Significance Factors

The significance of each coefficient in Table 5.2 was determined by its p-value. According to the present model of the biomass, the linear term (X_1 or KH_2PO_4) and squared term (X_3^2 or $CaCl_2.2H_20^{\ 2}$) were significant. For oil%, linear terms (X_1 and X_3 or KH_2PO_4 and $CaCl_2.2H_20$), interaction terms ($X_1.X_2$ and $X_2.X_3$ or $KH_2PO_4 \times MgSO_4.7H_20$ and $MgSO_4.7H_20 \times CaCl_2.2H_20$) were significant. For ARA%, linear terms (X_1, X_2 and X_3 or KH_2PO_4, $MgSO_4.7H_20$ and $CaCl_2.2H_20$) and squared term (X_1^2 or $KH_2PO_4^{\ 2}$) were significant. Except for oil% which had two significant interaction terms, responses to biomass and ARA% were only significantly affected by a single term or squared term.

Previous screening methods were performed in a PB design where interaction terms were confounded and not considered. Here, from the RSM design, the data showed insignificant effects of other factors on cross-interactions except for oil %. This may be due to the fact that the mineral interactions were minimal at high concentrations or that the current quadratic model was unable to detect significant terms.

5.1.2.6 Main Effect Analysis

Figure 5.2 to 5.4 show the main effect plots. In terms of biomass, the main effect plots for KH_2PO_4 and $CaCl_2.2H_20$ showed similarities, where biomass increased with increasing concentrations of KH_2PO_4 and $CaCl_2.2H_20$ until they peaked at 7.5 g L^{-1} and 1.4 g L^{-1}, respectively, and then biomass decreased to the end (Figure 5.2).

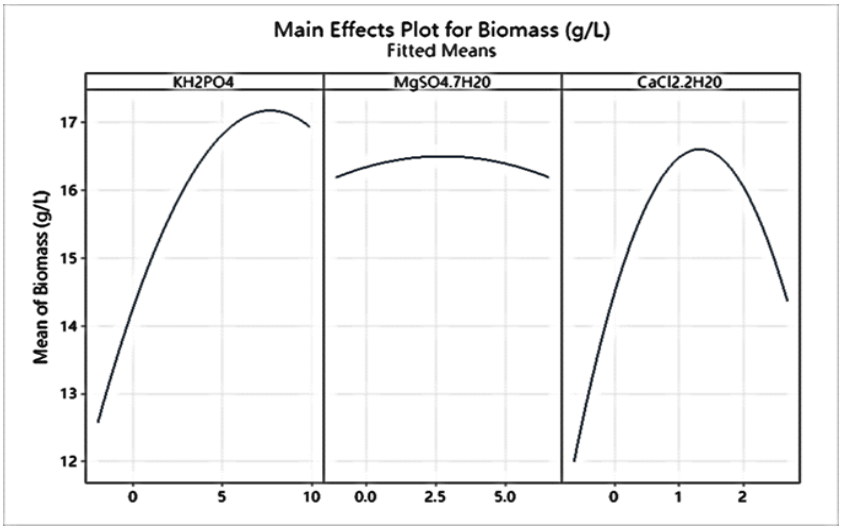

Figure 5.2: Main effects plots of significant minerals KH_2PO_4, $MgSO_4.7H_20$ and $CaCl_2.2H_20$ for response variables: Biomass DCW (g L^{-1}).

However, the changes of KH_2PO_4 and $CaCl_2.2H_20$ were opposite in terms of oil %, which increased when KH_2PO_4 increased linearly from 0 to 9.886 g L^{-1}, while it decreased when $CaCl_2.2H_20$ gradually increased (Figure 5.3).

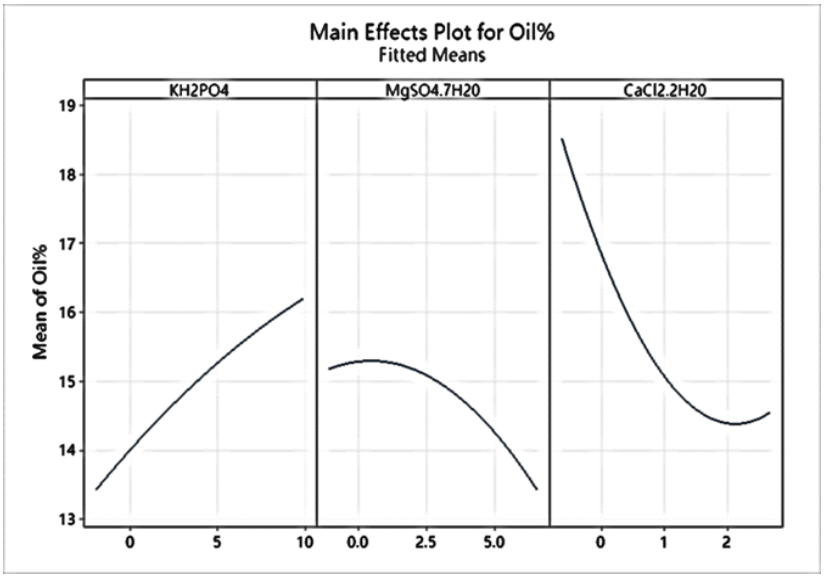

Figure 5.3: Main effects plots of significant minerals KH_2PO_4, $MgSO_4.7H_20$ and $CaCl_2.2H_20$ for response variables: Total oil content w/w%.

In terms of the contribution of ARA, all three factors were significantly affected. The variation of KH_2PO_4 was opposite to $CaCl_2.2H_20$ and $MgSO_4.7H_20$, in which the ARA%

decreased from 36% to 23% when KH_2PO_4 was decreased until the lowest peak at 5 g L^{-1}, and then it gradually increased. Meanwhile, increasing the concentration of $CaCl_2.2H_20$ and $MgSO_4.7H_20$, resulted in ARA% increasing from 20% to 31% (Figure 5.4).

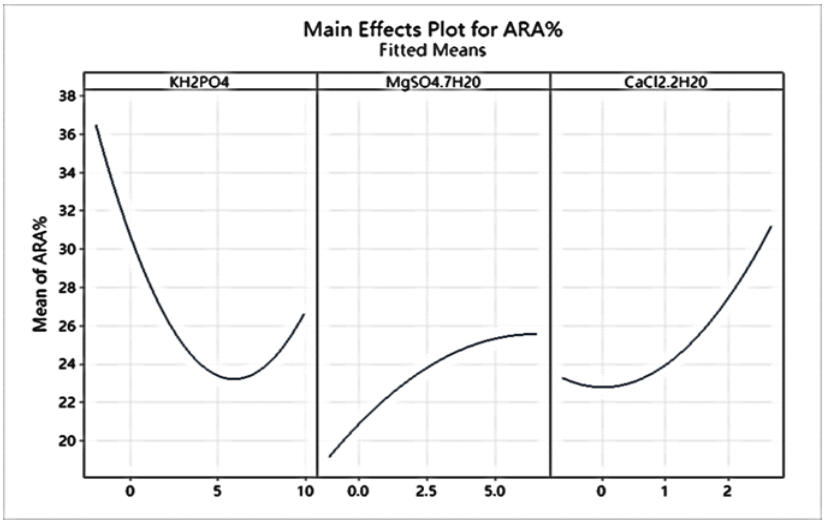

Figure 5.4: Main effects plots of significant minerals KH_2PO_4, $MgSO_4.7H_20$ and $CaCl_2.2H_20$ for response variables: ARA w/w%.

In terms of the significance of the main effect, all three responses were significantly affected by KH_2PO_4 and $CaCl_2.2H_20$. The biomass and oil rate % were increased at higher KH_2PO_4 concentration, whereas a lower KH_2PO_4 was favorable for ARA%. $CaCl_2.2H_20$ showed a sinusoidal wave with a maximum peak of 1.4 g L^{-1}, reaching 16.5 g L^{-1} biomass. In addition, increasing $CaCl_2.2H_20$ was beneficial for ARA%, but decreasing $CaCl_2.2H_20$ resulted in higher oil rates. $MgSO_4.7H_20$ only affected ARA%, where a higher concentration led to a higher ARA %.

5.1.2.7 Response Surface Plotting

Response surface and contour plots provide an understanding of the interaction of two factors while keeping the other factors constant at the level of the centroid (Myers et al., 2009; Yang et al., 2006). From previous ANOVA analysis, only interaction terms KH_2PO_4 × $MgSO_4.7H_20$ and $CaCl_2.2H_20$ × $MgSO_4.7H_20$ were significant to the response

of oil% while others were insignificant (Table 5.2). In this study, only significant interaction terms were analyzed in contour plots to determine the optimal level.

Figure 5.5 A & B shows the contour and surface plot of $CaCl_2.2H_20 \times MgSO_4.7H_20$ on the oil %, with KH_2PO_4 fixed at its central level (4.0 g L^{-1}). This contour plot revealed a hyperbolic shape, which demonstrated a saddle point that was a flexion point between a relative minimum and relative maximum, which was neither a maximum nor a minimum point (Breig & Luti, 2021). As $MgSO_4.7H_20$ and $CaCl_2.2H_20$ decreased from 5.0 to 0.0 g L^{-1} and 1.2 to 0.0 g L^{-1}, respectively, the oil rate increased from 15 to more than 18%. The oil rate may also reach 15-16% when $MgSO_4.7H_20$ and $CaCl_2.2H_20$ attained their highest edge points. This surface plot showed a sharp slope which corresponds to a higher response activity. The maximum oil rate can be achieved by reducing $CaCl_2.2H_20$ and $MgSO_4.7H_20$ to below 0.2 g L^{-1} and 0.5 g L^{-1}, respectively; or by increasing both factors to the highest edge of the out-of-range point.

Figure 5.5 C & D shows the contour and surface plot of $KH_2PO_4 \times MgSO_4.7H_20$ for the oil %, with $CaCl_2.2H_20$ fixed at its central level (1.025 g L^{-1}). When KH_2PO_4 increased while $MgSO_4.7H_20$ was maintained at a low level (approximately from 0 to 0.7 g L^{-1}), the oil % did not change significantly (remained at 15-16%). With the increase of $MgSO_4.7H_20$, and KH_2PO_4 kept below 5 g L^{-1}, oil accumulation would gradually be inhibited thus reducing oil%. The maximum oil % can be expected to exceed 16% when KH_2PO_4 and $MgSO_4.7H_20$ are higher than 7 g L^{-1} and 2 g L^{-1}, respectively. In general, the surface plot of oil % with $KH_2PO_4 \times MgSO_4.7H_20$ displayed a gentle slope that lowered the response sensitivity level. However, this surface plot had a maximum design point that was outside the area of experimentation. Consequently, the highest oil% (above 16 %) could be expected if KH_2PO_4 and $MgSO_4.7H_20$ were increased to the highest edge point that out of the scope. Optimal oil % could also be achieved if KH_2PO_4 was increased but $MgSO_4.7H_20$ was kept low. The interaction between $CaCl_2.2H_20 \times MgSO_4.7H_20$ was

stronger than KH_2PO_4 × $MgSO_4.7H_20$, which implied that $CaCl_2.2H_20$ × $MgSO_4.7H_20$ performed better prediction on the oil%.

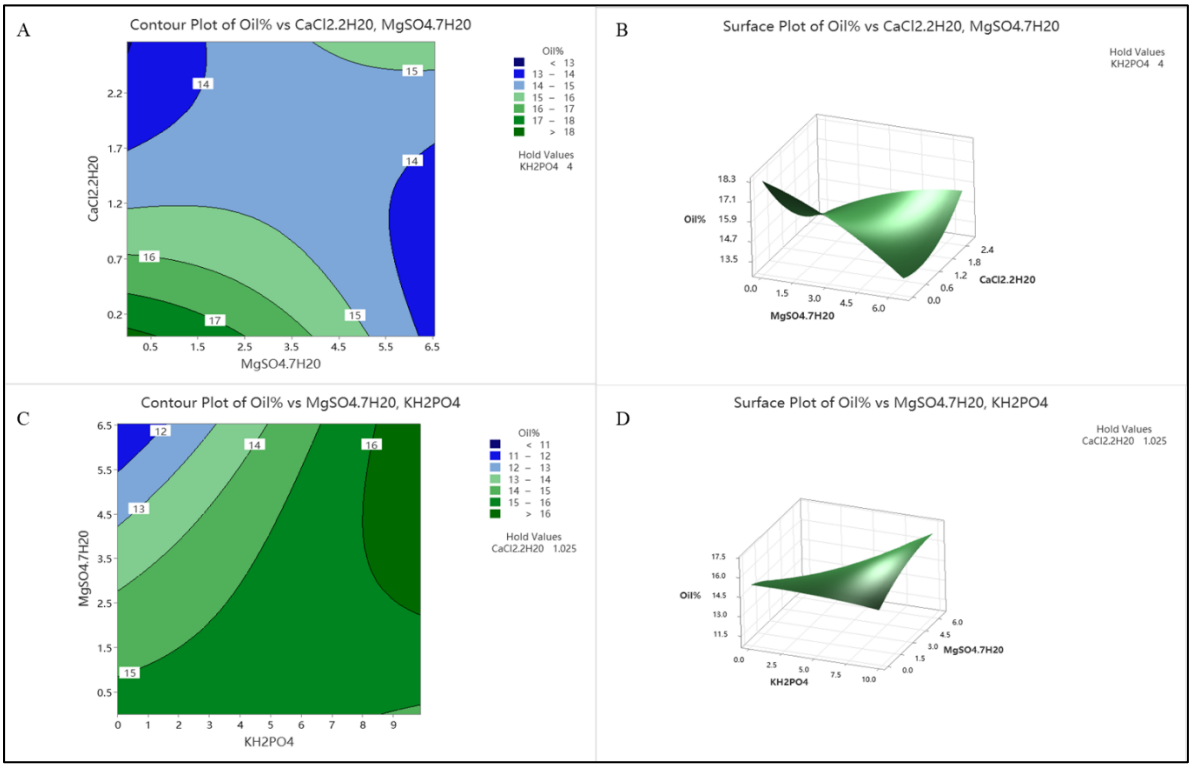

Figure 5.5: Two-dimension contour plots (A and C) and three-dimensional response surface plots (B and D) for total oil w/w% production by *M. alpina* MA2-2 showing interaction of two variables while the remaining factors were held constant: (A and B) contour and surface plots of $CaCl_2.2H_20$ × $MgSO_4.7H_20$; (C and D) contour and surface plots of KH_2PO_4 × $MgSO_4.7H_20$

5.1.2.8 Experimental Validation of the Optimized Culture Variables

Correlation coefficient R^2 was the proportion of change in the response values explained or accounted for by the model. The R^2 value must be close to 1.0 in a model which describes good prediction efficiency (Breig & Luti, 2021) and a higher value of R^2 indicates a better fit to the model (Nisha et al., 2011; Ekpenyong et al., 2017; Choudhary & Pramanik, 2021).The R^2 values for DCW, oil% and ARA% were 0.7582, 0.8463 and 0.8433 (Table 5.2). The biomass DCW response was less predicted than oil% and ARA%

since R^2 is the proportion of change in the response values explained or accounted for by the model. The results showed that oil% had a relatively higher recovery rate with a decent prediction compared to ARA%, and that biomass was the least predictable response.

To evaluate the model acquired by the RSM, an experiment was conducted in triplicate under the identified conditions (Ghobadi et al., 2022). The information from the equation models and plots, relating to the optimal levels of KH_2PO_4, $MgSO_4.7H_20$ and $CaCl_2.2H_20$ predicted two optimal solutions. Experiment A referred to the maximum of all responses, including biomass DCW, TFA% or Oil%, ARA% and ARA concentration; while experiment B referred to the maximum of ARA production, summarized in Table 5.3. The experimental values thus obtained were compared with the predicted values to test the applicability of the model equation for validating the optimum response values (Nisha et al., 2011). For experiment A, the deviations between the experimental and predicted values for the production of biomass, TFA %, ARA % and ARA concentration were 5.91%, 18.03%, 16.93% and 32.2%, respectively, while experiment B resulted in deviations of 11.4%, 21.4%, 3.94% and 13.6%, respectively. The deviation of experiment A was closer to the predicted value of R^2, while B is more divergent from the predicted value.

Among the multi-responses, the variation of ARA concentration was the highest, followed by oil% and ARA%, with biomass having the least variation. However, the concentration of ARA was largely dependent on the production of the remaining three effects, and therefore fluctuations in these effects can vary the concentration of ARA. Both experiments had relatively lower validity (68-96%) of the prediction models.

Almost all responses were predicted to be optimal in the edge (α) points, but this was outside the range of the model, which could lead to biased results because the model cannot accurately predict responses outside the range. The α range may represent some higher-order models, so low predictability was to be expected. The potential solution was to explore how higher levels of factors within the α ranges affected production performance of ARA. To investigate this, a second RSM design was established, where factors were

adjusted to the new levels (Section 5.1.3).

Table 5.3: Predicted and experimental value of responses at optimum condition

Exp. (g L^{-1})	KH_2PO_4[a]	$MgSO_4.7H_20$	$CaCl_2.2H_20$	Biomass [b]	Oil %	ARA%	ARA
A	9.886	6.534	2.296	15.21 ± 0.41 [c]	15.3 ± 0.38	30.86 ± 2.52	715.3 ± 26.43
				16.17 [d]	18.67	37.15	1054.5
B	3.060	6.534	2.665	15.63 ± 0.09	11.7 ± 0.96	36.81 ± 1.62	674.6 ± 35.81
				14.03	14.88	38.32	780.9

- A and B, experiments based on maximum all responses and maximum ARA production conditions, respectively.
- Basal medium: Glucose and Yeast Extract maintained at 20 g L^{-1} and 11 g L^{-1}.

[a] All factors were added in units of g L^{-1}.

[b] Represents mean of the responses for biomass DCW production (g L^{-1}), Oil content (%), ARA content (%) and ARA production (mg L^{-1}), based on triplicate experiments.

[c] Experimental results in Mean ± Standard Deviation (SD), n = 3.

[d] Theoretical solution for the optimal condition under each experimental result

5.1.3 Second RSM Optimization on KH_2PO_4, $MgSO_4.7H_20$ and $CaCl_2.2H_20$

Based on the first RSM analysis, the response surface contour plot indicated that there were additional points that should have been included in the model due to the behaviour at the edge points. This may have affected agreement of the predicted and experimental data. To improve the model, a second RSM experiment was designed so that the high and low levels of the factors were adjusted to include the edge points of the previous RSM.

5.1.3.1 Experimental Results of the Second RSM

The new levels for the factors included in the second RSM are shown in Table 5.4. The observed responses from CCD experiments were summarized in Appendix B – Table B.4, and the results were analyzed by standard ANOVA as shown in Table 5.5. The maximum responses of biomass, ARA%, Oil% and ARA yield were 16.6 ± 0.0 g L^{-1}, 31.21 ± 2.72%, 14.78 ± 0.6% and 642.2 ± 77.2 mg L^{-1}, respectively. Compared to the first RSM, the strain performance in respect to four responses was diminished. The central-level

performance in the second RSM was still lower than the first RSM. In addition, all responses in the second RSM were consistently low without any outliers except design #9 (Shown in Table B.4). A simple conclusion could be drawn that all responses were not significantly affected by different concentrations of three factors.

Table 5.4: Experimental variables at different levels used for the 2nd RSM approach.

Composition:	Unit	Coded Levels				
		$-\alpha$ (-1.683)	-1	0	+1	$+\alpha$ (+1.683)
KH_2PO_4	g L^{-1}	0	1	2.5	4	5.023
$MgSO_4.7H_20$	g L^{-1}	0.796	2.5	5	7.5	9.204
$CaCl_2.2H_20$	g L^{-1}	0.318	1	2	3	3.682

5.1.3.2 Diagnostic Checking of the Models Significance

The ANOVA of the quadratic regression models indicated, except for oil% and ARA concentration, that the residual models confirmed the insignificance of experimental data ($p > 0.05$) (Table 5.5). Therefore, the full quadratic model consisting of $CaCl_2.2H_20$, KH_2PO_4 and MgSO4.7H_20 (independent variables) had an insignificant effect on the biomass and ARA % responses (dependent variables). The ANOVA of the quadratic regression models for oil% and ARA concentration resulted in F values of 5.3, and 3.95, respectively, which confirm the experimental data are significant for both models ($p < 0.05$).

A second-order polynomial model, incorporating the different interactions according to the term significance ($p < 0.05$), was proposed with respect to total oil (Eq. 13) and the concentration (Eq. 14) of ARA.

$$Y_{Oil}(\%) = 15.72 + 0.016\ KH_2PO_4 - 3.231\ CaCl_2.2H_20 + 0.801\ CaCl_2.2H_20^2 \quad (13)$$

$$Y_{ARA\ conc.}\ (mg\ L^{-1}) = 510 + 84.5\ KH_2PO_4 + 32.5\ CaCl_2.2H_20^2 \quad (14)$$

5.1.3.3 Determination of Lack of Fit and/or Outlier

The lack of fit error was non-significant ($p > 0.05$) for oil%, which indicates that the model did not fail to include data in the experimental domain (Nisha et al., 2011). However, ARA exhibited a significant lack of fit ($p < 0.05$) in the current model. One possible reason is that the ARA concentration from run no. 9 (Appendix B – Table B.4) is an outlier that biases the experimental data. An outlier may cause the variation in the design points to be greater than the replicate mean values, thus biasing the runs (Ahmed, N.d.). If this outlier is removed from the data, the lack-of-fit becomes insignificant (Appendix A – Figure A.2).

5.1.3.4 Plot analysis (Normality Probability Plot, Residual vs. Fit)

The normality plots are shown for the significant models, Oil% and ARA concentration (Appendix A – Figure A.3). The normality plot for ARA concentration showed the data points are closely aggregated and follow a straight line (Figure A.3 C) whereas the plot for Oil% represented an approximate straight line, but with variation in the scattered data points (Figure A.3 A). The results from the normality plots show that both responses formed a normal distribution, but small variations indicated the prediction terms did not perfectly match the experimental results, which was consistent with the ANOVA analysis.

In terms of residuals vs. fitted plots, oil% shown more clustering of residuals, along with an uneven distribution of residuals over the fitted values of x, indicating dependence and non-constant variance (Figure A.3 B); while ARA concentration indicated a more random scatter with no clear pattern compared to oil% (Figure A.3 D). However, both plots showed a few inflectional points that were far away from other points in the x-direction. Consequently, the prediction assumptions of the two models were not perfect due to the variability around the normality plot, which was consistent with the relatively low prediction regression from the ANOVA.

Table 5.5: ANOVA analysis for response surface quadratic model of biomass DCW, oil%, ARA% and ARA concentration by the second RSM.

Term	DF[f]	Biomass DCW (g L^{-1}) [b]				TFA % [c]				ARA % [d]				ARA (mg L^{-1}) [e]			
		SS [g]	MS [h]	F- value	p value	SS	MS	F- value	p value	SS	MS	F value	p value	SS	MS	F value	p value
Model	9	62.86	6.98	1.75	0.199	19.4	2.2	5.3	**0.008**	80.8	9.0	1.27	0.357	147627	16403	3.95	**0.022**
X_1 [a]	1	28.98	28.98	7.25	**0.023**	2.0	2.0	4.94	**0.05**	21.5	21.5	3.04	0.112	57846	57846	13.92	**0.004**
X_2	1	0.93	0.93	0.23	0.64	1.0	1.0	2.51	0.144	3.0	3.0	0.43	0.528	497	497	0.12	0.737
X_3	1	2.15	2.15	0.54	0.48	4.1	4.1	10.04	**0.01**	0.1	0.1	0.02	0.901	16281	16281	3.92	0.076
$X_1 \times X_2$	1	0.00	0.00	0	0.989	0.1	0.1	0.21	0.656	19.1	19.1	2.7	0.132	9131	9131	2.2	0.169
$X_1 \times X_3$	1	1.28	1.28	0.32	0.584	0.0	0.0	0.01	0.932	13.6	13.6	1.92	0.196	1904	1904	0.46	0.514
$X_2 \times X_3$	1	0.28	0.28	0.07	0.798	0.5	0.5	1.16	0.308	5.0	5.0	0.71	0.418	1285	1285	0.31	0.59
X_1^2	1	19.64	19.64	4.91	0.051	0.1	0.1	0.15	0.706	16.3	16.3	2.31	0.16	19713	19713	4.75	0.054
X_2^2	1	3.14	3.14	0.79	0.396	1.5	1.5	3.61	0.087	1.0	1.0	0.14	0.718	9933	9933	2.39	0.153
X_3^2	1	3.61	3.60	0.9	0.365	10.5	10.5	25.8	**0**	0.0	0.0	0	0.984	26228	26228	6.31	**0.031**
Error	10	39.99	4.00			4.1	0.4			70.8	7.1			41543	4154		
Lack-of-fit	5	39.88	7.98	360.09	**0**	2.5	0.5	1.53	0.325	37.6	7.5	1.13	0.448	37736	7547	9.91	**0.012**
Pure Error	5	0.11	0.02			1.6	0.3			33.2	6.6			3806	761		
Total	19	102.85				23.4				151.6				189170			

The bold values indicate the significance at or above the 95.0% confidence level. The outlier was included in the ANOVA analysis.

[a] $X_1 = KH_2PO_4$ (g L^{-1}); $X_2 = MgSO_4.7H_20$ (g L^{-1}); $X_3 = CaCl_2.2H_20$ (g L^{-1}). [f] DF degree of freedom [g] SE sum of square [h] MS mean of square

[b] Biomass DCW production (g L^{-1}) note: $R^2 = 0.6112$; Adj. $R^2 = 0.2612$; Pred. $R^2 = 0$

[c] TFA content (%) note: $R^2 = 0.8266$; Adj. $R^2 = 0.6706$; Pred. $R^2 = 0.1023$

[d] ARA content (%) note: $R^2 = 0.5330$; Adj. $R^2 = 0.1126$; Pred. $R^2 = 0.027$

[e] ARA production (mg L^{-1}) note: $R^2 = 0.7804$; Adj. $R^2 = 0.5828$; Pred. $R^2 = 0$

5.1.3.5 Evaluation of Significance Factors

In present model of the oil%, the linear term (KH_2PO_4 and $CaCl_2.2H_20$) and squared term ($CaCl_2.2H_20$ ^{2}) were significant while the cross factor/2-way interaction had an insignificant effect. In terms of ARA concentration, the linear term (KH_2PO_4) and squared term ($CaCl_2.2H_20$ ^{2}) were significant (Table 5.5). Different from the first RSM, the $CaCl_2.2H_20$ mostly affected the performance on oil% and ARA concentration.

5.1.3.6 Main effect analysis

In the second RSM, most of the single or squared terms had significant effects on oil yield and ARA concentration. For oil%, the single and squared terms relating to $CaCl_2.2H_20$ mainly affected lipid accumulation. The maximum oil% reached 14.8% at the lowest concentration of $CaCl_2.2H_20$, which was about 0.318 g L^{-1}, it followed a parabolic curve where the minimum oil% was at a $CaCl_2.2H_20$ content of 2.5 g L^{-1} (Figure 5.6).

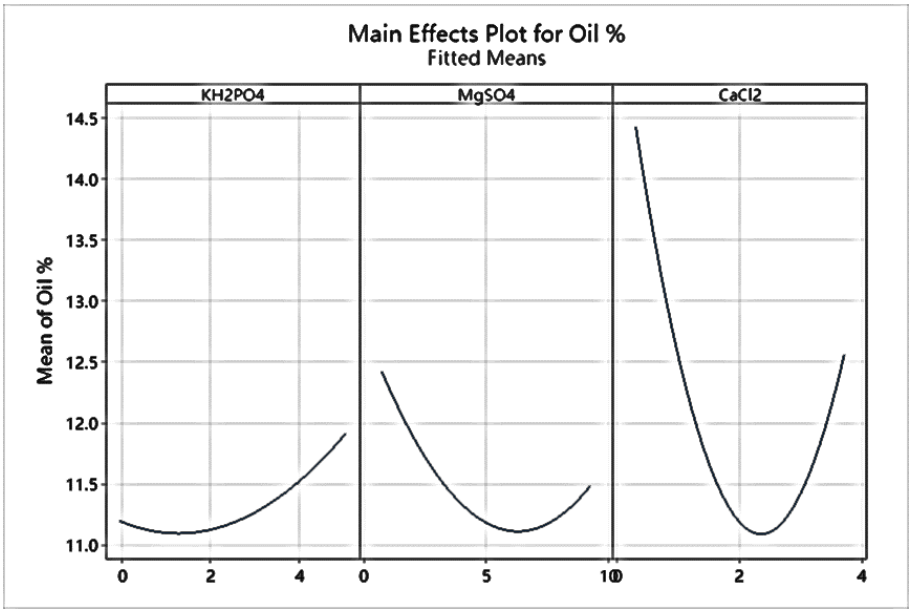

Figure 5.6: Main effects plots of significant minerals KH_2PO_4, MgSO4.7H_20 and $CaCl_2.2H_20$ for response variables: Total oil content w/w%.

For ARA concentration, the single factor KH_2PO_4 and the squared term $CaCl_2.2H_20$

had a significant effect. ARA concentration increased linearly with increasing KH_2PO_4 concentration. ARA concentration behaved similarly to the oil % with respect to $CaCl_2.2H_20$, following another parabolic curve with the lowest ARA concentration occurring at 2 g L^{-1} $CaCl_2.2H_20$ (Figure 5.7).

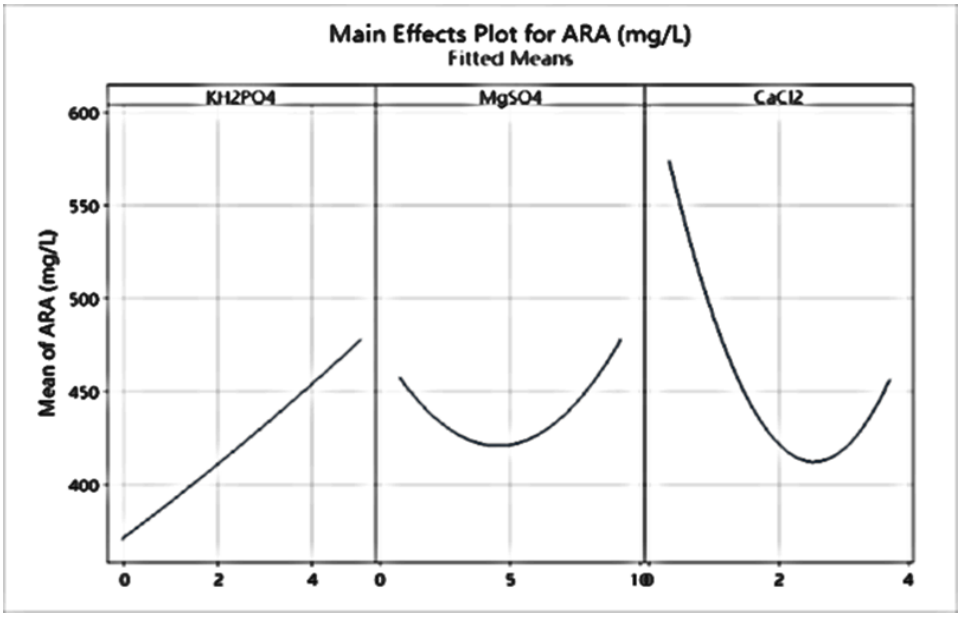

Figure 5.7: Main effects plots of significant minerals KH_2PO_4, MgSO4.$7H_20$ and $CaCl_2.2H_20$ for response variables: ARA concentration (mg L^{-1})

5.1.3.7 Experimental Validation of the Optimized Culture Variables

Table 5.6 summarizes the experiments from the first RSM (Experiments A and B) and second RSM (Experiment C) that were conducted to validate the predicted responses. Experiment C used concentrations of the culture variables that were predicted to give maximum values of all responses and the experimental and predicted values were found to deviate by 9.56%, 7.11%, 14.07% and 11.2% for DCW, TFA%, ARA % and ARA concentration, respectively. This represented 86-93% validity of the prediction models. In addition, significant models were obtained for Oil% and ARA concentration, where each showed a relatively high R^2 of 0.8266 and 0.7804, respectively (Table 5.5). The deviation

of experiment C was closer but higher than the predicted value of R^2, indicated the experimental validation results were better than predicted.

Compared to Experiments A and B from the first RSM validation, the second RSM exhibited a higher predictivity. Experiment B exhibited the highest ARA %, however, its TFA % was the lowest, meaning that the final ARA concentration would be lower. Experiments A and C gave results that were not significantly different; however, the improved predictivity from Experiment C's model indicates that its stability and consistency was better than A. Consequently, this study suggested that the final optimal culture conditions from both RSM would be at a KH_2PO_4 concentration of 5.023 g L^{-1}, $MgSO_4.7H_20$ concentration of 0.796 g L^{-1} and $CaCl_2.2H_20$ concentration of 0.318 g L^{-1}. These conditions would lead to maximum production of biomass of 14.57 ± 0.29 g L^{-1}, TFA % of 17.1 ± 0.43%, ARA% 30.00 ± 2.27% and ARA concentration of 744.28 ± 35.81 mg L^{-1}. Compared to the cell performance with the original medium, these are increases of 46.6%, 2.4%, 9.1% and 65.3%, respectively.

Table 5.6: Predicted and experimental value of responses at optimum condition in two RSM designs

Experiments	KH_2PO_4[a]	$MgSO_4.7H_20$	$CaCl_2.2H_20$	Biomass g L^{-1} [b]	Oil %	ARA%	ARA mg L^{-1}
A	9.886	6.534	2.296	15.2 ± 0.4 [A c] 16.2 [d]	15.3 ± 0.38 [A] 18.7	30.9 ± 2.52 [B] 37.2	715 ± 26.4 [A] 1054
B	3.060	6.534	2.665	15.6 ± 0.09 [A] 14.0	11.7 ± 0.96 [B] 14.9	36.8 ± 1.62 [A] 38.3	675 ± 35.8 [A] 781
C	5.023	0.796	0.318	14.8 ± 0.29 [A] 16.1	17.1 ± 0.43 [A] 16.0	30.0 ± 2.27 [B] 34.9	744 ± 35.8 [A] 838
Original medium [e]				10.1 ± 0.42 [B]	16.7 ± 1.78 [A]	27.5 ± 2.22 [B]	450 ± 89.0 [B]

- A and B, experiments based on maximum all responses and maximum ARA production conditions, respectively from the first RSM. C, experiment based on maximum all responses from the second RSM.
- Basal medium: Glucose and Yeast Extract maintained at 20 g L^{-1} and 11 g L^{-1}.

[a] All factors were added in units of g L^{-1}

[b] Represents mean of the responses for biomass DCW production (g L^{-1}), Oil content (%), ARA content (%) and ARA production (mg L^{-1}), based on triplicate experiments.

[c] Experimental results in Mean ± SD, n = 3. Letters refer to significant term comparison by Tukey ANOVA analysis within 95% confidence interval.

[d] Theoretical solution for the optimal condition under each experimental result

[e] Experimental results of the original condition (basal medium) in Mean ± SD, n = 3.

5.2 Macronutrients Studies

5.2.1 C:N Ratio Screening

Glucose and yeast extract were the main carbon and nitrogen sources evaluated for different C:N ratios. Results showing the fatty acid profile and biomass production from the experiments are shown in Figure 5.8. Here, two strategies were used to increase the C:N ratio from the initial 7.2 to 10, 15 and 20 by increasing the carbon source or decreasing the nitrogen source. These experiments not only determined the optimal C:N ratio but also investigated the relationship between different concentrations of carbon and nitrogen sources.

The results show that for both the carbon and nitrogen modification experiments, the oil content gradually increased to more than 20% when the C:N ratio was increased. Surprisingly, the highest oil content was achieved at a C:N ratio of 20 with a reduction of nitrogen, and increased from an initial 17.1% to 32.8%, resulting in a 0.92-fold increase in oil content. When carbon increased, the increase in oil content was slightly lower, from 17.1% to 27.8%, reaching a 0.63-fold increase at a C:N ratio of 20. Compared to the oil content of 16.2% achieved during the original cultivation conditions, without adding minerals nor adjusting the C:N ratio, the reduction of nitrogen and increase of carbon improved the TFA% in total biomass by 1.02-fold and 0.72-fold, respectively, at a C:N ratio of 20.

In contrast, biomass DCW showed opposite performance in the two improvement strategies. At a final C:N ratio of 20, biomass gradually decreased from 14.6 g L^{-1} to a final 8.8 g L^{-1} as the nitrogen source decreased; reaching a decrease of about 40%. In contrast, increasing the carbon source led to a significant increase in biomass, from 14.6 g L^{-1} to a maximum of 24.6 g L^{-1}, a 0.68-fold increase compared to initial ratio of 7.2. While 10.1 g L^{-1} in biomass was produced using the unmodified cultivation media, experiments with a C:N ratio of 20 showed a 12.9% decrease with the decrease in nitrogen, while a 1.44-fold increase was reached with the addition of carbon.

In terms of ARA concentration, no significant difference was found under the modified nitrogen condition, with ARA varying between 738 and 815 mg L^{-1} corresponding to C:N ratios between 10 to 20. This was due to the higher oil content and lower biomass content compensating for the final ARA concentration, resulting in no improvement in the ARA yield. The increase in ARA concentration under improved carbon conditions was significant, reaching a 1-fold increase from 835 mg L^{-1} at a C:N of 10 to a maximum of 1663 mg L^{-1} at a C:N of 20. The increase in biomass and oil content boosted ARA production to more than 1.6 g L^{-1}. The highest ARA concentration was a 2.7-fold and 1.2-fold increase compared to that achieved with the original and control conditions (added minerals), which were 450 mg L^{-1} and 744 mg L^{-1} respectively. The ARA contribution within the TFA was maintained throughout the experiment at between 24.3 – 31%, indicating that the increase in C:N ratio had minimal effect on ARA synthesis from cell metabolism.

In conclusion, an increase in C:N ratio had a positive effect on oil accumulation, especially for a C:N between 15 - 20. Although reducing the nitrogen source allowed more oil accumulation, the lower amount of biomass resulted in only a small increase in overall productivity. Increasing the carbon source improved biomass and oil content, thus increasing ARA production, and ultimately seemed to be a better option for further experiments.

For the later experiments, a C:N ratio of 15, containing 41.25 g L^{-1} glucose (with 16.5 g L^{-1} total carbon content) and 11 g L^{-1} yeast extract (with 1.1 g L^{-1} total nitrogen content) was chosen as the best ratio to use. This was because the C:N ratio of 15 depleted glucose by day 7, faster than the C:N ratio of 20 which lasted 10 days, thus the overall productivity in g $L^{-1}d^{-1}$ was higher at the C:N ratio of 15 due to the shorter fermentation time. Using the optimal C:N ratio of 15 resulted in a biomass concentration of 21.8 g L^{-1}, 25.8% TFA and 1479 mg L^{-1} of ARA. The new C:N ratio of 15 showed a significant increase in biomass, oil yield and ARA production by 1.16, 0.59 and 2.29 times, respectively, compared to the

original medium with a C:N ratio of 7.2, containing only glucose and yeast extract.

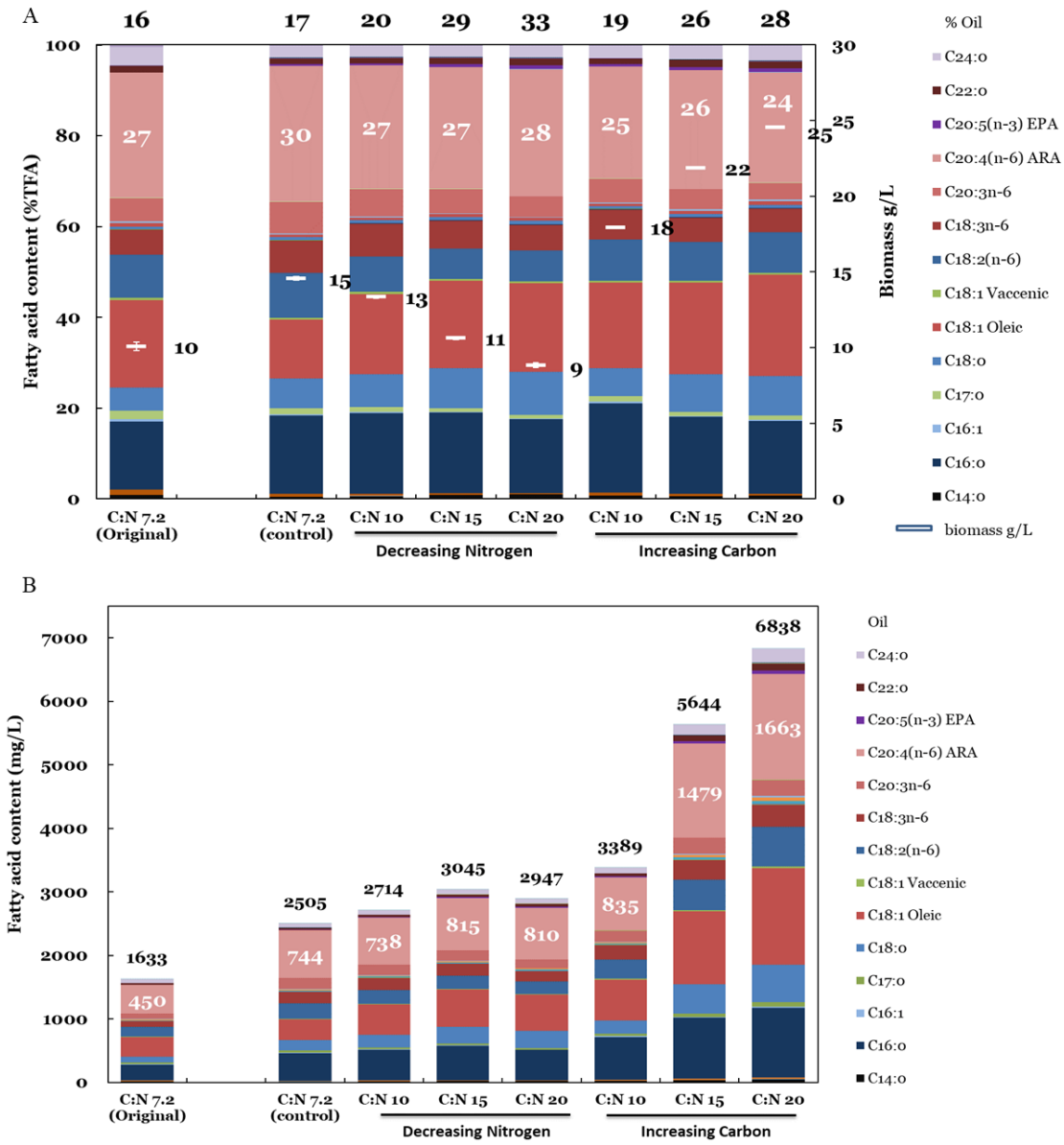

Figure 5.8: Fatty acid profile A) in w/w %; and B) in mg L^{-1} of carbon to nitrogen ratio screening of *M. alpina* MA2-2 strain. The stacked bar for each strain represents the fatty acid profile with the % contribution and concentration mg L^{-1} of each individual fatty acid to the TFAs indicated by a different colour (see legend). The chain length of the fatty acids increases from bottom to top of the bar graphs, likewise with saturated to unsaturated. ARA (20:4 n-6) is denoted in pink and labelled in both figures. Biomass production in g L^{-1} is indicated by a white line overlaid on the % TFA bar, aligning to the y-axis on the right side. The percentage and amounts (mg L^{-1}) of total oil within the biomass is given by the number at the top of each bar.

5.2.2 Nitrogen Pre-screening

The results for the nitrogen pre-screening experiments are shown in Table 5.7. Here, three organic nitrogen (yeast extract, peptone and urea) and three inorganic nitrogen ($NaNO_3$, MSG and $(NH_4)_2SO_4$) were supplemented with yeast extract and the C:N ratio was maintained at the control level of 7.2. The nitrogen source containing peptone or $NaNO_3$ supplemented with yeast extract increased the oil yield to about 30%, compared to yeast extract alone. Peptone showed the best improvement in oil yield and maintained a stable biomass and ARA% with the highest overall ARA yield of 956 mg L^{-1} at a C:N ratio of 7.2. The biomass produced with $NaNO_3$ was lower than when yeast extract or peptone was the main nitrogen source, but a higher oil content was obtained to compensate the lower biomass, so that the ARA concentration was similar to the conditions with the single yeast extract. Using MSG as the main nitrogen source resulted in no significant change in biomass and slightly higher oil content, but a lower percentage of ARA was obtained, reducing overall productivity. The addition of urea and ammonia sulfate strongly inhibited cell growth, resulting in low biomass production. The accumulation of ARA was extremely low because the growth phase did not reach the logarithmic stage, thus the overall productivity was low.

From these pre-screening results, the organic nitrogen sources of yeast extract and peptone, and inorganic nitrogen sources of $NaNO_3$ and MSG were selected for subsequent mixture design. In the mixture design, the optimum C:N ratio of 15 was selected, where glucose was increased to 41.25 g L^{-1} and yeast extract was kept at 11 g L^{-1}, so that the total nitrogen content was maintained at 1.1 g L^{-1}.

Table 5.7: Experimental design of pre-screening nitrogen for multi-response variables (biomass DCW, Oil%, ARA%, and ARA concentration

Yeast extract	Peptone	$NaNO_3$	Urea	MSG	$(NH_4)_2SO_4$	Biomass [c]	Oil %	ARA%	ARA
11(100) [a]	0	0	0	0	0	[d] 15.4 ± 0.54^{A}	14.4 ± 0.23^{B}	30.9 ± 2.90^{A}	687.7 ± 29.5^{AB}
1.1(10) [b]	9.52 (90)	0	0	0	0	12.3 ± 0.06^{BC}	30.0 ± 6.96^{A}	26.0 ± 0.31^{A}	956.3 ± 206^{A}
1.1(10)	0	6.01 (90)	0	0	0	8.6 ± 1.76^{D}	29.1 ± 1.87^{A}	28.0 ± 0.49^{A}	704.9 ± 200^{AB}
1.1(10)	0	0	2.12 (90)	0	0	9.3 ± 0.41^{CD}	9.7 ± 0.32^{B}	14.9 ± 0.44^{B}	134.4 ± 6.48^{C}
1.1(10)	0	0	0	11.9 (90)	0	13.2 ± 0.2^{AB}	18.0 ± 1.23^{AB}	17.6 ± 0.44^{B}	417.1 ± 32.3^{BC}
1.1(10)	0	0	0	0	4.71 (90)	2.0 ± 0.05^{E}	22.4 ± 4.90^{AB}	7.45 ± 0.42^{C}	33.73 ± 6.28^{C}

- Values in the same column followed by different alphabetical superscripts are significantly different at 5% level according to ANOVA Tukey multiple range test.

[a] Total Nitrogen source (100% composition of nitrogen) maintained at 1.1 g L^{-1}

[b] Table comprised of yeast extract with 10% composition of nitrogen mixed with other nitrogen sources with 90% compositions of total nitrogen

[c] Represents mean of the responses for biomass DCW production (g L^{-1}), Oil content (%), ARA content (%) and ARA production (mg L^{-1}), based on duplicate experiments.

[d] Mean ±SD, n = 2.

5.2.3 Nitrogen Mixture Design

5.2.3.1 Model fitting and regression analysis

The ANOVA analysis for the nitrogen mixture experiments is shown in Table 5.8. The regression quadratic model for the responses of biomass, ARA content and ARA concentration confirmed the significance of the experiment data ($p < 0.05$). For the total oil%, p value of the F test was 0.973, indicating non-significance ($p > 0.05$). The potential reason could be that the variation in oil content was minimal or even insignificant, as most terms were within the 95% confidence interval. Since the overall model was insignificant for the percentage of total oil content, subsequent analyses were performed only for the regression models that confirmed significance.

The F-test for the contribution of the quadratic term was significant in response to biomass with a p value of 0.011 ($P < 0.05$), indicating that a quadratic mixture model should be used. The statistics indicated that the quadratic model for biomass was superior to the linear model (Fortela et al., 2016). ARA content and concentration showed non-significant quadratic models ($P > 0.05$), indicating that individual nitrogen factors had a greater effect on both responses than additive effects. This implied that the linear model was applicable for ARA content and concentration studies.

Table 5.8: ANOVA analysis for response surface quadratic model of biomass DCW, ARA content and concentration by nitrogen mixture design

Term	DF [f]	Biomass DCW (g L^{-1}) [b]				Oil % [c]				ARA % [d]				ARA (mg L^{-1}) [e]			
		SS[g]	MS[h]	F	p	SS	MS	F	p	SS	MS	F	p	SS	MS	F	p
Model	9	615	68	17.57	**0**	122	14	0.25	0.973	475	53	3.99	**0.026**	8.89E+06	9.88E+05	4.07	**0.024**
Linear	3	330	110	28.24	**0**	6.6	2.2	0.04	0.988	175	58	4.41	**0.036**	4.58E+06	1.53E+06	6.29	**0.014**
Quadratic	6	131	22	5.6	**0.011**	76	13	0.24	0.953	116	19	1.47	0.29	1.73E+06	2.88E+05	1.19	0.392
Yeast Extract × Peptone [a]	1	2.0	2.0	0.52	0.488	7.8	7.8	0.15	0.711	2.7	2.7	0.21	0.661	1.56E+05	1.56E+05	0.64	0.444
Peptone × $NaNO_3$	1	22	22	5.79	**0.04**	3.9	3.9	0.07	0.791	96	96	7.29	**0.024**	8.45E+05	8.45E+05	3.48	0.095
Yeast Extract×MSG	1	52	52	13.46	**0.005**	27	27	0.51	0.493	13	13	1	0.343	6.88E+05	6.88E+05	2.84	0.126
Peptone × $NaNO_3$	1	46	46	11.8	**0.007**	5.6	5.6	0.11	0.753	0.01	0.01	0	0.985	3.66E+04	3.66E+04	0.15	0.707
Peptone × MSG	1	11	11	2.74	0.133	22	22	0.41	0.538	0.3	0.3	0.02	0.879	4.50E+03	4.50E+03	0.02	0.895
$NaNO_3$ × MSG	1	3.6	3.6	0.93	0.361	8.8	8.8	0.17	0.693	2.3	2.3	0.17	0.686	4.86E+03	4.86E+03	0.02	0.891
Error	9	35	3.9			478	53			119	13			2.18E+06	2.43E+05		
Total	18	650				600				594				1.11E+07			

The bold values indicate the significance at or above the 95.0% confidence level

[a] Factors added were in units of g L^{-1}

[b] Biomass DCW production (g L^{-1}) note: $R^2 = 0.9461$; Adj. $R^2 = 0.8923$

[c] TFA content (%) note: $R^2 = 0.2026$; Adj. $R^2 = 0$

[d] ARA content (%) note: $R^2 = 0.07996$; Adj. $R^2 = 0.5992$

[e] ARA production (mg L^{-1}) note: $R^2 = 0.8028$; Adj. $R^2 = 0.6057$

[f] DF degree of freedom

[g] SE sum of square

[h] MS mean of square

A second-order polynomial model, incorporating the different interactions, was proposed with respect to growth (Eq. 15) and the percentage (Eq. 16) and concentration (Eq. 17) of ARA with their term significance ($p < 0.05$).

$$Y_{DCW}(g\ L^{-1}) = 22.43\ Yeast\ Extract + 19.5\ Peptone + 2.65\ NaNO_3 + 5.00\ MSG + 20.23\ \text{Yeast Extract} \times NaNO_3 + 31.09\ \text{Yeast Extract} \times \text{MSG} + 28.82\ \text{Peptone} \times \text{NaNO}_3 \quad (15)$$

$$Y_{ARA}(\%) = 32.8\ Yeast\ Extract + 31.77\ Peptone + 18.45\ NaNO_3 + 19.35\ MSG + 29.9\ Yeast\ Extract \times NaNO_3 \quad (16)$$

$$Y_{ARA\ conc}\ (mg\ L^{-1}) = 2370\ Yeast\ Extract + 2098\ Peptone + 7\ \text{NaNO}_3 + 268\ \text{MSG} \quad (17)$$

5.2.3.2 Normality Plot Analysis

The normality probability plot was to assess whether the data was normally distributed or not shown in Appendix A – Figure A.4 (Dias et al., 2015). The normality plot of the response to biomass closely aggregated to follow a straight line (Figure A.4 A). The ARA responses were all approximately straight lines, but some rare events or outliers were observed, as well as a trend in the residuals relative to x, showing a less normal distribution plot (Figure A.4 C & E). The results of the normality plots showed that the biomass formed a normal distribution better than the ARA responses, which was consistent with the previous ANOVA. A lower predictivity could be expected when validating the ARA production model in comparison to the biomass model.

In terms of residuals vs. fitted plots, the experimental points for all three responses were reasonably scattered around zero randomly, which means that constant variance can be expected. However, a few rare outliers were also found that could imply dependence. Biomass showed more clustering of residuals (Figure A.4 B), while the residuals on the fitted values of x were unevenly distributed, suggesting dependence and non-constant

variance compared to ARA production (Figure A.4 D & F) (Fortela et al., 2016). In conclusion, biomass showed a better normal distribution with high predictability to verify the adequacy of the model, however, its independent distribution was not as good as the percentage and concentration of ARA.

5.2.3.3 Term Significance

From Table 5.8, it is evident that all linear models exhibited a significant effect ($P < 0.05$). In addition, the quadratic terms of yeast extract × $NaNO_3$, yeast extract × MSG and Peptone × $NaNO_3$ had p values of 0.04, 0.005 and 0.007 respectively, that were significant for biomass ($p < 0.05$). In terms of ARA%, the quadratic term of yeast extract × $NaNO_3$ was significant at p value of 0.024. For the response of ARA concentration, the quadratic model was not significant (Table 5.8).

According to the regression coefficients, four nitrogen sources had positive effects on the linear terms of biomass and ARA production (Eq. 15 to 17). In terms of the biomass, the significant interaction terms, yeast extract × $NaNO_3$, yeast extract × MSG and Peptone × $NaNO_3$, had positive regression coefficients, bringing synergistic blending effects. In terms of the percentage of ARA, the significant term yeast extract × $NaNO_3$ had a positive effect on ARA and therefore also a synergistic mixing effect.

5.2.3.4 Main Effect Plot Analysis

In mixture analysis, the traditional t-test is not used to assess the significance of each factor because all components were strongly correlated with each other. Instead, a special graph, the response trace plot in Cox direction, is usually used to find the behavior of each component in the mixture design (Cornell, 2002; Shariati et al., 2019). Appendix A – Figure A.5 shows the Cox trace plots for this study, where the reference blend was the centroid of the design, corresponding to 25% of total nitrogen for each component. Here, the x-axis is the deviation amount from the reference point, and the y-value is the fitted

response, thus the effects of a component depended on the range of the component and the steepness of the response trace (Cornell, 2002). In these plots, all responses indicated a steeper response for yeast extract or peptone, especially in terms of percentage and concentration of ARA, which had a more pronounced effect than biomass. In particular, yeast extract had the highest steepness and the greatest improvement for all responses. Thus, biomass and ARA production increased rapidly with the increase of organic nitrogen in the mixture, especially with the addition of yeast extract. In contrast, two inorganic nitrogen sources showed lower traces of steepness response, indicating that the sole inorganic nitrogen sources could cease cellular growth and lipid accumulation. The acceptability of all responses decreased rapidly as the proportion of $NaNO_3$ or MSG in the mixture increased. Consequently, organic nitrogen sources improved biomass and ARA production more than inorganic nitrogen sources.

5.2.3.5 Interpretation of Contour and Surface Plots

Mixture contour plots are shown in Figure 5.9. Contour plots were constructed for multi-responses except oil content due to its model insignificance. The single factor represented in the corner of the contour plot exhibited similar performance to the cox response trace plots, where organic nitrogen sources, yeast extract or peptone, were found to increase biomass and ARA production in comparison to the inorganic sources. In particular, yeast extract, was most effective in increasing ARA production. In addition, the combination of organic and inorganic nitrogen sources resulted in higher performance. For instance, the large proportion of yeast extract mixed with small portion of $NaNO_3$ brought more than 36% of ARA and 2.5 g L^{-1} ARA concentration, while the yeast extract source alone produced 32 – 36% ARA or a 2.0 g L^{-1} concentration, resulting in a 12.5% and 25% increase, respectively (Figure 5.9 B). Compared to $NaNO_3$, MSG brought insignificant additive effects. Consequently, the combination of yeast extract and $NaNO_3$ significantly improved the multi-response performance, including biomass DCW, percentage and

concentration of ARA.

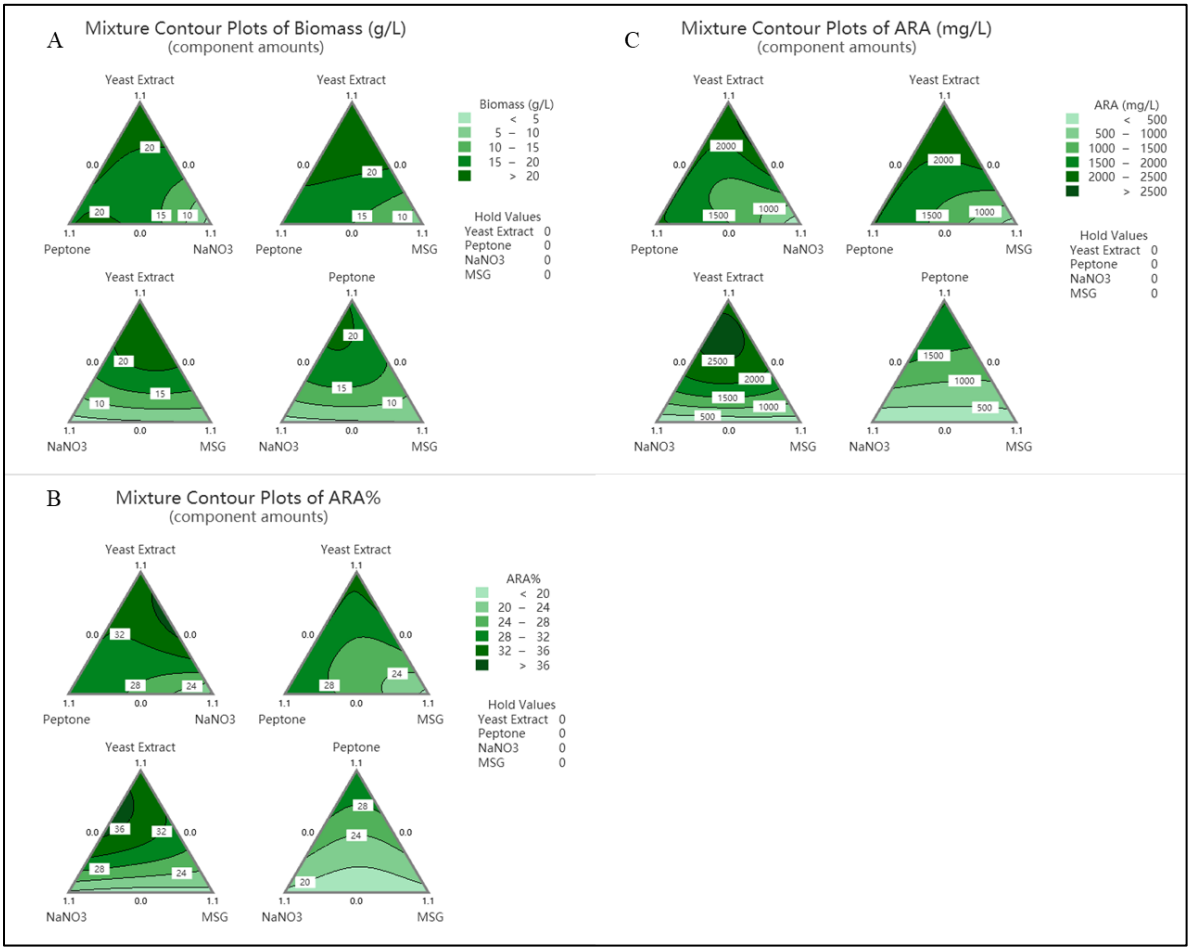

Figure 5.9: Ternary two-dimensional contour plots of significant response variables in mixture design for *M. alpina* MA2-2, with respect to the response of: A) Biomass; B) ARA content (%); C) ARA concentration.

5.2.3.6 Experimental Validation

The model for biomass exhibited a high R^2 and adjusted R^2, which were 0.9461 and 0.8923, respectively, which indicated that the regression model adequately fitted the experimental data, and the model can be used for predictive purposes. The models for ARA content and concentration showed a R^2 of 0.7976 and 0.8028; and an adjusted R^2 of 0.5992 and 0.6057, respectively (Table 5.8). Both models for ARA content and concentration expressed a relative lower regression prediction than biomass.

To evaluate the model determined by the mixture design, an experiment was conducted

in triplicate under the identified conditions. The information from the equation models and plots predicted one optimal solution (Table 5.9). Experiment A was designed to maximize all responses, including biomass DCW, TFA% or Oil%, ARA content and concentration. The high portion of organic nitrogen, 7 g L^{-1} of yeast extract accounted for 0.7 g L^{-1} of total nitrogen, combined with a small portion of inorganic nitrogen, 2.429 g L^{-1} of $NaNO_3$ which accounted for 0.4 g L^{-1} of total nitrogen.

Experiment A predicted responses for biomass DCW, TFA% or Oil%, ARA content and concentration of 20 g L^{-1}, 34.64%, 37.42% and 2518 mg L^{-1}, respectively. The actual experimental data resulted in values of 17.67 ± 0.16 g L^{-1}, 32.7 ± 0.02%, 39.33 ± 2.10% and 2270 ± 100.9 g L^{-1}, respectively. The corresponding deviations between the experimental and predicted values were 11.7%, 5.6%, 5.10% and 9.85%, respectively. These results confirmed the validity of the model and that the experimental designs used in this work were appropriate for predicting the optimized culture conditions.

Thus the modified media for the strain MA2-2 was determined and consisted of glucose 41.25 g L^{-1}, yeast extract 7 g L^{-1}, $NaNO_3$ 2.429 g L^{-1}, KH_2PO_4 5.023 g L^{-1}, $MgSO_4.7H_20$ 0.796 g L^{-1} and $CaCl_2.2H_20$ 0.318 g L^{-1}. The modified media resulted in biomass DCW, TFA% or Oil%, ARA content and concentration of 19 – 22 g L^{-1}, 30 – 35 %, 33 – 42% and 2.1 – 2.5 g L^{-1}, respectively. Compared to the original medium containing 20 g L^{-1} of glucose and 11 g L^{-1} of yeast extract, the response variables of biomass, Oil%, ARA content and concentration reached 10 – 12 g L^{-1}, 16 – 18 %, 25 – 27.5% and around 0.45 g L^{-1}, respectively; and therefore cell performance was improved by at least 0.9, 0.875, 0.32, 3.7 times, respectively.

Table 5.9: Predicted and experimental value of responses at the optimum condition in nitrogen mixture design

Exp.	Yeast Extract	$NaNO_3$	Biomass [b]	Oil %	ARA%	ARA
A	7 (0.7)	2.429 (0.4)	17.67 ± 0.16 [c]	32.7 ± 0.02	39.33 ± 2.10	2270 ± 100.9
			20 [d]	34.64	37.42	2518

- Experiment A based on maximum all responses
- Basal minerals: KH_2PO_4 5.023 g L^{-1}, $MgSO_4.7H_20$ 0.796 g L^{-1} and $CaCl_2.2H_20$ 0.318 g L^{-1}

[a] Factors were added in units of g L^{-1}

[b] Represents mean of the responses for biomass DCW production (g L^{-1}), Oil content (%), ARA content (%) and ARA production (mg L^{-1}), based on triplicate experiments.

[c] Experimental values corresponding to the predicted value in Mean ± SD, n = 3.

[d] Theoretical solution for the optimal condition under each experimental value

5.3 Random Mutagenesis

5.3.1 Development of UV Mutagenesis and Screening Method

5.3.1.1 UV Mutagenesis

Figure 5.10 shows the results after cells were exposed to UV radiation from 1 to 45 min with the petri dish lid on (Figure 5.10). Surviving cells were observed at all conditions even after 45 min of irradiation. The reason for this could be the limited ability of UV light to penetrate the lids of the Petri dishes, thus minimizing the irradiation effect. As reported by Turnbull et al., the penetrating ability of the UV can be extremely limited as the microstructural elements of nitrocellulose and similar membranes are able to substantially shield the spores (Turnbull et al., 2008).

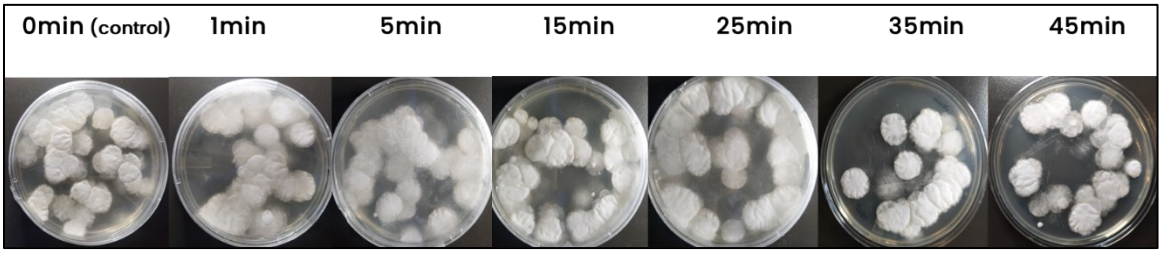

Figure 5.10: Screening of the UV mutagenesis condition 'Preset UV Time Exposure', showing surviving colonies with exposure times of 0, 1, 5, 15, 25, 35 and 45 min when the Petri dish lid was on.

To enhance UV penetration, a second exposure was set up with the Petri lid removed, for a period ranging from 0.1 min to 7.5 min (Figure 5.11). After the spore suspensions were directly exposed to UV light, 100% mortality was obtained for all conditions, indicating that the default UV energy intensity (~120,000 µJ cm^{-2}) was not suitable to be used for mutagenesis with the *M. alpina* spore suspension.

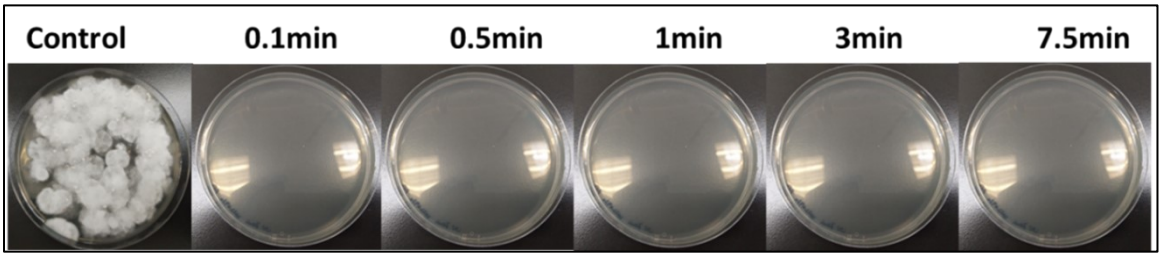

Figure 5.11: Screening of the UV mutagenesis condition 'Preset UV Time Exposure' showing surviving colonies with exposure times ranging from 0, 0.1, 0.5, 1, 3 and7.5 min when the Petri dish lid was removed

Next, the intensity of UV energy irradiation was tested to find a suitable intensity for mutagenesis. Measured doses of UV exposure to the samples were monitored at different intensities and the results are shown in Figure 5.12. In this study, the energy intensity of UV irradiation ranged from 0 to 12,000 µJ cm^{-2}. The exposure intensity was set and applied to Petri dishes with the lids removed in order to improve the penetration of UV light. As shown in Figure 5.13, a clear trend of inhibition was found. About 86% of the spores were killed at 8,000 µJ cm^{-2} UV, and this was chosen as the best intensity for mutant recovery.

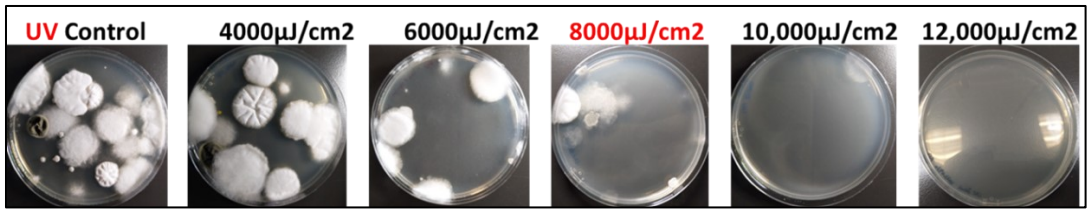

Figure 5.12: Screening of UV mutagenesis 'Preset UV Energy Exposure', ranging from 0, 4000, 6000, 8000, 10,000 and 12,000 µJ cm^{-2} when the Petri dish lid was removed

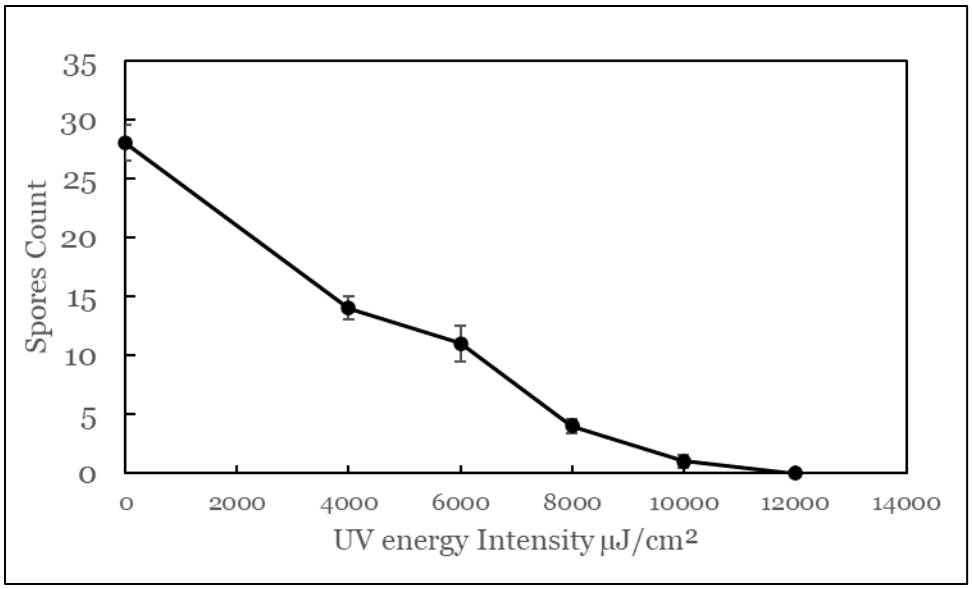

Figure 5.13: Mortality plot with respect to UV exposure to the MA2-2 strain spore suspension

5.3.1.2 FAs Inhibitor Cerulenin Screening

Figure 5.14 shows the results from the initial screening of cerulenin in PDA agar plates where the tested concentrations ranged from 0 to 0.8 µM. The inhibition increased with concentrations above 0.4 µM, especially at 0.8 µM, where growth was severely inhibited and about 83.1% of the spores were killed (Table 5.10).

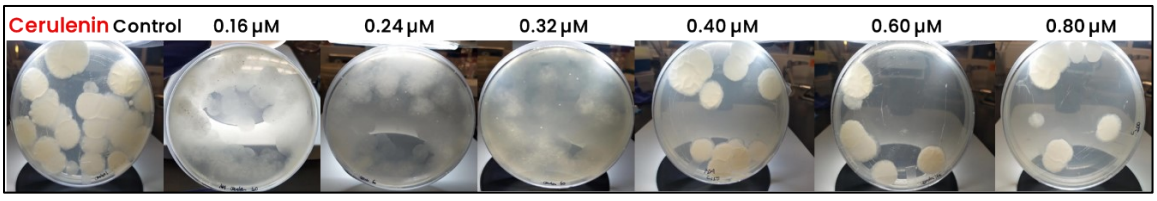

Figure 5.14: Screening of different concentrations of FAs inhibitor cerulenin supplemented with PDA plates, ranging from 0, 0.16, 0.24, 0.32, 0.40, 0.60 and 0.80 µM

Table 5.10: Effect of various cerulenin concentrations on mycelial growth for the first screen results

Cerulenin Concentration		Observation	Spores count
[µM]	[mg L^{-1}]		
0	0	Normal growth with intact colony	~77 spores
0.16	0.036	Normal growth with intact colony	64 spores: 16.8% killed
0.24	0.054	Normal growth with intact colony	65 spores: 15.6% killed
0.32	0.071	Growth was slightly inhibited with intact colony	58 spores: 24.7% killed
0.4	0.089	Growth was inhibited with slow growth	23 spores: 69.2% killed
0.6	0.13	Growth was severely inhibited with little mycelium can be seen.	17 spores: 77.9% killed
0.8	0.18	Growth was severely inhibited with little mycelium can be seen	13 spores: 83.1% killed

Subsequently, a second screening was performed with a wider range of cerulenin concentrations, similar to Yao et al. (2019), ranging from 0.1 to 4.5 µM. The results are shown in Figure 5.15, where the concentration of 1 µM resulted in a strong inhibition, while the growth of mycelium was slower with a mortality rate of about 42.3% compared to the lower concentrations (Table 5.11).

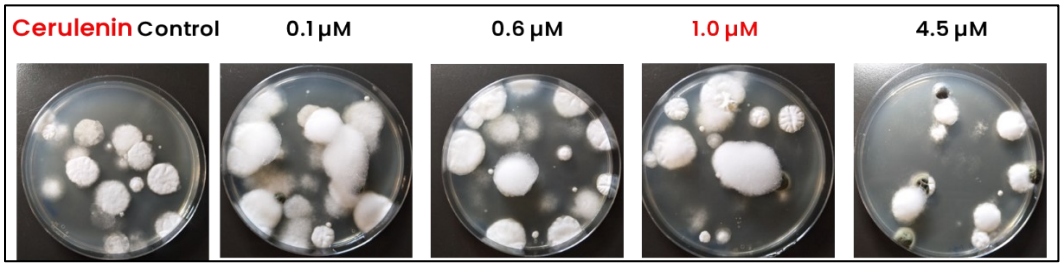

Figure 5.15: Screening of different concentrations of FAs inhibitor cerulenin supplemented with PDA plates, ranging from 0, 0.1, 0.60, 1.0 and 4.5 µM

The mortality rate of the second cerulenin screening experiment was found to be lower than the first one. This was possibly due to having fewer control cells in the second screening experiment. Furthermore, some colonies were aggregated together, making the spore count less precise. Consequently, visual observation of the size of colonies and the growth rate grown on plates were the main factors to be considered. When the

concentration was higher than 0.6 μM for both screening experiments, smaller colony sizes were observed in comparison to the relatively larger cells in the control. In addition, the growth time of mycelium was prolonged at higher concentrations of cerulenin supplementation. Mycelium in the control usually took two to three days to germinate intact colonies with pale white morphology; however, at higher cerulenin concentrations, four to five days were required for the mycelium to germinate and form intact colonies. There was severe inhibition at concentrations of 0.8 to 1 μM, which was consistent with the study of Yao et al (2019). Therefore, the concentration of cerulenin was set to 1 μM to exclude strains with low FA synthesis activity.

Table 5.11: Effect of various cerulenin concentrations on mycelial growth for the second screen results

Cerulenin Concentration		Observation	Spores count
[μM]	[mg L^{-1}]		
0	0	Normal growth with intact colony	~26 spores
0.1	0.022	Normal growth with intact colony	21 spores: 19.2% killed
0.6	0.13	Growth was slightly inhibited with intact colony	17 spores: 34.6% killed
1.0	0.22	Growth was severely inhibited with little mycelium seen.	15 spores: 42.3% killed
4.5	1	Growth was severely inhibited with little mycelium seen.	13 spores: 50% killed

5.3.1.3 TTC Screening

Figure 5.16 shows the results from screening experiments with TTC, where various concentrations of TTC (0, 0.15, 0.3, 1.5 and 3 mM) were added to PDA plates to determine a suitable concentration for screening. The results showed that the colony color turned deeper red as the concentration of TTC increased (Table 5.12). Based on these results, a TTC concentration of 1.5 mM would be suitable as an indicator and was chosen for

screening and selecting mutagenized cells. The results were also compared with those of Yao et al. (2019) who showed that dark colonies could be obtained with the same concentration of TTC. An interesting observation was that the colony size became smaller with increasing TTC supplementation, especially above 1.5 mM.

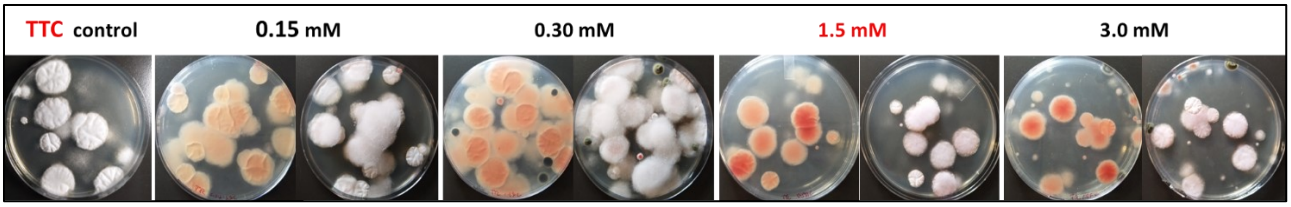

Figure 5.16: Screening of different concentrations of TTC supplemented with PDA plates, ranging from 0.15, 0.30, 1.5 and 3.0 mM

Table 5.12: Effect of various TTC concentrations on mycelial growth

TTC Concentration		Observation
[mM]	[g L^{-1}]	
0	0	Normal growth with milky white colony
0.15	0.05	Some stained red
0.30	0.1	Most redness can be observed
1.5	0.5	Darker red can be differentiated, less spores
3.0	1.0	Darkest red compared to above, less spores

5.3.2 Isolation and identification of oleaginous filamentous fungi

After UV mutagenesis was applied by exposing to 8,000 µJ cm^{-2} UV, the mutagenized spore suspensions were spread on PDA plates containing 1 µM cerulenin and 1.5 mM TTC and incubated at 25°C for 3 days. Most surviving cells would be prevented from forming normal large colonies, and only mutants with enhanced FA synthesis activity would grow into large colonies (Li et al., 2015). Thus 39 colonies that were larger and darker than the un-mutagenized spores were selected and evaluated for FAMEs after fermentation in 250-mL shake flasks at normal conditions. The fatty acid profiles are shown in Figure 5.17.

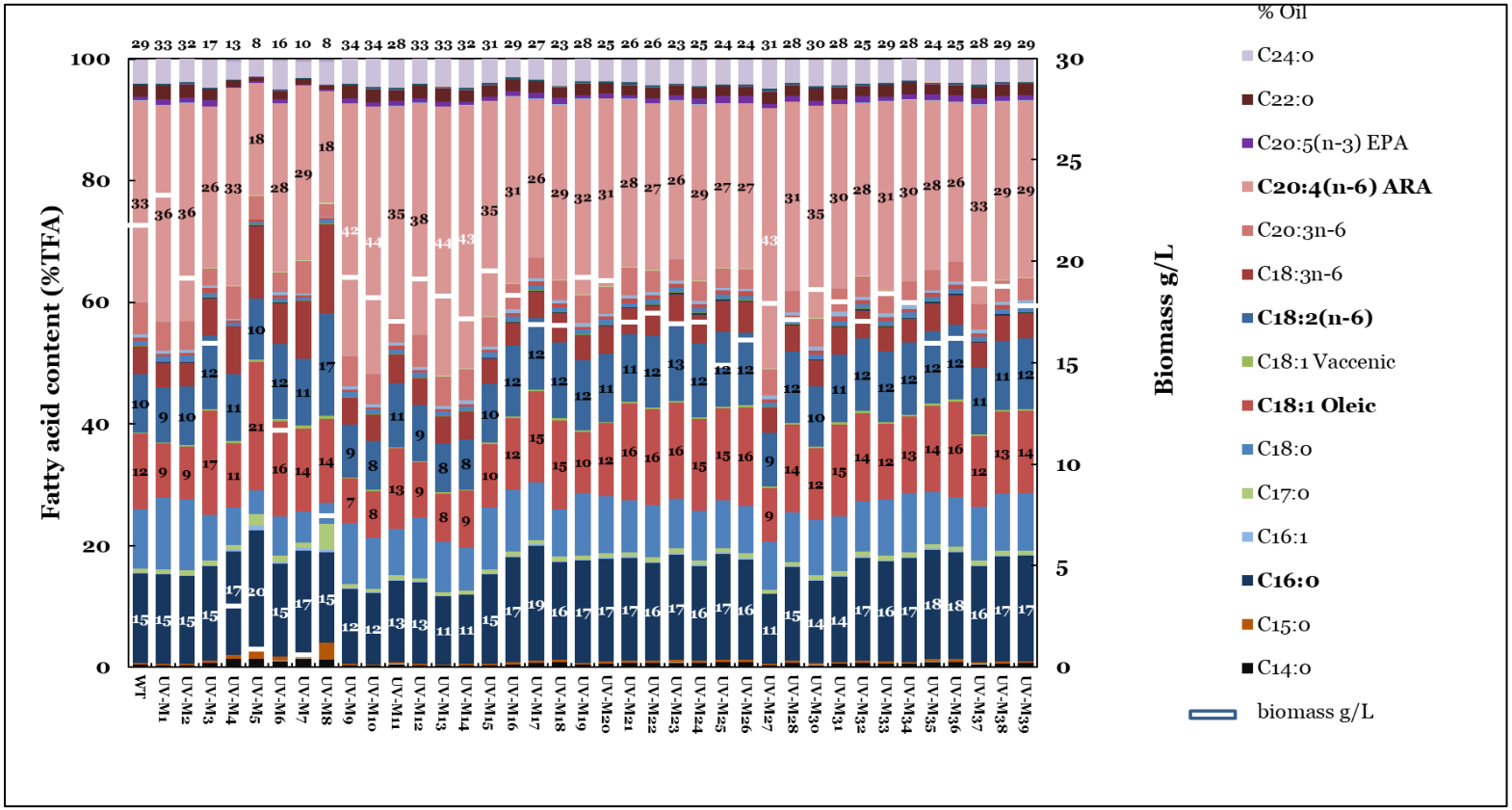

Figure 5.17: Fatty acid profile in w/w % of TFA of UV-mutagenized cells from *M. alpina* MA2-2 strain. The stacked bar for each strain represents the fatty acid profile with the % contribution of each individual fatty acid to the TFA indicated by a different colour (see legend). The chain length of the fatty acids increases from bottom to top of the bar graphs, likewise with saturated to unsaturated. ARA (20:4 n-6) is denoted in pink and labelled. Biomass production in g L^{-1} is indicated by a white line overlaid on the % TFA bar, aligning to the y-axis on the right side. The percentage of total oil within the biomass is given by the number at the top of each bar.

5.3.3 Fatty acid profiles of oleaginous fungal isolates

The biomass of most of the fungal isolates fluctuated between 15 and 23 g L^{-1}, as shown in Figures 5.21 and 5.22. Five isolates, namely M4, M5, M6, M7 and M8, produced biomass below 15 g L^{-1}, significantly lower than the wild type, suggesting that these mutants were derived from plates with the same mutagenic spore suspension and that they experienced a strong inhibitory effect on normal growth. Most of the mutants achieved normal growth similar to the wild type, however, no significantly higher growth was observed.

In terms of total oil content, all the fungal isolates were rich in C16 and C18 fatty acids. The most abundant fatty acids produced were palmitic acid (C16: 0), oleic acid (C18: 1), linoleic acid (C18: 2), and ARA (C20: 4) (Figure 5.17). The wild type typically accumulated 29% to 33% of total oil in biomass, with most mutants reaching over 25% and up to 34% in mutants M9 and M10. In addition, the mutants with the lowest biomass discussed above also accumulated the lowest TFA, below 16% (Figure 5.18). The reason for this may be that the long logarithmic growth has not yet reached the point of starvation for nitrogen and carbon sources, so there were not many nutrients to initiate the accumulation of lipids. Still, no significant improvement in total lipid content was found.

The content of ARA in TFA varied from 18% to 44% in the isolates, with most of them fluctuating around 30% (Figure 5.18). The synthesis of ARA (C20:4) as a PUFA followed the opposite trend to that of SFA (saturated fatty acids), especially the most abundant fatty acids such as palmitic acid (C16:0), oleic acid (C18:1) and linoleic acid (C18:2). Most mutants had around 30% of C20:4, followed by 17% of C16:0, 14% of C18:1 and finally 11% of C18:2 (Figure 5.17). Among them, five mutants were capable of accumulating more than 40% of ARA, namely M9, M10, M13, M14 and M27, which also reduced their SFAs content to about 8-11%.

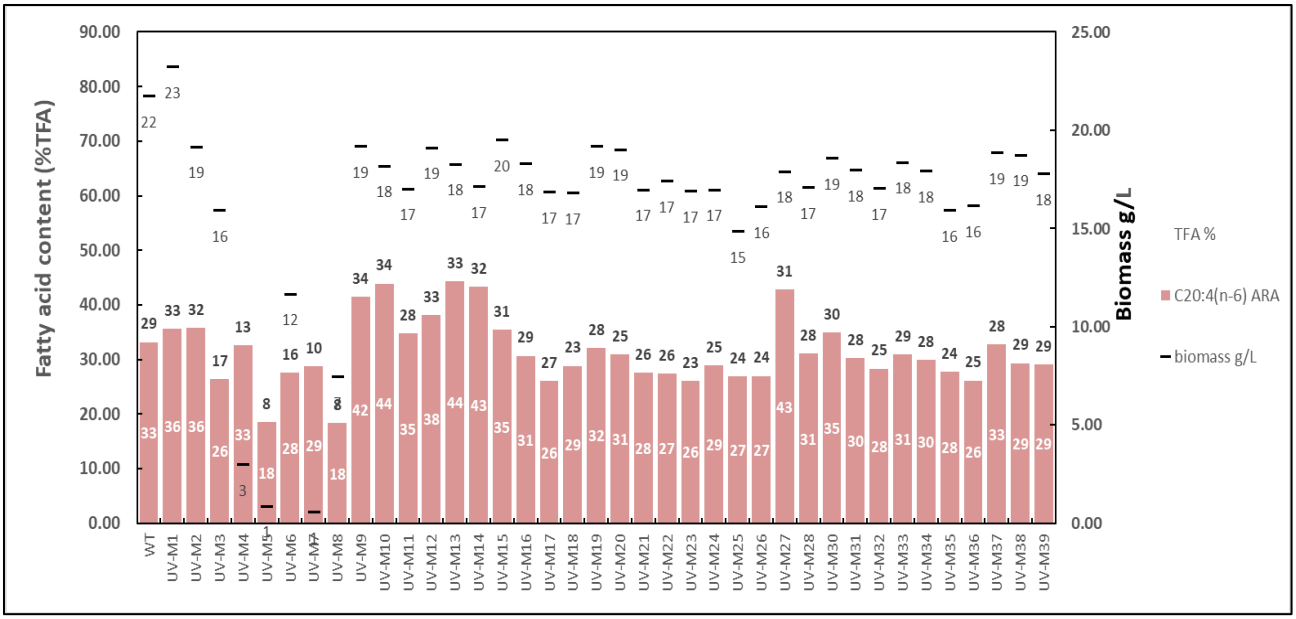

Figure 5.18: Fatty acid profile of UV-mutagenized cells from *M. alpina* MA2-2 strain. The simplified version of Figure 5.17. Fatty acid content of ARA (20:4 n-6) in TFA is denoted in pink and labelled in white within each bar. Biomass production in g L^{-1} is indicated by a black line overlaid on the % TFA bar, aligning to the y-axis on the right side. The percentage of total oil (TFA%) within the biomass is given by the number at the top of each bar, labelled in black.

To determine the stability of the beneficial mutants, five mutants with more than 40% ARA content, namely M9, M10, M13, M14 and M27, were selected for flask screening experiments in triplicate, data is shown in Table 5.13. In general, the results of biomass and fatty acid profiles showed minimal standard errors and good stability. However M27 exhibited poor growth in flask assays and could not undergo FAME esterification, indicating its high sensitivity to growth in flasks and poor stability. Among the selected mutants, M9 and M13 retained ARA (C20:4) by more than 40%, and M10 and M14 were both below 40% insignificantly. Followed by SFAs, with C16:0 at around 11-14%. The remaining abundant fatty acids were lower than 10% in TFA (Table 5.13). As a result, the stability of M9 and M13 was slightly better. However, the four best mutants exhibited a non-significant difference compared to wild-type MA2-2 strain, indicating that the four mutants did not exhibit a beneficial phenotype, but maintained a wild-type phenotype.

Table 5.13: Fatty acid content (% in TFA) of UV mutagenized strains, namely M9, M10, M13 and M14 in comparison to the wild-type MA2-2 (WT)

	C16:0	C18:0	C18:1	C18:2	C18:3	C20:3	C20:4	C22:0	C24:0
WT	12.5±0.15	8.56±0.35	9.06±0.56	8.25±0.16	5.34±0.18	5.50±0.06	41.1±0.39	1.88±0.05	3.47±0.10
M9	12.2±0.35	8.58±0.28	9.37±0.37	8.30±0.14	5.19±0.16	5.33±0.28	41.4±0.39	1.85±0.09	3.56±0.06
M10	14.1±0.39	9.19±0.06	10.7±0.71	8.85±0.33	5.14±0.33	5.58±0.25	36.8±1.03	1.78±0.06	3.30±0.32
M13	11.9±1.23	8.00±0.98	8.76±0.39	8.12±0.47	5.07±0.08	5.37±0.23	42.9±3.01	1.83±0.05	3.61±0.12
M14	13.3±0.91	8.78±0.37	9.84±1.12	9.03±0.11	4.99±0.07	5.27±0.06	39.3±2.89	1.78±0.28	3.29±0.11

5.4 High-Temperature ALE

5.4.1 High Temperature Screening

To develop a high temperature process for ARA production, it is important to find a strain that can resist high temperatures and simultaneously accumulate relatively high amounts of ARA. An adaptive evolution strategy can then be used, where a suitable adaptive pressure, such as high temperature, should be determined before adaptive evolution (Hu et al., 2021).

5.4.1.1 First High-Temperature Screen and ALE Attempt 1

5.4.1.1.1 Observation of Cell Morphology at Different High Temperatures

For the first high-temperature screening, the effects of different temperatures (28℃ (control), 32℃, 35℃, 38℃) on cell growth of *M. alpina* 2-2 were explored and results are shown in Figure 5.19. Inoculation of the shake flasks was done by adding mycelium-covered agar at different temperatures. Biomass production and glucose consumption were the main determinants for stress inducer selection. The cell growth of MA2-2 strain was not affected at 30°C, but was significantly inhibited when the temperature was further increased to 32°C. It could be easily observed on day 4 that thick mycelium was obtained in the control at 30°C, while very little of mycelium was observed at temperatures higher

than 32°C (Figure 5.19) The morphogenesis was different at different temperatures. For example, dispersed or filamentous morphology was observed for cultures grown at 28°C and 30°C, and under the microscope it could be seen that the branches were filled with spores, indicating that the cells readily absorbed nutrients, resulting in glucose depletion by day 8. In contrast, the few mycelia grown at 32°C were granular and consumed little glucose, suggesting that their granularity makes it difficult to absorb energy and carbon as a source of lipid synthesis. In addition, the cells that were present at 32 °C were in the form of a large entangled fuzzy ball, where all branches were swirling to form a loose pellet, and more vesicles were observed, but with fewer intracellular spores. No growth was observed at 35 to 38°C, showing a 100% killing rate at these temperatures.

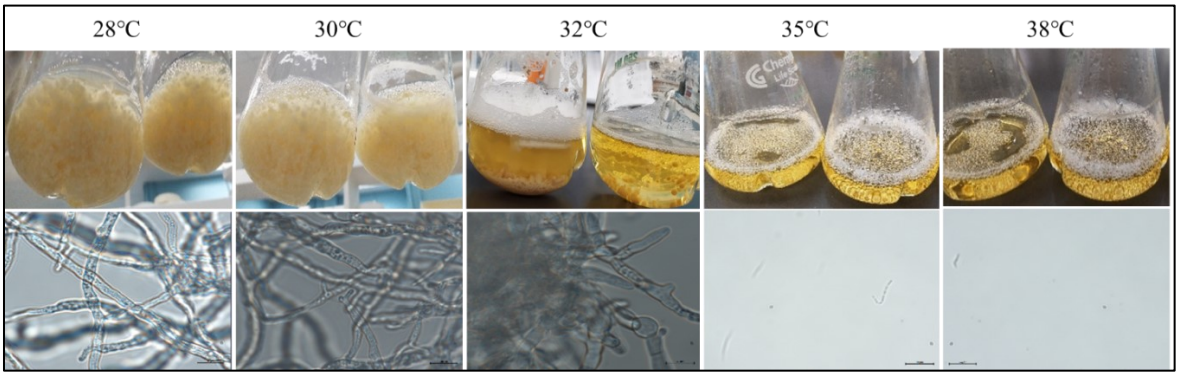

Figure 5.19: Growth performance and microscope pictures of MA2-2 strains at various high temperatures for the initial temperature screen (scale bars: 10µm)

5.4.1.1.2 Observation of Glucose Consumption, Biomass and Fatty Acid Profiles at Different High Temperatures

It was observed that at 28°C and 30°C, 100% of the glucose was consumed. Glucose consumption decreased significantly at day 3 and eventually all glucose was consumed by day 8. At 32°C, glucose was barely consumed until day 7, and later only 5 g L^{-1} was consumed at the end point, reaching a consumption of 14.3%. There was neither growth nor glucose depletion in the experiments at 35°C and 38°C. The growth phase was different at 32 °C compared to 28°C or 30°C due to incomplete glucose consumption.

There was no significant difference in the results obtained at 28°C and 30°C, with around 22 g L^{-1} of biomass, 23% of total oil and 23% of ARA in TFA. At 32 ℃, only 2.97 g L^{-1} of biomass, 10.8% of total oil and 13% of ARA accumulated; in the early growth phase, more SFA than PUFA was formed, so the accumulation of C16:0 palmitic and C18:1 oleic was higher than ARA (Figure 5.20). To conclude, the condition at 32℃ had a stronger inhibitory effect on wild-type MA2-2 growth, which can be used the stress factor throughout the adaption.

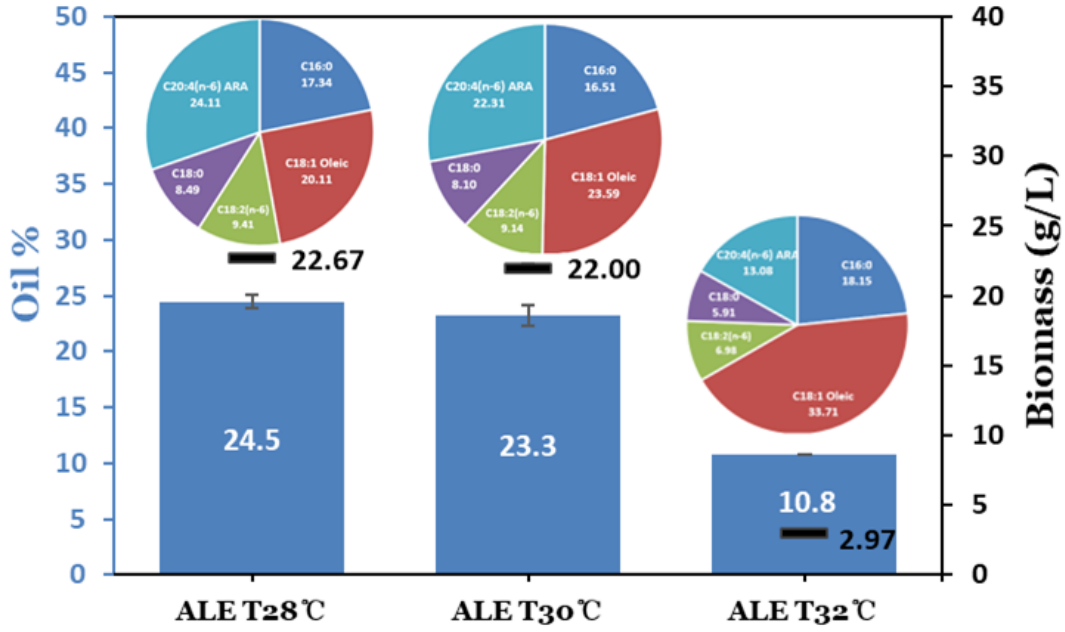

Figure 5.20: Fatty acid profile of MA2-2 strain growing at 28℃, 30℃ and 32℃. The percentage of total oil within the biomass is given by the number at each column, aligning to the y-axis on the left side. Biomass production in g L^{-1} is indicated by a black line overlaid on the % TFA bar, aligning to the y-axis on the right side. The pie chart represents the fatty acid profile with the % contribution of most abundant fatty acids to the TFA by a different colour, C16: 0 (blue); C18: 0 (purple); C18: 1 (red); C18: 2 (green) and ARA (C20: 4) (light blue).

5.4.1.1.3 High temperature ALE attempt at 32°C

When ALE was started by transferring 10% of the liquid culture in shake flasks at 32°C, the mycelia grew relatively fast within 24 hours. Previously, temperature screening was done by inoculating mycelia from PDA plates (Section 5.4.1.1), so fewer cells were introduced into the medium which would have introduced less mycelia, and may have enhanced temperature sensitivity and decreased thermotolerance. However, the starting point for ALE was the addition of 10% liquid culture, which may have caused inconsistencies in cell concentrations. At higher cell concentrations, the temperature of 32°C appeared to be less inhibitory for the early generation. The first attempt of high temperature ALE was terminated after the first cycle at 32°C, because the initial growth of liquid cultures at this temperature indicated that there would be insufficient inhibition.

5.4.1.2 Second High-Temperature Screen and ALE Attempt 2

5.4.1.2.1 Observation of Cell Morphology at Different High Temperatures

The initial temperature screening (Section 5.4.1.1) enabled the appropriate range of stress temperatures used for ALE to be determined. However, when ALE started (Section 5.4.1.1.3), the different inoculation cultures caused inconsistencies in cell concentration, making them tolerate temperature differently. To better understand thermotolerance during the adaptive strategy, a second temperature screen was conducted to study inhibitory effects at different temperatures while maintaining consistency in the inoculation culture.

From the first temperature screening, the glucose consumption decreased from 14.2% to 0% between 32℃ to above 35℃. It was worth trying to see how cell growth would be affected at temperatures of 32°C, 34°C and 36°C. The 34°C temperature was between 32°C and 35°C, and also appeared in the high-temperature ALE experiment for DHA production study by Hu et al. (2021) who used 34.5°C as the stress. In addition, 36°C was between 35°C and 38°C, filling the previous gap in temperature screening. The second temperature screen followed the ALE protocol of adding 10% liquid cultures at different temperatures, which were initially derived from seed cultures grown at the control temperature. Since the

biomass, glucose consumption and fatty acids were studied in a previous temperature screen, the second screen lasted only 72 hours and was used for daily monitoring of cell growth (Figure 5.21).

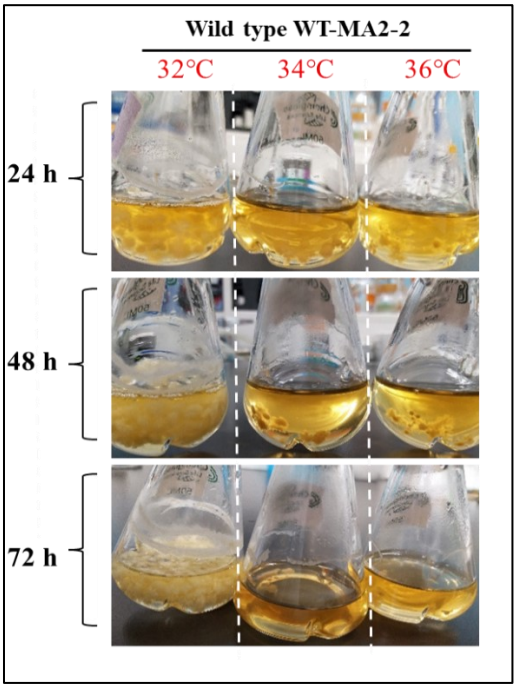

Figure 5.21: Growth performance of wild-type MA2-2 strains at temperatures 32°C, 34°C and 36°C within 72 h in flask assays for the second temperature screen

As shown in Figure 5.21, the mycelia grew well within 24 h at 32°C, similar to the first attempt of ALE. In contrast, mycelium growth was much slower at 34°C and 36°C, especially at 36°C where there was hardly any growth. At 34°C, a few mycelia formed biomass rings at the edge of the flask after 72 h, indicated that 34°C can be expected to have a high inhibitory effect and was therefore selected as the new stress temperature.

5.4.1.2.2 High temperature ALE attempt at 34°C

As shown in Figure 5.22, when the second high temperature ALE started at 34°C, cell growth was clearly observed at the end of the first cycle, i.e. biomass rings and more mycelium growth. However, from the beginning of the second ALE cycle, the mycelium

prolonged its growth, so that a few mycelia grew after the second cycle. In the subsequent cycles, as no new mycelium formed, the original ALE parental strain was gradually reduced and the concentration of cells in each culture decreased until the mycelium shrank and was considered dead at the end of cycle 5.

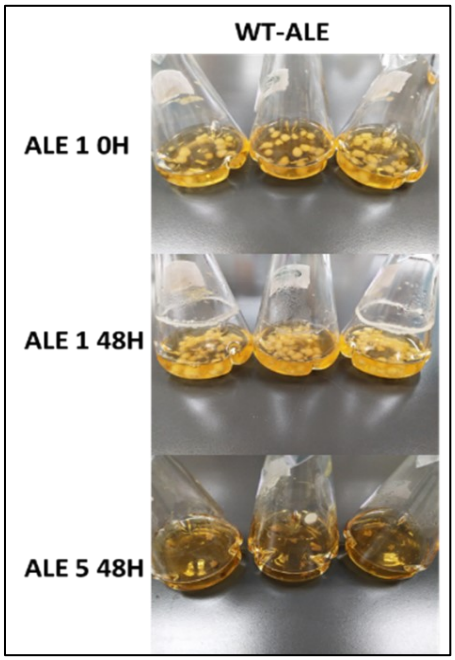

Figure 5.22: Adaptive evolution of cell performance at 34°C for the first 5 cycles, and ALE terminated at cycle 5

5.4.1.3 Third High-Temperature Screen and ALE Attempt 3

The second temperature screen (Section 5.4.1.2) used a more consistent inoculant culture and its results showed that the thermotolerance of mycelia gradually decreases as ALE progresses through more generations, which suggests a greater temperature sensitivity when exposed to high temperatures for longer periods of time. The original hypothesis with high temperature ALE was that cell growth would be greatly affected by high temperatures from the outset, and over time, evolved strains could eventually overcome growth at such stressful temperatures. However, after five cycles of ALE at 34°C, it was seen that the early evolved strains were extremely sensitive to high temperatures.

Since their former parental strains struggled in growth, their subsequent daughter cells resembled their parental cells and developed unhealthy growth in later generations. The stress temperature of 34°C was too inhibitory for the formation of new, healthy daughter cells, and eventually all the cells died.

To further select the stress temperature that both inhibited normal cell growth and allowed the cells to still survive, a third temperature screening was conducted by comparing the cell growth in different high temperature ALEs in parallel. Previous screening indicated normal growth at 32℃ and a strong inhibition at 34℃, thus the re-screening occurred at temperatures 32℃, 32.5℃ and 33℃, and lasted for 10 days for the first five ALE cycles with culture transferred simultaneously for the three temperatures. The results are shown in Figure 5.23 and indicate that the first two cycles were less inhibited at temperatures of 32°C and 32.5°C, but were more inhibited and grew slowly at 33°C. No significant differences between the three temperatures were observed at 100x magnification, and germinated branches filled with spores could be easily observed. However, cell growth ceased at all conditions starting from ALE cycle 3, especially at 33°C when there was almost no growth. At 33°C, the microstructure appeared to be disrupted, as most of the swirling branches were separated and also filled with large cell membrane vesicles rather than spores. The sporangial stage was greatly affected and hardly any individual spores were observed floating in the background. The mycelium shrank and decreased in size and was considered dead after the third cycle at 33°C. Cell growth was slightly better at 32°C because there were fewer vesicles in the microstructure than at 32.5°C, as well as more mycelium growth at 32°C. Although cell growth was much slower at 32.5°C, there was still mycelia surviving at the end of the fifth cycle. Therefore, a temperature of 32.5°C was selected for subsequent ALE generations (Figures 5.23).

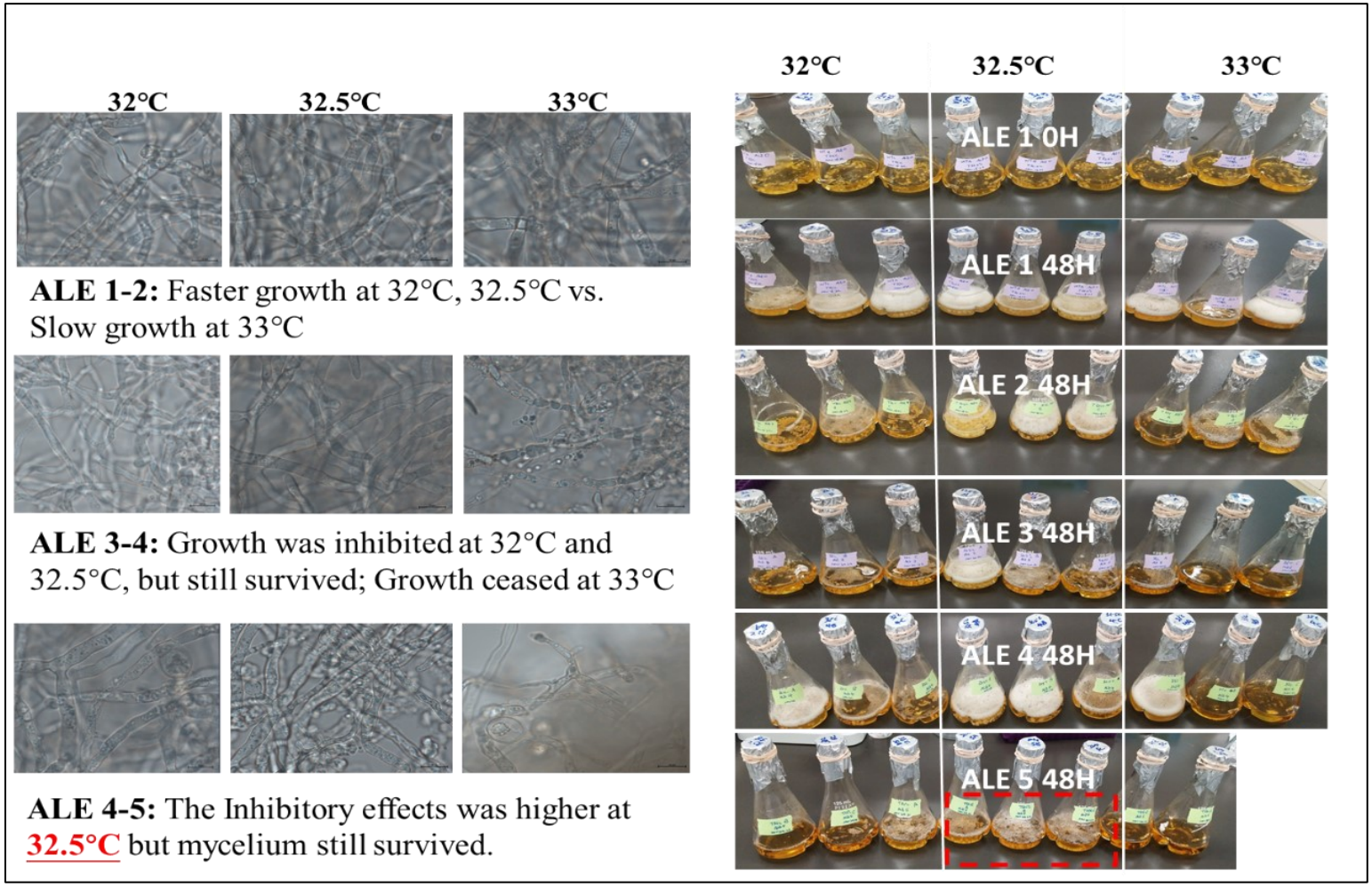

Figure 5.23: Growth performance and microscope pictures of MA2-2 adaptive strains for the first 5 ALE cycles, at temperatures 32°C, 32.5°C and 33°C for the third temperature screen (scale bars: 10µm)

5.4.2 High Temperature ALE at 32.5°C - Observation of Cell Performance during Adaptation

Subsequent adaptive evolution experiments continued at 32.5°C starting from cycle 5 and lasted for a period of 90 days. The evolved strains were recorded as ALE5, ALE10 for every 5 cycles until ALE45 was used as the end point, and each cycle lasted 48 h as the default setting for recovery. Results illustrating the cell performance are shown in Figure 5.24.

The evolved strains of early adaptations struggled to grow at high temperatures, especially in the first 10 cycles, with very little and extremely slow growth. At the end of each cycle, not many seeds were ready for passage. The mycelia exhibited a pellet-shaped morphology in the early stages, indicating nutrients were not easily absorbed from the medium. In addition, the pellet shapes in different sizes formed extremely heterogeneous cultures, making passage difficult. When passing from ALE10 to ALE15, the mycelia tended to gradually adapt to 32.5°C as more filamentous forms were observed, which allowed for faster cell growth. A clear observation showed that on approaching ALE15, more mycelia germinated into hyphae and the culture became more homogeneous and could be passed on more easily. The first 15 cycles were defined as the high temperature adaptive period, in which the strain was greatly inhibited by high temperatures in the early stages, and with successive passes to ALE15, cell performance became normal growth (Figure 5.24).

From ALE16 to ALE30, cell growth returned to normal, and more mycelia and faster growth was achieved within 48 hours. Up to this point, 10% of the cultures contained more seeds than in the first 15 cycles. To enhance the stress on cell growth, the passage culture was reduced to introduce fewer parental cells in the new cycle by gradually reducing the culture from 10% to 2.6% culture at the end of the final ALE30. Consequently, the strain was able to grow with fewer seeds in each cycle (Figure 5.24).

In order to keep increasing the pressure on cell growth, the recovery period was

shortened in the last 15 cycles. The strain was successfully grown in 48 hours with only 2.6% of the culture introduced at 32.5°C at the end of ALE30. Subsequent cultures were maintained at 3% of the culture passaged to the next generation, and the culture time was gradually reduced from 48 hours to a final 24 hours at ALE45. Initially, the adapted strain exhibited inhibited growth for a shorter period of time. However, as the incubation time was shortened from 48 to 40, 36 and finally 24 hours, the endpoint of the evolved strain ALE45 exhibited faster growth within 24 hours. In conclusion, visual observations of cell performance during adaptation suggested that the endpoint evolved strain ALE45 exhibits rapid growth in a shorter inoculation time (Figure 5.24).

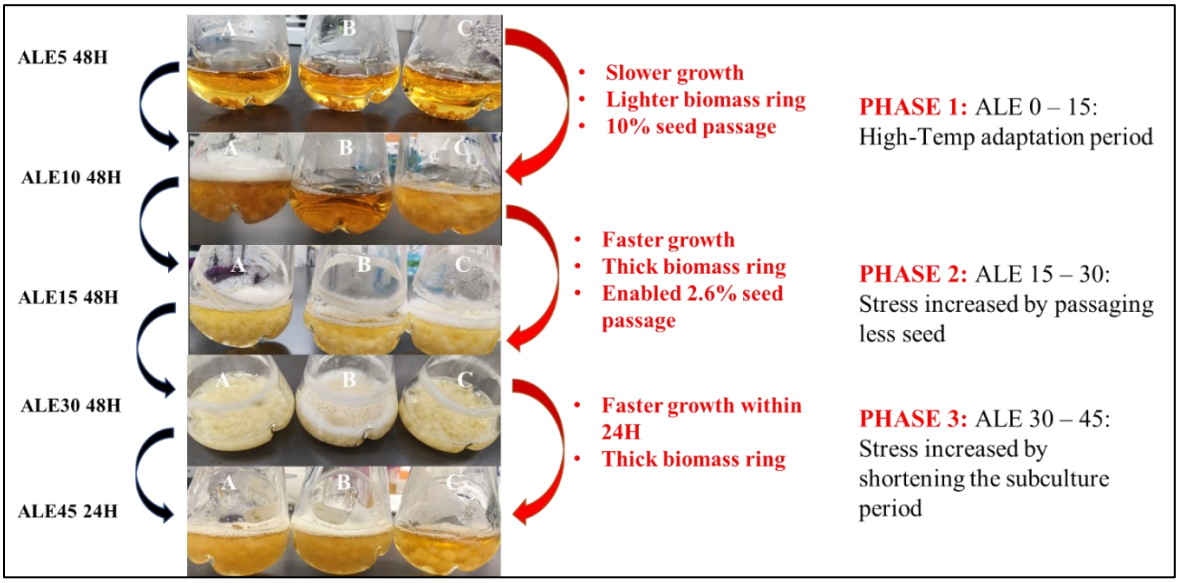

Figure 5.24: Adaptive laboratory evolution of cell performance at 32.5°C

5.4.3 ALE Characteristic Results after Adaptation

In order to obtain the most promising adapted strains as well as to test the sensitivity of the strain to temperature, the fermentation characteristics were compared between the starting strain and adapted strains every 5 cycles, namely ALE5, ALE10, ALE15 till ALE45. Fermentation periods were determined by the time of glucose exhaustion or the end of 12 days (288 h). The characteristics experiment was intended to explore the cell

performance of the adaptive strains at normal conditions. To maintain consistency throughout the experiment, experiments were carried out in 250 mL shake flasks at 28°C and 32.5°C. The culture was inoculated by adding mycelia covered agar from PDA plates, which was passaged from -80°C glycerol stocks. A comprehensive analysis included biomass DCW (g L^{-1}), total oil%, ARA%, ARA concentration (mg L^{-1}) and ARA productivity (g $L^{-1}d^{-1}$) and fermentation periods (h) were discussed and compared in both temperatures.

5.4.3.1 Fermentation of the Adaptive Strains at High Temperature 32.5°C

The fermentation of the adapted strains was similar to the experiments performed for the initial temperature screening, that had inoculated mycelia grown on PDA plates. The introduction of fewer mycelium in the culture broth was supposed to improve the sensitivity to temperature. Consequently, pellet-like morphology was formed during the fermentation at 32.5°C, and their entangled large pellets prevented the mycelium from absorbing major nutrients for cell growth and lipid accumulation. This resulted in most adapted strains (including wild-type (WT)) being slowly depleted of glucose by the end of 288 hours. Most of them only depleted 5 – 10 g L^{-1} glucose at the end point; However, subsequent evolved strains gradually depleted more glucose, until ALE45 was capable of consuming all glucose to 0 g L^{-1} at 264 h (Figure 5.25). This indicated that the evolved strain exhibited better glucose uptake performance as well as faster growth rate, suggesting that adaptive strains had a more vigorous metabolism, resulting in higher growth rates and glucose consumption rates (Hu et al., 2021).

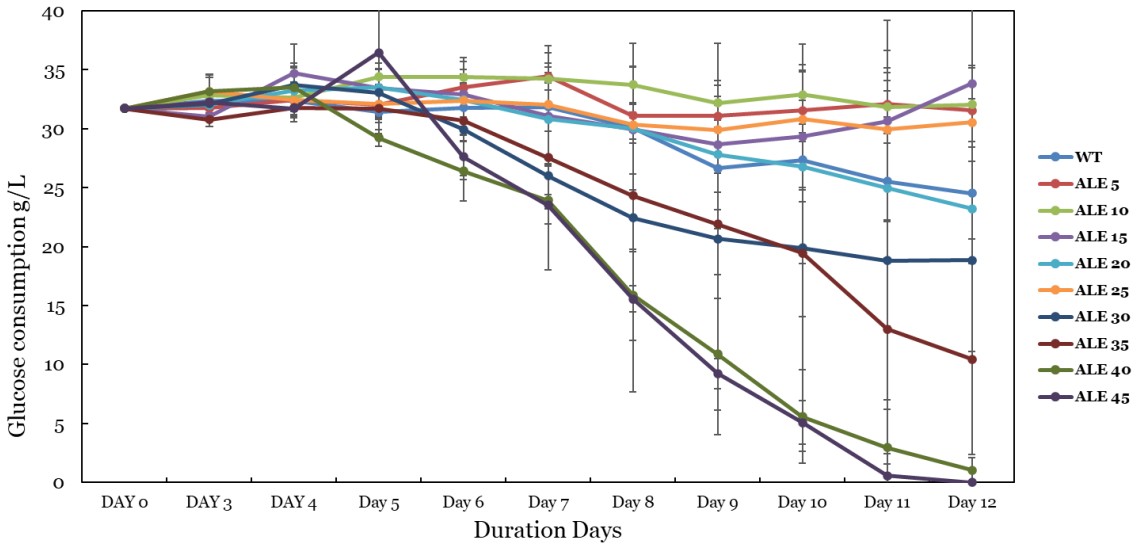

Figure 5.25: Glucose depletion (g L^{-1}) of MA2-2 starting strain and ALE adapted strains grown at high temperature (32.5°C) in every 5 ALE cycles

In terms of biomass, cell growth showed an increasing trend from ALE5 to ALE45, ranging from 3.51 ± 0.32 to 17.8 ± 0.36 g L^{-1} compared to 8.98 ± 3.01 g L^{-1} for the wild type (WT). The strain exhibited a struggling growth period, especially for the first 15 cycles, with growth below 4.93 ± 4.33 g L^{-1} at ALE15. In the following cycles, DCW gradually increased, eventually reaching 17.8 ± 0.36 g L^{-1}, a 1-fold increase compared to WT, indicating that the strain started to adapt to high temperatures (Figure 5.26 A and Table 5.14).

In terms of fatty acid contribution, all these evolved strains were rich in C16 and C18 fatty acids. The main lipids included myristic acid (C14: 0), C16: 0, stearic acid (C18: 0), C18: 1, C18: 2, linolenic acid (C18: 3), eicosatrienoic acid (C20: 3), ARA (C20: 4) and tetracosanoic acid (C24: 0) (Yao et al., 2019). At 32.5°C, C18:1 was the most abundant fatty acid, accounting for about 30% of the total fatty acids, followed by ARA (C20:4) at about 18% and C16:0 at about 16%. However, there were no significant differences in the different adaptations (Figure 5.26A and Table 5.14). High temperatures only increased the synthesis of saturated fatty acids, but the fatty acid structure was consistent throughout the adaptation.

Lipid accumulation increased during the adaptations. The original strain accumulated 11.9 ± 1.11% of total oil in biomass, and adapted strains increased from 15.2 ± 0.96% in ALE5 to 22.4 ± 2.34% in ALE45, indicating a 0.9-fold increase in total oil rate (Figure 5.26 A and Table 5.14). Lipid accumulation was mainly based on carbon sources. Glucose depletion is a key factor in determining whether the strain can take up carbon sources for growth and lipid accumulation (Cao et al., 2015; A. Singh & Ward, 1997). The aforementioned glucose consumption indicated the evolved strains were able to deplete glucose by the end of fermentation, which also contributed to the accumulation of more lipids.

ARA concentrations were mainly based on biomass, oil % and ARA%. Therefore, ARA concentration was expected to increase with increasing above mentioned factors; from 97.5 ± 10.7 mg L^{-1} in ALE5 to 759 ± 96.6 mg L^{-1} in ALE45, which was a 3.5-fold increase compared to 170 ± 30.0 mg L^{-1} in WT (Figure 5.26 B and Table 5.14). Considering the fermentation period, the final ARA productivity of ALE45 was 0.052 ± 0.009 g $L^{-1}d^{-1}$, which was a 4.2-fold increase compared to 0.01 ± 0.002 g $L^{-1}d^{-1}$ of WT (Table 5.14).

The final evolved strain still exhibited a pellet-like morphology similar to the mycelial morphology at high temperatures in the first round of temperature screening, when inoculated from the plates. Remarkably, cell performance of the evolved strain at 32.5°C was comparable to that of the WT strain at 28°C in the first round of temperature screening. After 45 cycles of long-term high temperature acclimation, it was shown that the evolved strain exhibited better cellular performance in terms of cell growth and lipid accumulation.

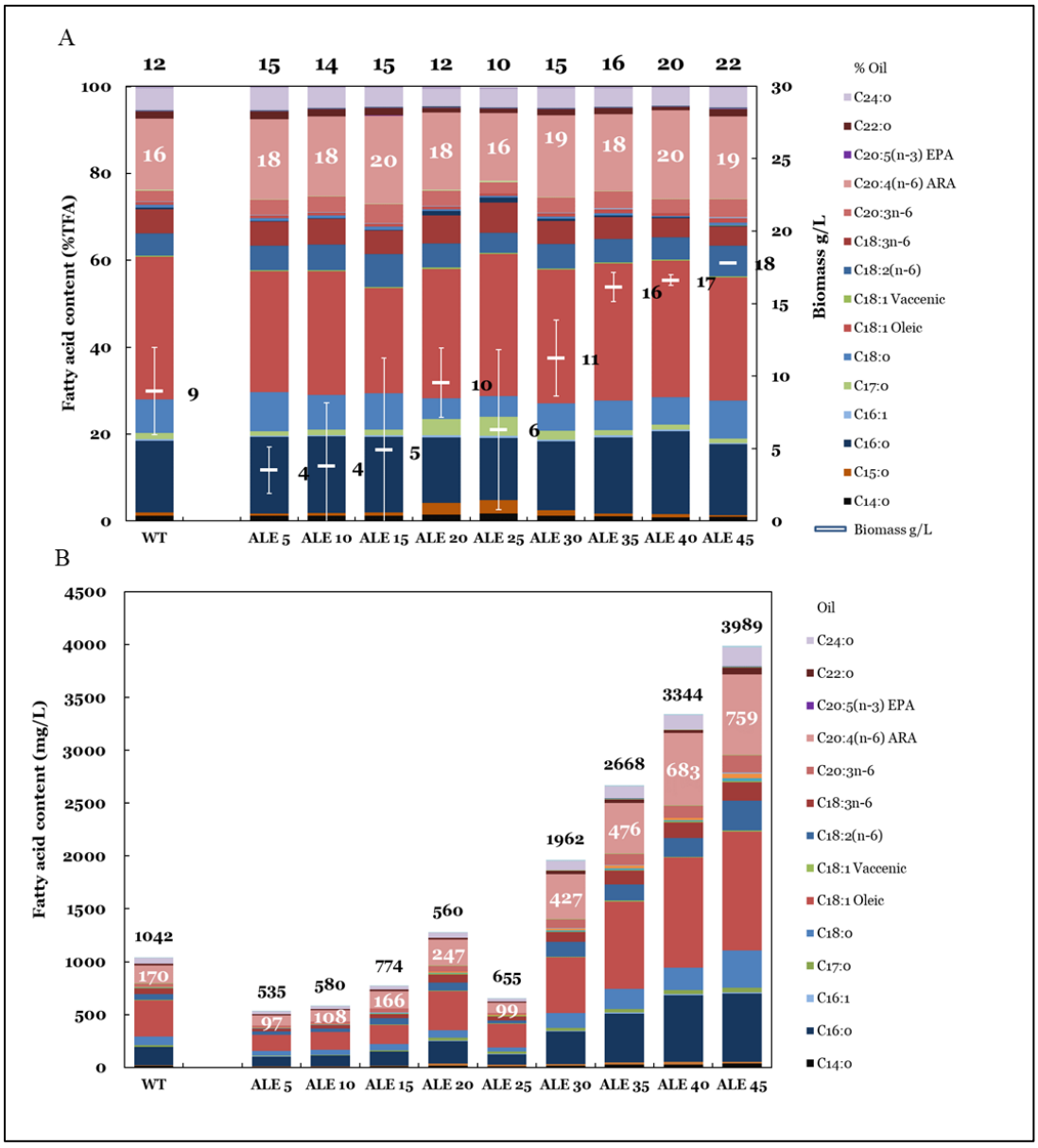

Figure 5.26: Fatty acid profile A) in w/w %; and B) in mg L^{-1} of MA2-2 starting strain and ALE adapted strains grown at high temperature (32.5°C) in every 5 ALE cycles. The stacked bar for each strain represents the fatty acid profile with the % contribution and concentration mg L^{-1} of each individual fatty acid to the TFAs indicated by a different colour (see legend). The chain length of the fatty acids increases from bottom to top of the bar graphs, likewise with saturated to unsaturated. ARA (20:4 n-6) is denoted in pink and labelled in both figures. Biomass production in g L^{-1} is indicated by a white line overlaid on the % TFA bar, aligning to the y-axis on the right side. The percentage and amounts (mg L^{-1}) of total oil within the biomass is given by the number at the top of each bar.

5.4.3.2 Fermentation of the Adaptive Strains at Normal Temperature 28°C

Mycelial morphology was different from that at 32.5°C, and a more dispersed or filamentous morphology was observed in all strains grown at 28°C. The dispersed mycelium absorbed nutrient sources more readily than the granular mycelium and therefore consumed glucose more rapidly. In particular, evolved strains exhibited faster glucose consumption, ranging from 144 ± 1.73 h in ALE5 to 136 ± 1.15 h in ALE15, which was approximately 40 h faster compared to 176 ± 0.58 h in WT. However, the glucose consumption was not a linear increasing trend, but a hyperbolic trend. Glucose consumption was completed at 144±1.73 h in ALE5, then decreased to 104±0.58 hours in ALE35, and then increased slightly to 136±1.15 h at the endpoint (Figure 5.27). This may indicate the adaption to control temperature varied in evolved strains.

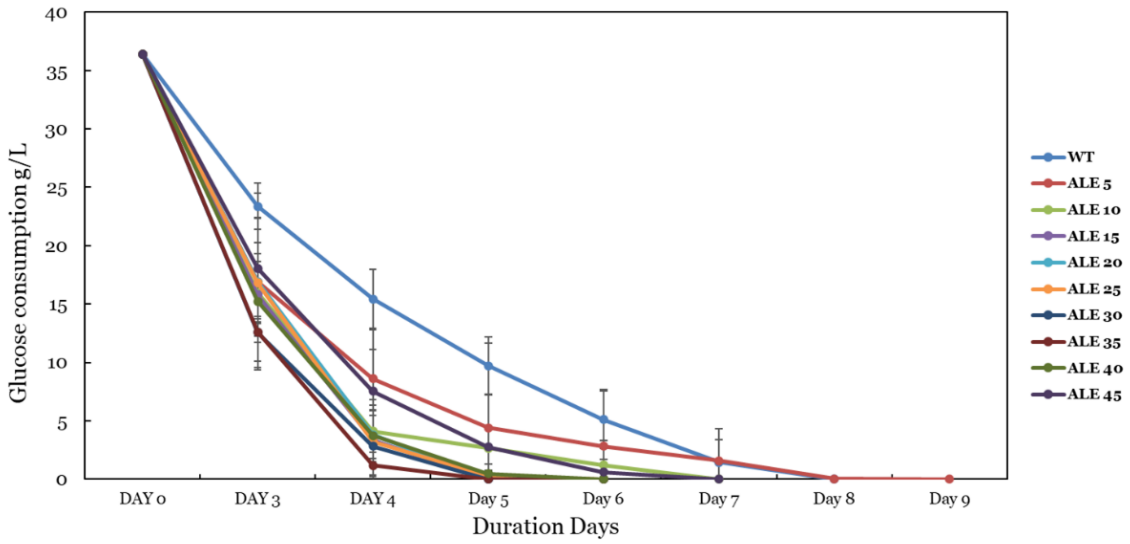

Figure 5.27: Glucose depletion (g L^{-1}) of MA2-2 starting strain and ALE adapted strains grown at control temperature (28°C) in every 5 ALE cycles

Biomass, oil% and ARA% remained high during acclimation, but there were no significant differences among all strains. The performance of all strains, including WT, was about 21 g L^{-1} of DCW, 32% total oil in biomass and 31% ARA in TFA, indicating that the genotypes of all strains should be similar and not altered or destroyed by high temperature incubation (Figure 5.28 A and Table 5.14). The MA2-2 evolved strain maintained a high performance comparable to WT, but with a shorter fermentation time under normal conditions, unlike the investigation of Hu et al. (2021) on high temperature ALE for DHA-producing strains, where they had a shorter fermentation time and 59.65% higher biomass than the original strain, but their TFA% decreased by 23.32%.

ARA concentration remained consistent for all strains, reaching around 2324 mg L^{-1} (Figure 5.28 B and Table 5.14). However, the final ARA productivity was different due to the variation in fermentation time, initially increasing from 0.417 ± 0.12 g $L^{-1}d^{-1}$ in ALE5 to 0.538 ± 0.08 g $L^{-1}d^{-1}$ in ALE35 and slightly decreasing to 0.421 ± 0.04 g $L^{-1}d^{-1}$ in ALE45, which was still 27.6% higher than of the original strain of 0.330 ± 0.04 g $L^{-1}d^{-1}$ (Table 5.14). In conclusion, cell performance of the adapted strains was comparable to that of the original strains, but their shorter fermentation time resulted in higher ARA productivity.

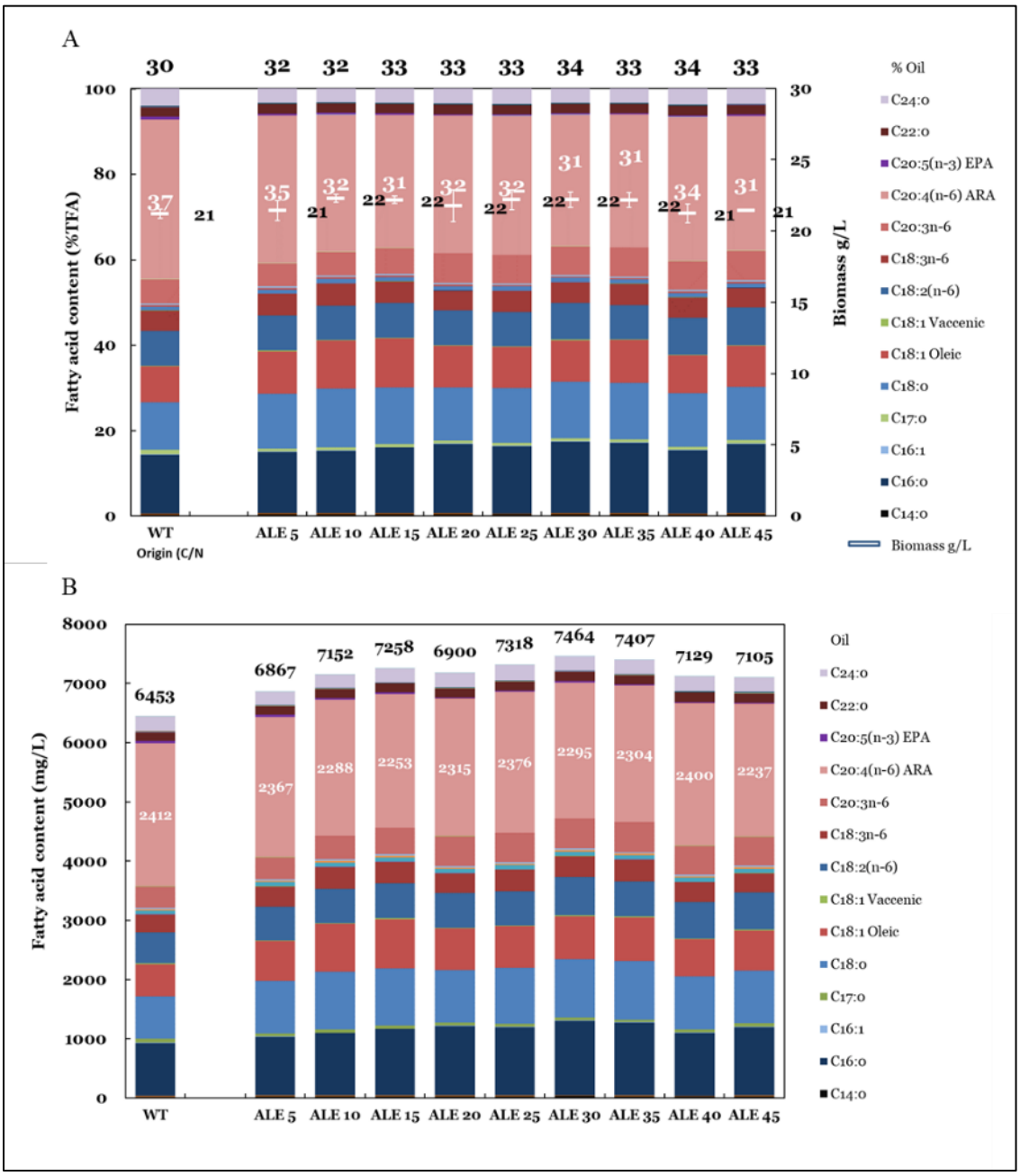

Figure 5.28: Fatty acid profile A) in w/w %; and B) in mg L^{-1} of MA2-2 starting strain and ALE adapted strains grown at control temperature (28°C) in every 5 ALE cycles. The stacked bar for each strain represents the fatty acid profile with the % contribution and concentration mg L^{-1} of each individual fatty acid to the TFAs indicated by a different colour (see legend). The chain length of the fatty acids increases from bottom to top of the bar graphs, likewise with saturated to unsaturated. ARA (20:4 n-6) is denoted in pink and labelled in both figures. Biomass production in g L^{-1} is indicated by a white line overlaid on the % TFA bar, aligning to the y-axis on the right side. The percentage and amounts (mg L^{-1}) of total oil within the biomass is given by the number at the top of each bar.

5.4.3.3 Temperature sensitivity of the starting and adaptive strains

To compare the sensitivity of the strains to temperature at 28°C to 32.5°C, the rates of reduction in the performance of biomass DCW (g L^{-1}), total oil%, ARA%, ARA concentration (mg L^{-1}) and ARA yield (g $L^{-1}d^{-1}$) were compared and formula was shown in Eq. 9. The smaller the rate of reduction (%), the smaller the effect of temperature on this performance. As shown in the Table 5.15, the indices ΔALE5, ΔALE10... until ΔALE45 was the change extent per 5 adaptation cycles.

When the temperature increased from control at 28°C to 32.5°C, the reduction rate of DCW decreased from 83.6% for ALE5 to 17.2% for ALE45, a 0.7-fold reduction compared to 57.6% for WT. Similar observations were found in oil% and ARA%, where the reduction rate decreased from 52.7% and 47.0% in ALE5 to 32.5% and 39.7% in ALE45, a 0.47-fold and 0.29-fold decrease compared to 60.9% and 55.8% in WT, respectively (Table 5.15). Thereby, smaller reduction rates in endpoint evolved strains indicated that long-term adaptation could reduce the sensitivity of cell growth, lipid accumulation and ARA synthesis to temperature.

The starting strain showed high temperature sensitivity to cell growth, lipid accumulation and ARA synthesis, and its ARA final concentration (mg L^{-1}) reached only 170 ± 30.0 g L^{-1} at 32.5°C, thus its reduction rate reached 92.9% at 2411 ± 166 mg L^{-1} at control temperature. Since the temperature sensitivity was much slower in the endpoint evolved strain, its ARA concentration reached 759 ± 96.6 mg L^{-1} at 32.5°C, compared to 2237 ± 203 mg L^{-1} at 28°C, and its reduction rate reached 66.1% (Table 5.15).

In addition, ARA productivity (g $L^{-1}d^{-1}$) also relied on fermentation time. As discussed earlier, fermentation of final evolved strain was around 40 h faster than starting strain at normal condition, thus a lower temperature sensitive can be expected. Starting strain obtained 0.01 ± 0.002 g $L^{-1}d^{-1}$ at high temperature, compared to 0.330 ± 0.04 g $L^{-1}d^{-1}$ at normal temperature, reached a 92.9% reduction rate. In contact to evolved strain, ALE45 had a 0.052 ± 0.009 g $L^{-1}d^{-1}$ at 32.5°C, an 87.6% reduction ratio was achieved compared

to 0.421 ± 0.04 g $L^{-1}d^{-1}$ at 28°C (Table 5.15). Overall, the temperature sensitivity of ARA concentration and final productivity of the evolved strain reduced 28.9% and 9.7% compared to the starting strain. These results showed that the evolved strain successfully enhanced the thermotolerance for cell growth, lipid and ARA accumulation.

Table 5.14: Difference of fermentation performance between the original strain and adaptive strains under 28°C and 32.5 °C

	28°C						32.5°C					
	DCW ($g\ L^{-1}$)	TFA %	ARA %	ARA concentration ($mg\ L^{-1}$)	ARA productivity ($g\ L^{-1}d^{-1}$)	Fermentation period (h)	DCW ($g\ L^{-1}$)	TFA%	ARA %	ARA conc. ($mg\ L^{-1}$)	ARA productivity ($g\ L^{-1}d^{-1}$)	Fermentation period (h)
WT	21.2±0.32 Aa	30.4±0.99 B	37.3±1.61 A	2411±166 A	0.330±0.04 A	176±0.58 A	8.98±3.01 B	11.9±1.11 B	16.5±0.87 A	170±30.0 B	0.01±0.002 B	288±0.00 A
ALE5	21.4±0.81 A	32.0±0.80 AB	34.5±0.79 AB	2367±96.1 A	0.417±0.12 A	144±1.73 AB	3.51±0.32 B	15.2±0.96 AB	18.3±2.30 A	97.5±10.7 B	0.008±0.001 B	288±0.00 A
ALE10	22.3±0.70 A	32.1±1.03 AB	32.1±2.02 B	2288±60.5 A	0.452±0.13 A	120±1.73 AB	3.81±1.60 B	14.4±3.15 AB	18.3±0.71 A	108±64.0 B	0.015±0.02 AB	288±0.00 A
ALE15	22.2±0.28 A	32.7±0.93 AB	31.1±1.36 B	2252±70.4 A	0.489±0.07 A	112±0.58 B	4.93±4.33 B	14.7±1.82 AB	20.2±3.14 A	166±169 B	0.014±0.01 AB	288±0.00 A
ALE20	21.8±0.24 A	33.0±0.81 AB	32.2±2.56 B	2314±203 A	0.463±0.04 A	120±0.00 AB	9.56±6.32 AB	11.7±3.89 B	17.7±2.52 A	247±268 AB	0.021±0.02 AB	288±0.00 A
ALE25	22.2±1.12 A	33.0±1.20 AB	32.5±0.19 B	2375±161 A	0.518±0.10 A	112±0.58 B	6.29±2.39 B	10.0±1.69 B	15.6±1.46 A	98.8±44.7 B	0.008±0.004 B	288±0.00 A
ALE30	22.2±0.72 A	33.7±1.84 A	30.7±0.77 B	2294±92.0 A	0.496±0.05 A	112±0.58 B	11.3±5.52 AB	15.0±7.93 AB	18.7±4.76 A	427±501 AB	0.041±0.05 AB	272±1.15 A
ALE35	22.2±0.55 A	33.4±0.59 AB	31.1±1.52 B	2304±120 A	0.538±0.08 A	104±0.58 B	16.1±2.63 A	16.1±3.67 AB	17.7±0.70 A	476±195 AB	0.040±0.02 AB	288±0.00 A
ALE40	21.2±0.50 A	33.6±0.17 A	33.7±0.54 AB	2400±88.1 A	0.454±0.06 A	128±0.58 AB	16.6±1.02 A	20.0±2.80 AB	20.4±0.81 A	683±162 AB	0.059±0.02 AB	280±0.58 A
ALE45	21.5±0.67 A	33.2±1.27 A	31.5±2.54 B	2237±203 A	0.421±0.04 A	128±1.15 AB	17.8±0.36 A	22.4±2.34 A	19.0±0.38 A	759±96.6 A	0.052±0.009 A	264±0.00 A

[a] Experimental results in Mean ± SD, n = 3. Letters refer to significant terms comparison by Tukey ANOVA analysis within 95% confidence interval.

Table 5.15: Difference of temperature sensitivity between the original strain and adaptive strains under 28°C and 32.5 °C

Temp Sensitivity ratio	DCW (g L^{-1})	Oil (w/w %)	ARA (w/w %)	ARA production(mg L^{-1})	ARA production (g/L/d)
ΔWT[a] (28~32.5℃)	57.6%	60.9%	55.8%	92.9%	97.0%
ΔALE5 (28~32.5℃)	83.6%	52.5%	47.0%	95.9%	98.1%
ΔALE10 (28~32.5℃)	82.9%	55.1%	43.0%	95.3%	96.7%
ΔALE15 (28~32.5℃)	77.8%	55.0%	35.0%	92.6%	97.1%
ΔALE20 (28~32.5℃)	56.1%	64.5%	45.3%	89.3%	95.5%
ΔALE25 (28~32.5℃)	71.6%	69.7%	52.0%	95.8%	98.4%
ΔALE30 (28~32.5℃)	49.1%	55.5%	39.1%	81.4%	91.7%
ΔALE35 (28~32.5℃)	27.5%	51.8%	43.1%	79.3%	92.6%
ΔALE40 (28~32.5℃)	21.7%	40.8%	39.5%	71.5%	87.0%
ΔALE45 (28~32.5℃)	17.2%	32.5%	39.7%	66.1%	87.6%

[a] The reduction ratio is calculated $\Delta(T_{28}\sim T_{32.5}) = \frac{X_{32.5}-X_{28}}{X_{28}}$

5.4.3.4 Comparison in modified media, ALE 15, 30, 45 vs. WT

An additional experiment was performed regarding the comparison of evolved strains in a final modified fermentation medium at room temperature, to investigate if lipid and ARA accumulation could be improved in the media-experiments as in the MA2-2 wild type. The difference between the ALE working medium and the final modified medium was the combination of nitrogen sources, i.e., a combination of organic and inorganic

nitrogen sources was added to the modified medium. The nitrogen mixture design showed that the lipid and ARA content of the MA2-2 strain could be increased to more than 30% and 35%, respectively. However, as shown in the data for the evolved strains at normal temperature, oil% and ARA% reached more than 30% in all strains, while ARA% remained stable at around 31% (Figure 5.28 A). This experiment was to explore if the evolved strain could still be improved under modified medium. Evolved strains in every 15 adaption cycles, namely ALE15, ALE30, ALE45 were compared to the starting strain.

As shown in the table, no significant differences were found between all strains in terms of the most abundant fatty acid profile as well as cell growth, lipid content and ARA concentration, except for ARA content which increased to more than 35% in all strains. The most abundant fatty acid was classified as ARA (C20:4) with more than 35%, followed by C16:0 with about 14%, C18:0, C18:1 and C18:2 with about 8-10%, and C18:3 and C24:0 in TFA with about 3-4% (Table 5.16). The results showed that the modified medium seemed to have less of an effect on cell growth and lipid accumulation, but slightly increased the synthetic content of ARA by more than 35% of the adaptation strain.

Table 5.16: Biomass and fatty acid of the original strains and adaptive strains in every 15 ALE cycles

	C16:0	C18:0	C18:1	C18:2	C18:3	C20:3	C20:4 ARA	C24:0	Cell dry weight g/L	Lipid %	ARA production(g/L)
WT	14.0±1.46 Aa	9.45±1.04 A	9.07±0.96 A	9.10±0.09 A	4.98±0.19 A	5.62±0.32 A	38.0±3.64 A	3.43±0.22 A	21.2±0.80 A	30.7±0.62 A	2467±121 A
ALE15	13.4±2.25 A	9.50±0.27 A	8.81±1.23 A	8.75±0.40 A	4.90±0.48 A	5.77±0.77 A	38.8±1.76 A	3.59±0.08 A	20.7±0.14 A	30.7±1.07 A	2649±61.3 A
ALE30	15.7±1.80 A	10.4±1.24 A	7.96±0.86 A	8.86±0.47 A	4.60±0.25 A	6.59±0.37 A	36.3±3.86 A	3.43±0.43 A	21.1±0.79 A	34.4±0.71 A	2624±214 A
ALE45	15.5±2.98 A	10.8±0.61 A	8.51±0.45 A	8.84±0.60 A	4.63±0.43 A	6.91±0.58 A	35.2±2.32 A	3.35±0.29 A	21.4±0.60 A	34.3±1.15 A	2581±192 A

[a] Experimental results in Mean ± SD, n = 3. Letters refer to significant terms comparison by Tukey ANOVA analysis within 95% confidence interval.

5.5 Summary of ARA productivities

In addition to the percent (%) and concentration (g L^{-1}) of ARA, the volumetric productivity (g $L^{-1}d^{-1}$) of ARA is also a measure of fermentation performance. In this study, ARA productivity (g $L^{-1}d^{-1}$) is calculated by dividing the ARA concentration (g L^{-1}) by the fermentation time (d). ARA productivities are shown and compared in Table 5.17.

The original medium only contained the main carbon and nitrogen source at original C:N ratio, and normally grew for 11 days to reach the ARA concentration of 0.45 g L^{-1}, and the ARA produtctivity was around 0.041 g $L^{-1}d^{-1}$. After micronutrients were optimized and added in the basal medium to form a blend for mineral sources by PB and RSM designs (section 5.1), the ARA concentration increased to around 0.744 g L^{-1}, after 5-day incubation, thus ARA productivity reached 0.149 g $L^{-1}d^{-1}$, which was a significant 63.7% increased compared to the original performance. When C:N was adjusted to a ratio of 15 (section 5.2.1), after 7 days fermentation, ARA concentration was around 1.48 g L^{-1} and productivity was around 0.211 g $L^{-1}d^{-1}$, corresponding to a 4.15-fold increase compared to original medium. When nitrogen sources were combined and modified (section 5.2.3), after 8 days fermentation, ARA concentration was around 2.1 – 2.5 g L^{-1}, and ARA productivity was around 0.284 g $L^{-1}d^{-1}$, leading to a significant 5.9-fold increase over the original performance.

In UV mutagenesis (section 5.3), the best performing mutant M13 retained an ARA concentration of 2.8 g L^{-1}, and ARA productivity was around 0.327 g $L^{-1}d^{-1}$ after 8 days incubation, which resulted in a 7.0-fold and 0.15-fold increase in comparison to the original medium and wild-type final modified medium, respectively. After high-temperature ALE (section 5.4), when final adapted strain ALE 45 grew at normal temperature, its fermentation time reduced to around 5.3 days, and its ARA concentration was around 2.24 g L^{-1}, and ARA productivity was around 0.421 g $L^{-1}d^{-1}$, leading to a significant 9.3-fold and 0.48-fold increase over original medium and wild-type final modified medium, respectively.

Table 5.17: Summary Table of ARA productivities (g $L^{-1}d^{-1}$)

Exp #	Ingredients	ARA productivity (g $L^{-1}d^{-1}$)
Original	Glucose 20 g L^{-1}, yeast extract 11 g L^{-1}	$0.041 \pm 0.008^{a\ E}$
PB / RSM	Glucose 20 g L^{-1}, yeast extract 11 g L^{-1}, KH_2PO_4 5.023 g L^{-1}, $MgSO_4.7H_20$ 0.796 g L^{-1} and $CaCl_2.2H_20$ 0.318 g L^{-1}	0.149 ± 0.006^{D}
C:N ratio	glucose 41.25 g L^{-1}, yeast extract 11 g L^{-1}, KH_2PO_4 5.023 g L^{-1}, $MgSO_4.7H_20$ 0.796 g L^{-1} and $CaCl_2.2H_20$ 0.318 g L^{-1}	0.211 ± 0.023^{C}
Nitrogen design (Final modified)	glucose 41.25 g L^{-1}, yeast extract 7 g L^{-1}, $NaNO_3$ 2.429 g L^{-1}, KH_2PO_4 5.023 g L^{-1}, $MgSO_4.7H_20$ 0.796 g L^{-1} and $CaCl_2.2H_20$ 0.318 g L^{-1}	0.284 ± 0.013^{B}
UV mutagenesis – M13	glucose 41.25 g L^{-1}, yeast extract 7 g L^{-1}, $NaNO_3$ 2.429 g L^{-1}, KH_2PO_4 5.023 g L^{-1}, $MgSO_4.7H_20$ 0.796 g L^{-1} and $CaCl_2.2H_20$ 0.318 g L^{-1}	0.327 ± 0.012^{B}
High-temp ALE – ALE45	glucose 41.25 g L^{-1}, yeast extract 11 g L^{-1}, KH_2PO_4 5.023 g L^{-1}, $MgSO_4.7H_20$ 0.796 g L^{-1} and $CaCl_2.2H_20$ 0.318 g L^{-1}	0.421 ± 0.037^{A}

[a] Experimental results in Mean ± SD, n = 3.

Letters refer to significant terms comparison by Tukey ANOVA analysis within 95% confidence interval.

Chapter 6: Discussion

6.1 Micronutrient Studies

In PB screening, the most common minerals named KH_2PO_4, $MgSO_4$ and $CaCl_2$ had a significant positive effect on more than one response variables and were selected for RSM optimization. Various studies suggested that a combination containing certain amounts of potassium, phosphorus, magnesium, calcium supplementation was effective for *M. alpina* growth and ARA synthesis (Chen et al., 1997; Higashiyama et al., 1998b; Totani et al., 2002; Nisha et al., 2011; Liu et al., 2012; Sun et al., 2015; Leth & McDonald, 2017).

Other ingredients in the PB design, including NaCl, $MgCl_2$, sodium citrate, trace elements and vitamins, showed negative effects on multiple responses, inhibiting cell growth or suppressing lipid accumulation. The results from the current work showing the negative effects of NaCl are consistent with the results of Chen et al. (2022), indicating that no significant improvement was found with the addition of sea salt or NaCl in various *Mortierella* strains (Chen et al., 2022). The addition of excess NaCl revealed the possibility of inhibiting ARA production (Higashiyama et al., 1998a). Higashiyama et al. (1998b) studied the effect of adding sodium sulphate, $CaCl_2$, and $MgCl_2$ and found that these did not improve the production of ARA, but resulted in a pellet shape that hindered the absorption of nutrients to accumulate lipids. Citrate has an important role in the metabolism of mammalian cells. After its synthesis in mitochondria by citrate synthase from acetyl CoA, it is part of the tricarboxylic acid cycle and may affect fatty acid synthesis (Iacobazzi & Infantino, 2014). However, the addition of sodium citrate has been found to negatively affect total lipids, indicating that its high concentration can inhibit fatty acid synthesis in this work.

In this study, the effect of metal ions was investigated by using a combination trace element solution patented by Mara. This trace element solution contained manganese, zinc, cobalt, copper, nickel and iron ions. Although Hansson & Dostalek (1998) showed that

copper and zinc ions had a positive effect on lipid accumulation, the current study indicated that the mixed solution had a negative effect on all response variables, suggesting that higher ARA yields were obtained in the absence of metal ions, which was consistent with studies by other researchers (Liao et al., 2007; Sun et al., 2015).

Zeng et al (2012) optimized vitamin B-group ingredients supplementation. The mixed B-group vitamins (shown in Table 4.1) increased ARA up to 10.0 g L^{-1}, which was 1.7 times higher than the control group. The rationale was that B-group vitamins can act as cofactors for key enzymes involved in ARA biosynthesis or form precursors for NADPH and acetyl CoA, which are essential for ARA synthesis (Zeng et al., 2012). However, after adding the exact amounts in the current study, all responses were negatively affected by PB results compared to their studies, suggesting that metabolic activity can vary from strain to strain. For MA2-2, vitamins negatively affected ARA production.

In this study, at higher concentrations of KH_2PO_4 in the first RSM (Section 5.1.2), biomass increased while total oil increased slowly, and ARA percentage decreased. Increasing the amount of KH_2PO_4 in the medium led to an increase in the production of fungal cell weight and cell growth. This can be attributed to phosphorus being an essential element required for the formation of cell membranes (Totani et al., 2002; Leth & McDonald, 2017). KH_2PO_4 also provided the nitrogen flux essential for a high biomass buildup thus improving cell growth (Nisha et al., 2011). However, a different outcome was observed in a study by Markou et al. (2012), where a decrease in both biomass and lipid yield was observed in all *Mucoromycota* fungi when grown in the presence of a high concentration of inorganic phosphorus source. Similarly, Nisha et al. (2011) reported lower levels of biomass, lipids, and ARA, as phosphorus could not accelerate the production of total lipids that occur in nitrogen-depleted media. In that case, higher levels of KH_2PO_4 may have had an inhibitory effect on ARA because higher KH_2PO_4 resulted in a differential increment in cell division and a subsequent reduction in the rate of lipid synthesis. In addition, KH_2PO_4 can provide buffering capacity in the growth media (Chen et al., 1997),

which can stabilize the growth medium and reduce the inhibition of lipid and ARA fatty acid formation (Dzurendova et al., 2020). In the second RSM (Section 5.1.3), the final concentration of 5.023 g L^{-1} KH_2PO_4 preserved higher cell dry weight but reduced the inhibitory effect on ARA accumulation.

In terms of $MgSO_4$ and $CaCl_2$, the first RSM indicated that moderate to higher concentrations could increase both biomass and ARA percentage, while lower concentrations favored lipid production. The optimized condition predicted by the model was achieved when both salts were increased to the highest edge points. However, the experimental results for model validation had large a deviation in comparison to predicted models. In order to verify the predictions made in the first design, a second RSM was conducted at even higher concentration ranges. Eventually, the second RSM showed that higher lipid and ARA production can be achieved at lower levels of $MgSO_4$ and $CaCl_2$. As discussed by Hansson & Dostalek (1988), small amounts of these ions are usually required for cell growth and enzyme activity, and low amounts of magnesium and calcium are desirable for lipid and ARA production (Higashiyama et al., 1998a; Sun et al., 2015). In their study, Totani et al. (2002) used media containing 0.5 g L^{-1} of $MgSO_4$ and 0.75 g L^{-1} of $CaCl_2$, which resulted in the highest DCW of 18.7 g L^{-1} and high yields of ARA (Totani et al., 2002). This was similar to the present study, where the final modified medium contained 0.796 g L^{-1} of $MgSO_4$ and 0.318 g L^{-1} of $CaCl_2$. Experimental validation of the optimal conditions showed much lower deviation when compared to the first RSM validation, indicating that the modified concentrations are more suitable for further ARA production.

From experiments conducted to validate the optimal conditions obtained in the first RSM, it was seen that the higher concentrations of KH_2PO_4, $MgSO_4$ and $CaCl_2$ were chemically active and prone to interacting with each other. For instance, magnesium phosphate or magnesium ammonium phosphate are fairly insoluble and could precipitate. Additionally, high concentrations of $MgSO_4$ may react with reagents such as NaOH to form

magnesium hydroxide, a white precipitate that would affect the consistency of the media pH (Leth & McDonald, 2017). The validation results using lower concentrations of mineral salts in the second RSM indicated better stability, with the reduced possibility of unwanted reactions and precipitation.

It was also observed that the addition of minerals salts altered the mycelial morphology from a smooth pellet shape to hairy pellet or dispersed filaments. The addition of KH_2PO_4 has been associated with filamentous growth (Higashiyama et al., 1998b) and calcium ions with inducing mycelial aggregation and pellet formation (Braun, 1991). Researchers have reported that mycelia from either fluffy-pellet and dispersed filaments can exhibit high biosynthetic activity, causing rapid glucose consumption and high enzyme production, to bring higher cell growth rate and lipid production (Teng et al., 2009).

6.2 Macronutrient Studies

6.2.1 Discussion on Carbon Sources and C:N Relations

In the present work, glucose was used as the sole carbon source for *M. alpina* MA2-2 strain. Based on the research by Lu et al. (2011), an optimal C:N ratio of 15-20 was reported for ARA production in a culture of *M. alpina* CBS 754.68. When the C:N ratio was higher than 20, cell growth was inhibited, and ARA decreased due to nitrogen limitation. An optimal C:N ratio between 15-20 was also reported by other researchers (Higashiyama et al., 2002; Mamani et al., 2019). The C:N ratio in present work was originally around 7.2 when glucose was at 20 g L^{-1} and yeast extract at 11 g L^{-1}. The C:N ratios of 10, 15 and 20 were compared by increasing the carbon source or decreasing the nitrogen source while keeping another source fixed. In comparison to previous work, two strategies were performed by the study of Koike et al. (2001) by studying how consumed C:N ratios affected ARA production, while this is the study to use both strategies to examine how initial C:N ratios affect ARA performance.

The results from this work showed that lipid content increased with rising C:N ratio, similar to that reported in other studies (Hansson & Dostalek, 1988; Cao et al., 2015; Sun et al., 2015; Malaiwong et al., 2016). Interestingly, the growth rate of lipids showed a slightly greater improvement when the nitrogen level was reduced at a C:N ratio of 20, resulting in a total lipid content of 33%. In comparison, a 28% lipid content was achieved with an increase in carbon source. This result indicated at a higher carbon source and lower nitrogen source were suitable for lipid accumulation (Sun et al., 2015; Malaiwong et al., 2016).

On the other hand, there was a significant difference in biomass when comparing the two approaches for modifying the C:N ratios. When yeast extract reduced from 11 g L^{-1} to 4 g L^{-1} and glucose was fixed at 20 g L^{-1} (C:N ratio increased from 7.2, 10, 15 and 20), the biomass was decreased from 14.6 g L^{-1} (control) to a final 8.8 g L^{-1}. A low nitrogen content has been reported as being unfavorable for cell growth and results in a low level of ARA production (Zhu et al., 2003). With lower nitrogen concentrations, nitrogen starvation would have occurred earlier, resulted in rapid glucose depletion and ultimately led to lower biomass. This was not ideal for ARA production since the low biomass and high lipid content did not improve ARA productivity. To achieve a higher ARA yield, a greater biomass concentration is required, which can only be achieved by increasing the nitrogen source (Higashiyama et al., 1998b). However, when glucose increased from 20 g L^{-1} to 55 g L^{-1} and yeast extract was fixed at 11 g L^{-1} (C:N ratio increased from 7.2, 10, 15 and 20) the biomass was improved to a final 24.6 g L^{-1}. The rise in glucose concentration resulted in an increase in lipid content in the dry biomass, suggesting that higher levels of glucose are advantageous for lipid synthesis in this fungus (Lu et al., 2011; Cao et al., 2015; Singh et al., 2017).

Other researchers have noted that high glucose concentrations above 100 g L^{-1}can inhibit the growth and suppress lipid accumulation of *M. alpina*, and reported an optimal glucose concentration range of 20 - 40 g L^{-1} (Ji et al., 2014). In the current study, the glucose

concentration is maintained within this safe range. According to the study from Koike et al. (2001), cell growth and lipid production increased in proportion to the initial concentrations of carbon and nitrogen sources until the carbon and nitrogen sources were 120 and 40 g L^{-1}, respectively. Above this concentration, ARA production decreased due to high osmotic pressure and viscosity. In the present study, the optimal concentrations of carbon and nitrogen were lower than the upper limits used in the study by Koike et al. (2001) in order to obtain a high biomass and high lipid content.

In terms of the synthesis of ARA in TFA, the present work showed that the C:N ratio had no effect on the accumulation of ARA. This contradicts the results of Koike et al. (2001) and Cao et al. (2015). These two studies showed differences in the contribution of ARA at different C:N ratios. In the study by Cao et al. (2015), the ARA content in total fatty acids was found to decrease with increasing substrate concentration and DCW. Koike and colleagues (2001) investigated different consumed C:N ratios by adjusting glucose and soybean meal. In their study they found that for a fixed amount of the carbon source, the ARA concentration increased with increasing amounts of nitrogen sources; for a fixed amount of the nitrogen source, ARA concentrations increased with decreasing amounts of carbon sources. These results may have been due to the fact that their study used relatively higher concentrations of carbon and nitrogen sources to adjust the C:N ratio, which could have resulted in a higher level of metabolic activity and ARA synthesis.

To summarize, the findings of this study were consistent with those of Higashiyama et al. (2002) in demonstrating that an excess of nitrogen source increased biomass yield, which was dependent on nitrogen concentration. Additionally, the presence of a higher C:N ratio in the carbon source resulted in an increase in TFA yield while maintaining a constant ARA percent in TFA.

6.2.2 Discussion on Nitrogen Sources

In this study, potential organic and inorganic nitrogen sources were initially screened,

and minimal amounts of yeast extract were added to compensate for growth performance. $NaNO_3$, MSG, $(NH_4)_2SO_4$, yeast extract, peptone and urea were examined in this study, although, urea and $(NH_4)_2SO_4$ were excluded from further consideration due to their poor performance during screening.

The combination of $(NH_4)_2SO_4$ resulted in the lowest biomass (2.0 g L^{-1}) and a lengthy lag phrase. In addition, the degree of unsaturation of fatty acids was significantly lower compared to other nitrogen sources, leading to the lowest ARA% of 7.45% (Table 5.7). The poor cell performance observed in this study was consistent with the findings of Lu et al. (2011), who reported that ammonia salts have negative effects on DCW and ARA percentage. The main reason for the poor performance of $(NH_4)_2SO_4$ may be its poor pH buffering capacity. In this study, the final pH measured at harvest was lower than 3 when using ammonia salt. This was because poorly buffered media containing ammonium salts tend to become more acidic during growth (Papagianni, 2004). In the case of ammonium sulfate, the ammonium ions $[NH_4]^+$ are oxidized to yield nitrate $[NO_3]^-$ ions (Fageria et al., 2010). Assimilation of ammonia is associated with release of $[H]^+$ cations, resulting in acidification of the medium (Patrovsky et al., 2019). Generally, *M. alpina* is strongly inhibited when pH is lower than 3 or higher than 8 (Mironov et al., 2018; Patrovsky et al., 2019). Therefore, $(NH_4)_2SO_4$ was not a suitable nitrogen source for ARA production in the present work.

When urea was used as a nitrogen source, it resulted in low biomass (9.3 g L^{-1}), low lipid content (9.7%), and low ARA percentage (14.9%) as shown in Table 5.7, which led to the second-lowest ARA concentration (134.4 mg L^{-1}) among the tested nitrogen sources. Therefore, urea acted as one of the poorest nitrogen sources. This result was also consistent with various studies (Obukowicz et al., 1998; Nisha, 2009; Nisha & Venkateswaran, 2011; Sun et al., 2015), this may due to urea acting as an inhibitor for delta 5 desaturase, a key enzyme that catalyzes the conversion of dihomo-γ-linolenic acid to ARA (Obukowicz et al., 1998; Nisha & Venkateswaran, 2011). In addition, urea contained minimal metal ions

or other essential nutrients for cell growth (Sun et al., 2015). Urea also had a slightly lower final pH to around 4 after the mycelia were harvested. However, the magnitude of the pH decrease was greater with ammonium sulfate than urea (Fageria et al., 2010).

Yeast extract is an excellent nitrogen source for the abundant growth of fungi due to the presence of metal ions and micronutrients that are essential for microbial growth (Yuan et al., 2002; Nisha, 2009; Nisha & Venkateswaran, 2011; Ling et al., 2016). Organic yeast extracts can be used as a source of nitrogen and phosphorus for oleaginous fungi (Chang et al., 2021). In addition to important growth factors, high concentrations of yeast extract alone can provide sufficient nitrogen, magnesium and sulfur to promote the growth of *M. alpina* and its ARA production (Chen et al., 1997). According to the study by Lu et al. (2011), yeast extract alone resulted in higher biomass compared to other organic or inorganic nitrogen sources.

Peptone for some *Mortierella* strains-enhanced mycelial growth was also found to improve ARA production. It has been shown to reduce the lag phase prior to growth and promote metabolite production in submerged cultures (Nisha, 2009; Nisha & Venkateswaran, 2011). The current study showed a significant increase in total lipids up to 30% when the cultivation media contained peptone combined with a very small amount of yeast extract (Table 5.7), consistent with the results of (Nisha & Venkateswaran, 2011; Fang et al., 2018). Although total nitrogen was kept constant in each experiment within this study, the complex nitrogen source may have been able to provide more essential elements for lipid accumulation (Fang et al., 2018).

As a nitrogen source, glutamate plays an important role in nitrogen metabolism and is required as an essential precursor for protein and nucleotide synthesis, and a substrate for energy metabolism (Wice et al., 1981). Moreover, glutamate enables activation of acetyl-CoA carboxylase, used for fatty acid synthesis (Kowluru et al., 2001). The results from the present work showed no difference in biomass and oil% from cultivation media with glutamate compared to the control, while ARA content was lower (17.6%). This result is

contrary to the findings reported by Lan and colleagues (2002), who noted that biomass and ARA production were higher in cultures containing glutamate than in control cultures, and both reached a maximum of 25 g L^{-1} and 1.4 g L^{-1}, respectively, after 7 days (Lan et al., 2002). Other studies have shown that glutamate addition improved the activity of glucose-6-phosphate dehydrogenase, a key enzyme for the formation of NADPH to form more PUFA (Hao et al., 2015; Mhlongo et al., 2021), though this was not observed in the current study.

When $NaNO_3$ was used as the main nitrogen source, lower biomass (8.6 g L^{-1}) and higher lipid (29.1%) production were achieved (Table 5.7). Lu et al. (2011) reported that the use of $NaNO_3$ as the only source of nitrogen could result in a desirable level of unsaturation. If $NaNO_3$ was used, the resulting pH increased or remained constant due to consumption of $[H]^+$ during nitrate assimilation (Patrovsky et al., 2019).

A mixture design approach was used in this study to investigate the synergistic effects of combining complex nitrogen sources, where different proportions of yeast extract, peptone, MSG, and $NaNO_3$ were added while the total nitrogen amount was fixed. Surprisingly, the study found that the accumulation of total lipids and the activity of desaturated fatty acids were significantly increased when complex nitrogen sources comprised mostly of organic nitrogen and minimal inorganic nitrogen sources were used. Combining yeast extract and $NaNO_3$ was found to be effective in promoting lipid accumulation and ARA percentage, with values reaching 35% and 42%, respectively. Previous studies suggested that $NaNO_3$ was a favorable nitrogen source for ARA accumulation by *M. alpina*, with moderate to high ARA values delivered (Lu et al., 2011; Rayaroth et al., 2021). Zhu et al. (2003) also noted that combining $NaNO_3$ with organic nitrogen sources was more effective than using yeast extract alone in enhancing cell growth and ARA production. To reduce nitrogen costs, Chen et al. (1997) recommended the use of cheaper and simpler nitrogen sources for microbial lipid accumulation. $NaNO_3$ has been suggested as a better nitrogen source when combined with organic nitrogen for enhancing

lipid content, ARA percentage, and reducing nitrogen costs.

To summarize, this study found that significant improvements in biomass DCW, lipid content, and ARA percentage were achieved by optimizing the C:N ratio to 15, increasing glucose to 41.25 g L^{-1}, and using a combined nitrogen source of 7 g L^{-1} yeast extract and 2.429 g L^{-1} $NaNO_3$, while keeping the total nitrogen amount at 1.1 g L^{-1}. This resulted in an increase in ARA productivity of over 2.1 g L^{-1}, which was a 3.7-fold increase compared to the original performance.

6.2.3 Comparison to Other Statistical Optimization Studies on ARA Producers

A comparison of this work with other statistical optimization studies on ARA production by fermentation is given in Table 6.1. The table shows results from submerged and solid-state fermentation.

Cheng et al. (1997) found that ARA production by *M. alpina* Wuji-H4 increased to 3.85 g L^{-1} after RSM was used to determine the optimal concentration of soluble starch being 99.7 g L^{-1}, yeast extract being 12.6 g L^{-1} and KH_2PO_4 being 3.0 g L^{-1}. Jin et al. (2009) used traditional mycelium aging technology with RSM optimization for *M. alpina* ME-1, and achieved a maximum ARA yield of 19.02 g L^{-1} , which was 1.55 times higher than that of traditional aging technology, at a temperature 13.7°C, ethanol 42.44 g L^{-1}, and potassium nitrate 2.62 g L^{-1}. Rocky-Salimi et al. (2011) used PB and RSM to improve the ARA production from *M. alpina* CBS754.68, where the results indicated that conducting the fermentation with glucose 50 g L^{-1}, yeast extract 14 g L^{-1}, temperature 22°C, and agitation rate of 180 rpm would increase the ARA production to 6.22 g L^{-1}. Nisha et al. (2011) improved the ARA production by *M. alpina* CBS754.68 using RSM, with four independent variables selected (glucose, corn solids, KH_2PO_4 and potassium nitrate) and the optimal conditions resulted in a maximum production of ARA of 1.39 g L^{-1} and biomass of 12.49 g L^{-1}. Samadlouie et al. (2012) improved the ARA production from *M. alpina* CBS754.68 to 5.64 g L^{-1} using RSM, with the results indicating that glucose and soybean were the

major impact factors with optimal concentrations at 50.35 g L^{-1} and 18.30 g L^{-1}, respectively (Samadlouie et al., 2012).

Saelao et al. (2011) used PB and RSM to optimize biomass and ARA production in *Aureispira maritima* shake-flask cultures, where tryptone and culture temperature had a significant effect on biomass production, and pH and agitation rate had a significant effect on ARA production. The validity of the optimum conditions was verified by separate experiments in which biomass and ARA yield were increased 4.02-fold (2.05 g L^{-1}) and 3.59-fold (21.50 mg g^{-1}). Malaiwong et al. (2016) used PB and RSM to maximize biomass and ARA for *M. alpina* PRAO7-10. The optimal values for the temperature, % v/v, glucose concentration and soy isolate concentration were 25.06°C, 14.16%, 6.67% and 0.48%, respectively, the maximum DCW and ARA production were 52.64 g L^{-1} and 6.76 g L^{-1}, respectively. In the study by Goyzueta-Mamani et al. (2021), wastes from the potato chip industry were used as a carbon source to develop an economical culture medium for the production of ARA by *M. alpina* CBS 528.72. A synthetic culture medium was optimized using PB and RSM and was able to achieve 24 g L^{-1} of DCW, 45% of lipids and 40% of ARA in lipids (Goyzueta-Mamani et al., 2021).

Kavitha et al. (2016) used RSM for optimizing ARA and eicosapentaenoic acid (EPA) production from a red marine microalgae *Porphyridium purpureum*. Results indicated that maximum biomass 0.95 g L^{-1} was achieved at the concentrations of sodium chloride 14.89 g L^{-1}, magnesium sulfate 3.93 g L^{-1} and sodium nitrate 0.96 g L^{-1} and potassium dihydrogen phosphate 0.09 g L^{-1}. The maximum total lipid 17.9 % and EPA 34.6 % content was at the concentrations of sodium chloride 29.98 g L^{-1}, magnesium sulfate 9.34 g L^{-1} and $NaNO_3$ 1.86 g L^{-1} (Kavitha et al., 2016). Antimanon et al. (2018) also reported that ARA improved after optimizing cultivation medium and parameters of solid-state fermentation by *Mortierella sp*. Validation of the regression equation was conducted using the optimal conditions of initial moisture content 60%, culture temperature 25°C and inoculum size 10% (v/w). The experimental result showed that 46.72 ± 2.54 mg g^{-1} dry fermented mass of

ARA. Asadi et al. (2018) investigated simultaneous production of ARA and EPA by *M. alpina* CBS 528.72 in solid-state fermentation. Date waste and soybean meal served as carbon and nitrogen sources, respectively. By using PB and RSM, the optimal parameters were determined as substrate initial moisture content 70-75%, linseed oil 10% w/w and nitrogen 4% w/w, substrate particle size 1.2-1.7 mm and seed age 96 h resulting in ARA and EPA production of 14.37 ± 0.06 and 11.35 ± 0.09 mg g^{-1}, respectively (Asadi et al., 2018). Finally, Ghobadi et al. (2022) used PB to determine that sunflower oil cake was the best out of four oil cakes for improving ARA production from *M. alpina* CBS 754.68, in a solid-sate fermentation. The optimal fermentation time, temperature, and substrate particle size from RSM was 8.75 days, 18.5°C, and 1.3 mm–1.7 mm, respectively. Under these conditions, the actual ARA yield, determined in evaluation tests was 4.48 ± 0.16 mg g^{-1} (Ghobadi et al., 2022).

Table 6.1: Comparison of statistical optimization studies on ARA production.

Mortierella Species	Fermentation time d	DCW g L^{-1}	Oil%	ARA%	ARA yield g L^{-1} or mg g^{-1}	Reference
M. alpina MA2-2 (current study) C/N 15, RSM & Mixture optimized	7-9	17-21	30-35 (~6.4 g L^{-1} in my study)	30-36	2 – 2.5 g L^{-1} Or (~127 mg g^{-1} in my study)	
M. alpina Wuji-H4	5				3.85	Chen et al., 1997
M. alpina ME-1 (5 L fermenter)	5.6				19.02	Jin et al., 2009
M. alpina CBS 754.68	8				6.22	Rocky-Salimi et al., 2011
M. alpina CBS 528.72	7	12.49	5.87 g L^{-1}		1.39	Nisha et al., 2011
M. alpina CBS754.68	10				5.64	Samadlouie et al., 2012
A. maritima TISTR 1715	3	2.05±0.06			21.5±0.25 mg g^{-1}	Saelao et al., 2011
M. alpina PRAO7-10	10	52.64			6.76	Malaiwong et al., 2016
M. alpina CBS 528.72	7	20	40	35		Goyzueta-Mamani et al., 2021
Porphyridium purpureum	28	0.95	17.9			Kavitha et al., 2016
Mortierella sp.	9				46.72 ± 2.54 mg g^{-1}	Antimanon et al., 2018
M. alpina CBS 528.72	6				14.37 ± 0.06 mg g^{-1}	Asadi et al., 2018
M. alpina CBS 754.68	9				10.13±0.26 mg g^{-1}	Ghobadi et al., 2022

6.3 Random UV Mutagenesis Coupled with High-Throughput Screening

This study used UV radiation as a physical method for random mutagenesis followed by a cerulenin-TTC based mutant screening assay. In the present work, *M. alpina* MA2-2 strains died after prolonged exposure to UV radiation at different exposure times. Cell viability was greatly affected by exposure to UV, even for short periods of time. This is similar to what was found in the study by Beacham et al. (2005) as *M. alpina* is a non-phototrophic organism and therefore less likely to be adapted to high levels of natural UV exposure for long periods of time. In the present work, after screening for fungal growth at different concentrations of cerulenin supplemented in agar medium, a final concentration of 1 μM was selected which agreed with the results of Yao et al. (2019). In addition, the PDA medium was supplemented with different concentrations of TTC and a red color was observed for some colonies at 1.5 mM, which was selected as the optimal concentration for mutant screening, in line with Yao et al. (2019). When cerulenin was supplemented, it was observed that there was a synergistic effect which helped to maintain the desired strains visually.

After UV mutagenesis coupled with cerulenin and TTC screening, 39 fast-growing, red-stained mutants were isolated and their fatty acid profiles were measured. Five of the mutants showed more than 40% contribution of ARA, while M9 and M13 retained more than 40% of ARA after replicate experiments. However, no significant improvement was found compared to wild type MA2-2. Mutants M9 and M13 maintained beneficial phenotypes that were similar to the wild type, whereas most of the other strains exhibited either neutral or negative traits. For most mutants, high biomass and total oil content were still retained, but ARA accumulation was lower, which can be explained by the fact that TTC reflected the overall desaturase activity in *M. alpina*, and not just the activity of key fatty acid desaturases taking part in ARA biosynthesis (such as Δ9, Δ12, Δ6 and Δ5 fatty acid desaturase) (Li et al., 2015).

A possible reason for not finding significant improvements in mutants from the present study was that only one round of UV mutagenesis was applied, and this may have induced fewer mutagenic effects, compared to other physical mutagenesis methods such as gamma rays, X-rays or heavy-ion beams. For instance, heavy-ion beam utilizes heavier charged particles, which lead to higher mutation rates and a wider spectrum of mutations due to their high linear energy transfer (Arora et al., 2020). Zheng et al. (2021) also state that most physical mutagenesis methods can be rapid and easy to carry out, however, nonbeneficial mutations are generated frequently (Zheng et al., 2021). Conventional mutagenic strategies are random and the probability of finding desirable mutants is minimal (Muthuraj et al., 2019). For further developing mutagenesis on *M. alpina*. Multiple rounds of mutagenesis or a combined physical and chemical mutagenesis can enhance the mutational effects as well as expand genetic diversity.

Other studies have successfully produced higher FA synthesis activity in *M. alpina* strains by using combined physical and chemical mutagenesis, including heavy-ion and 5-flurouracil, coupled with screenings using triclosan and octyl gallate. For example, in the study by Zhang et al. (2018), the best mutant achieved an ARA yield of 5.26 g L^{-1}, which was 3.24 times higher than that of the wild-type strain. In another study, when atmospheric and room temperature plasma mutagenesis combined with diethyl sulfate and TTC were used for *M. alpina,* the ARA yield of the isolated mutant strain was 5.09 g L^{-1}, an increase of 40.61% over the original strain (3.62 g L^{-1}) and the relative content of ARA increased from 38.99% to 45.64%. (Li et al., 2015). After UV radiation-mediated mutagenesis followed by screening with iodine vapor staining, starchless mutants of *Tetradesmus obliquus* were isolated with a 41% increment in TFA productivity (de Jaeger et al., 2014). Moreover, Sarayloo et al. (2018) used a combination of UV radiation and EMS to mutate *Chlorella. vulgaris* and its isolated mutants exhibited a 67% increase in lipid content and a 35% increase in biomass than those of the wild-type (Sarayloo et al., 2018). These findings revealed that the use of different combinations of classical mutagenesis resulted in efficient

performance for *M. alpina* and other microorganisms. Although no improvement was found using a single round of UV mutagenesis in *M. alpina* MA2-2, this strategy was fast and efficient for isolating mutants with deleterious effects.

6.4 High-Temperature ALE

6.4.1 Discussion of High-Temperature ALE Experiments for the MA2-2 strain

High temperature was used as a stressor to induce evolutionary adaptation in the *M. alpina* MA2-2 strain. The adaptation process firstly involved three temperature screenings to identify the optimal temperature range. The first two screenings used different inoculation methods, resulting in varying cell densities and performance in high temperatures. The sample inoculated with fewer cells exhibited strongly inhibited growth at 32℃, while normal growth was observed in cultures with more cells. However, the culture was unable to grow at temperatures above 35℃ during the temperature screenings, which agreed with the findings by Chen et al. (1997) that *M. alpina* Wuji-H4 isolate could barely grow at 36℃ (1997). Although the wild-type MA2-2 strain was capable of growing at temperatures below 35℃, the adapted strains showed inhibition above 33℃ during long-term high temperature adaptation. Therefore, a temperature of 32.5℃ was chosen for the long-term adaptive evolution.

After the adaption, MA2-2 evolved strains in every 5 ALE cycles were compared to starting strain at normal temperature (28℃) and stress inducer (32.5℃). At 32.5℃, the evolved strain ALE45 successfully depleted glucose while other strains were struggled to absorb nutrients, indicating the evolved strain exhibited better glucose uptake performance. As well, the biomass of DCW, total oil% and ARA yield gradually improved up to 4 times in comparison to the starting strain. These results agreed with what was reported by Peng et al. (2010), that a relatively high culture temperature was favorable for glucose

consumption. The evolution of the cell dry weight showed that a higher initial growth rate was achieved at higher temperatures. This means that maximal biomass was reached in a shorter amount of time at higher temperatures, where it is likely that the faster metabolism rate at higher temperatures promoted rapid cell division, leading to shorter lag growth phases (Shinmen et al., 1989; Singh & Ward, 1997; Cao et al., 2015). At 28°C, no distinct difference was found between biomass, total oil% and ARA production. This may be due to the fact that cells grown in the laboratory may be evolutionarily limited and have lower genetic variation due to smaller population sizes, which may prevent or delay the isolation of mutants with the desired phenotype (Trovão et al., 2022). However, the fermentation time was faster in adapted strain, reaching up to 40 h faster than starting strain.

The overall ARA productivity (g $L^{-1}d^{-1}$) of adapted strain was 27.6% higher than the starting strain, and the synthesis of total oil and ARA increased to around 32% and 31% throughout all conditions, respectively. This was in contrast with the findings by Hansson & Dostalek (1988), where there was a tendency for the composition of unsaturated fatty acids to increase in cells containing low amounts of lipids, and the degree of unsaturation to decrease with increasing lipid content. PUFA synthesis of ARA did not seem to affect the accumulation of total lipids. There was no opposite trend for total lipids and ARA, while they both showed a high percentage of accumulation. However, more ARA accumulated in total lipids at normal temperatures, with more than 30%, compared to about 18-20% ARA synthesis at 32.5°C. This suggested that lower temperatures increased the unsaturation of fatty acids, as this was essential for cells to maintain membrane fluidity (Shinmen et al., 1989; Singh & Ward, 1997; Cao et al., 2015). At a temperature of 32.5°C, oleic acid (C18:1) made up the largest proportion of fatty acids, whereas it decreased at normal temperatures. According to Hu et al. (2021), increasing the cultivation temperature resulted in an increase in the percentage of saturated fatty acids but a decrease in the percentage of PUFAs. After long-term adaptation at higher temperatures, the percentages of fatty acid profiles tended to change in the opposite direction compared to normal

conditions (2021).

An interesting phenomenon was that the cell growth did not increase linearly but followed a hyperbolic trend. i.e. the growth rate increased considerably until reaching the ALE35 cycle and then gradually decreased near the end point. This is similar to the study by Daskalaki et al. (2019) where the lipid accumulation capacity of *Y. lipolytica* decreased early in evolution compared to the starting strain. Subsequently, oily strains dominated, resulting in populations able to accumulate large amounts of lipids (Daskalaki et al., 2019). To adapt to abiotic stressors, such as high temperature, strains can alter their biochemical composition, leading to stress-induced accumulation of storage molecules, such as lipids (Arora et al., 2022). In this process, cells undergo acclimation to restore cellular homeostasis, and supra-optimal temperatures cause imbalances in cellular metabolism, which ultimately result in reduced growth and productivity. Acclimation helps to achieve a more stable cellular state, but growth is still impeded when non-optimal growth conditions are maintained (Barten et al., 2022).

The adapted strain ALE45 decreased temperature sensitivity among all response variables. When the temperature increased from the control at 28°C to 32.5°C, the reduction rate of the temperature sensitivities between starting strain and final evolved strain of DCW, total oil%, ARA% reduced 2.35, 0.87 and 0.41-fold, respectively. Overall, the temperature sensitivity of ARA concentration and final productivity of the evolved strain reduced 28.9% and 9.7% compared to starting strain. The modified strain significantly improved temperature tolerance and shortened fermentation time, thus avoiding energy consumption and saving more fermentation costs.

6.4.2 High Temperature Strategies on Various Microorganisms

Moreover, more studies have been conducted on strategies to improve the heat resistance of microorganisms. A high temperature ALE was carried out for DHA producer, *Schizochytrium sp.*; after long-temperature adaption at 34°C, the evolved strain improved

thermotolerance, as well as improved lipid and DHA concentration at 34℃ which reached 4.31 and 4.33 times higher than the starting strain (Hu et al., 2021). After transcriptomic and lipidomic studies regarding response mechanism of *Schizochytrium sp.* to temperature stress, it was found that high temperature stress accumulated more phosphatidyl glycerol, diglyceride and fatty acids while low temperatures resulted in the synthesis of more shorter monounsaturated fatty acids and phosphatidylethanolamine (Hu et al., 2022). Barten et al. (2022) performed high temperature ALE to increase the maximum temperature of already thermotolerant microalgae *Picochlorum sp.,* which resulted in an increase of 1.5°C in thermotolerance so that its upper temperature boundary was up to 49°C (2022).

The effects of day- and night-time temperature on *Haematococcus pluvialis* were studied, and the results indicated that raising the daytime or night temperature could stimulate night accumulation of astaxanthin until reaching a temperature of up to 28°C; The net biomass and astaxanthin yields increased 5 and 2.9-fold when the culture temperature was 28°C (Wan et al., 2014). Directed laboratory evolution in *Symbiodinium* has been proposed as a strategy to enhance coral halobiont thermal tolerance. Selected cells showed superior photophysiological performance and growth rate at 31°C (Chakravarti et al., 2017). The capacity for adaptation to warming in the marine diatom *Thalassiosira pseudonana*.c was shown in its ability to survive at a severe 32°C (Schaum et al., 2018).

A two-prong strategy of random mutagenesis and adaptive laboratory evolution was performed for robust thermotolerant strains of *Nannochloropsis oculata*. The best mutants increased productivity at 35°C. Biomass and lipid productivity were 1.43-fold and 2.24-fold higher, respectively, than wild type at 25°C (Arora et al., 2022). *Kluyveromyces marxianus* JKH5, a thermotolerant ethanologenic yeast implanted high temperature ALE for improving cellulosic bioethanol production. The improved strain showed 3.3-fold higher specific growth rate, 56% reduced lag phase and 80% enhanced fermentation efficiency at 42°C (Hemansi et al., 2022). A green marine microalgae *Tetraselmis sp.*

compared growth performance of UV mutants at a slightly high temperature 31°C, where the mutant showed an accelerated growth (Lo et al., 2022).

A high temperature ALE was applied to the lactic acid bacteria *Streptococcus thermophilus* at 60°C to enhance thermotolerance for adapting manufacturing processes, such as pasteurization. Increased heat tolerance of ALE strains showed higher survival rate during long-term storage at sub-zero temperatures as well as the adaptation to upper thermal threshold. Also fatty acid analysis indicated that saturated fatty acid ratio was higher than for the wild-type strain (Min et al., 2019). *Tisochrysis lutea* was used to increase the thermal stress of 12 isolates for 6 months. Two of them survived, indicating a doubling of the improvement in lipid content (Gachelin et al., 2021).

In conclusion, employing high-temperature ALE can enhance thermotolerance of industrial microorganisms against different environmental stresses, leading to reduced energy consumption and fermentation costs. The development of high-temperature strategies for producing ARA, an omega-6 fatty acid, was successful, and the ALE-evolved strain demonstrated improved temperature sensitivity while maintaining high cell performance and ARA production.

6.4.3 Other ALE Strategies on Various Microorganisms

In addition to temperature adaptation, various ALE strategies, including environmental or nutritional stress, have been explored for microalgae as producers of fatty acids, particularly omega-3 fatty acids. One factor ALE has been extensively studied for various microorganisms. The yeast *Saccharomyces cerevisiae* was used to study salt stress tolerance, because it contained several highly conserved pathways that mediate the salt stress response. All evolved strains had faster growth rate in high salt conditions than their ancestor (Dhar et al., 2011). A freshwater microalga *Parachlorella sp.* went through a high salt ALE. After eight consecutive ALE cycles, microalgal growth rate was remarkably increased to close to that of the culture without salt stress. Furthermore, FA content in

microalga was improved from 7.5% to 25% (Kim et al., 2021). A high oxygen ALE was applied to improve the production capacity of *Schizochytrium sp*. Endpoint strains improved 32.4% of CDW compared to starting strain. But slight lipid accumulation impairment was observed (Sun et al., 2016).

Later, two-stage ALE was developed to compensate for the performance degradation caused by single-stress ALE. A two-stage ALE strategy was applied to the thraustochytrid *Aurantiochytrium sp*., a DHA producer. Heavy-ion irradiation technique was first used before the ALE to increase the genetic diversity of strains, and low temperature supplemented with Acetyl CoA Carboxylase inhibitor were employed in enhancing the DHA production. The end-point strain with a DHA content 51% higher than that of the parental strain was obtained (Wang et al., 2021). A low temperature and high salinity was applied to improve the production capacity of *Schizochytrium sp* as a DHA producer. Low-temperature conditions were used to improve the DHA content, and high salinity was applied to stimulate lipid accumulation and enhance the antioxidative defense systems (Sun et al., 2018). A low temperature and oxygen ALE was developed to improve the exergy efficiencies of DHA. The adapted microalgal strain improved biomass yield which had the most important effect on enhancing the exergy efficiencies of DHA and yield (Ren et al., 2020).

Nutritional stress was also applied for ALE to improve the molecular mechanism of lipidome. Nutrient-limiting medium was used as stress inducer for *Y. lipolytica*, aimed to improve lipid accumulation. The evolved strain was able to accumulate 44% of lipid, which was 30% higher than that of the starting strain under nutrient-limiting medium (Daskalaki et al., 2019). High glucose concentration was supplemented to DHA strain *Crypthecodinium cohnii* for 260 ALE cycles. The glucose-tolerant strain showed that DHA-rich lipids increase by 15.49% at 45 g L^{-1} glucose concentrations (Li et al., 2017).

6.4.4 Challenges and Current Phase of ALE on Filamentous Fungi

ALE technology is still plagued by a number of challenges. Firstly, the creation of large mutant libraries and the necessity for large-scale screening of the necessary evolutionary bodies pose difficulties. Secondly, due to cell division, effective genes can disappear. Lastly, ALE experiments require a significant amount of time, and the endpoint is entirely at the discretion of the researcher (Wang et al., 2021). Experimental evolution studies often define a generation as a single cell division, which enables them to achieve thousands of generations quickly in laboratory conditions (Fisher & Lang, 2016). Filamentous fungi have cytoplasm filled with multiple nuclei, even in asexual spores, and there is no uninucleate stage in the life cycle. Such characteristics complicates the development of high-producing industrial strains, for instance, by mutagenesis and selection (Streekstra, 2010). One reason why adaptive evolution has not been applied to filamentous fungi is because of their multi-cellular characteristics. However, many fungal species have simple and rapid life cycles that can produce hundreds to thousands of generations over a relatively short period of time. Therefore, experimental evolution in fungi has the potential to provide a more comprehensive understanding of the evolutionary process (Fisher & Lang, 2016).

This study was the first to use microbial evolution adaptation to improve oleaginous filamentous fungi, specifically *M. alpina* MA2-2. High temperature was used as the stress inducer for the ALE. One challenge with adapting filamentous fungi was that the whole population was studied rather than individual cells, making it difficult to select specific genes. However, this ALE provided a good starting point for exploring the fitness of the entire population within the evolved strain. The results showed a clear improvement, indicating the successful application of adaptation to filamentous fungi and an improvement in thermotolerance of the evolved strain.

6.5 Summary of ARA productivities

Section 5.5 summarizes the ARA productivities for each part of this study, and Table 6.2 summarizes the ARA productivities for different literature including this study. By comparison with other work, the ARA productivity of the MA2-2 adapted strain ALE45 was able to approach extensively studied or scaled up ARA producing strains when grown in optimized fermentation media, indicating the potential of MA2-2 strain for further research aimed at commercialization and industrialization.

Table 6.2: Literature Summary of ARA productivities (g L^{-1} d^{-1})

Mortierella alpina Strains	Fermentation time d	ARA yield g L^{-1}	ARA productivity g $L^{-1}d^{-1}$	Reference
MA2-2 Current study-ALE45	5-7	2 – 2.5	0.421	
Wuji-H4	5	3.85	0.77	Chen et al., 1997
ME-1	5.6	19.02	3.40	Jin et al., 2009
CBS 754.68	8	6.22	0.78	Rocky-Salimi et al., 2011
CBS 528.72	7	1.39	0.20	Nisha et al., 2011
CBS754.68	10	5.64	0.564	Samadlouie et al., 2012
A. maritima TISTR 1715	3	21.5±0.25 mg g^{-1}		Saelao et al., 2011
PRAO7-10	10	6.76	0.676	Malaiwong et al., 2016
ATC3222	11	11	1	Singh & Ward, 1997
ME-1	7	9.2	1.3	Peng et al., 2010
1S-4	10	13	1.3	Higashiyama et al., 1998a
1S-4	8	3	0.4	Higashiyama et al., 1998b
LU166	5	6.2	1.24	Ling et al., 2016
Mortierella sp.	9	46.72 ± 2.54 mg g^{-1}		Antimanon et al., 2018
CBS 528.72	6	14.37 ± 0.06 mg g^{-1}		Asadi et al., 2018
CBS 754.68	9	10.13±0.26 mg g^{-1}		Ghobadi et al., 2022

Chapter 7: Conclusions and Recommendations

7.1 Conclusions

The overall goal of this research was to explore a new isolated filamentous fungus that has high potential for ARA production, an omega-6 fatty acid supplemented in infant formula. The main focus of the project was first to develop a medium using multiple statistical optimization strategies that focused on increasing multiple responses regarding increased ARA production in terms of biomass cell weight, percentage of total lipids in the biomass, percentage of ARA accumulated in the lipids, and ARA production; followed by a second part based on MA2-2 strain improvement, including random mutagenesis with screening methods and microbial evolution experiments to obtain beneficial mutants with better cell growth, high lipid and ARA accumulation, and better environmental adaptability, resulting in a robust strain capable of increasing ARA production.

Through this work, the following results have been achieved in relation to the specific objectives:

1. The final modified media for the strain MA2-2 consisted of glucose 41.25 g L^{-1}, yeast extract 7 g L^{-1}, $NaNO_3$ 2.429 g L^{-1}, KH_2PO_4 5.023 g L^{-1}, $MgSO_4.7H_20$ 0.796 g L^{-1} and $CaCl_2.2H_20$ 0.318 g L^{-1}. The modified media resulted in biomass DCW, TFA% or Oil%, ARA content, concentration and productivities of 19 – 22 g L^{-1}, 30 – 35 %, 33 – 42%, 2.1 – 2.5 g L^{-1}, and 0.284 g L^{-1} d^{-1}, respectively. Compared to the original medium containing 20 g L^{-1} of glucose and 11 g L^{-1} of yeast extract, responses variables of biomass, Oil%, ARA content, concentration and ARA productivity reached 10 – 12 g L^{-1}, 16 – 18 %, 25 – 27.5%, 0.45 g L^{-1}, and around 0.041 g L^{-1} d^{-1}, respectively; and therefore cell performance was improved by at least 0.9, 0.875, 0.32, 3.7 and 5.9 times, respectively. In addition, the final performance in modified medium reached the project targets.

2. UV mutagenesis coupled with a FAs inhibitor (cerulenin) and staining reagent (TTC) was developed for random mutagenesis. Among them, 39 relatively large colonies were pre-screened and evaluated FAMEs results. Five of them, namely M9, M10, M13, M14 and M27 had comparable biomass and lipid percent, but retained more than 40% of ARA. After replicating the experiment in triplicate, M9 and M13 retained ARA by more than 40% with minimal variation. However, no mutant exhibited a significantly better phenotype in comparison to the wild type.

3. High-temperature ALE was performed on wild-type MA2-2 at high temperature inducer of 32.5°C for up to 90 days acclimation, for a total of 45 ALE cycles. The evolved strain ALE45 was able to grow at high temperature of 32.5°C for 24 hours. ARA final productivity in ALE45 retained around 0.421 g L^{-1} d^{-1} which was 27.6% higher than of the original strain of 0.330 ± 0.04 g L^{-1} d^{-1}. Temperature sensitivity of ALE45 was dramatically lower than original strain, indicating the thermotolerance of evolved strain was improved.

7.2 Recommendations

1. Plackett-Burman screening can be an effective way to screen various factors in a limited number of experiments, but the interaction term is always negligible. It is recommended that the one factor at a time approach be used to investigate each mineral and possible interactions. A mixture design could also be an optimal choice to screen various minerals in a limited number of runs where their interaction terms can be adequately detected.

2. Predictions of the two rounds of RSMs were still relatively poor in relation to the experimental data. The main problem was the choice of level, which chose a wider range domain, making it less predictable in quadratic polynomial order. To overcome this problem, narrowing the range could be an optimal choice to detect a more accurate model.

3. Although the random mutagenesis scheme was effective for the MA2-2 strain, no

significant improvement was found. More rounds of mutagenesis or a combination of different mutagenesis strategies could be used to expand more phenotypes.

4. ALE has been successfully studied on the filamentous fungus MA2-2. More ALE strategies such as single rounds or combined ALE can be designed for this type of strain in the future.

5. The strain could undergo bioreactor fermentation to test the feasibility of scaling up with the potential aim of commercializing and industrializing this ARA strain producer.

References

Ademakinwa, A. N., Ayinla, Z. A., & Agboola, F. K. (2017). Strain improvement and statistical optimization as a combined strategy for improving fructosyltransferase production by Aureobasidium pullulans NAC8. *Journal of Genetic Engineering and Biotechnology*, *15*(2), 345–358. https://doi.org/10.1016/j.jgeb.2017.06.012

Ahmed, S. (N.d.). *Response Surface Methodology: Analyze & Explain*. The Open Educator. https://www.theopeneducator.com/doe/Response-Surface-Methodology/Analyze-and-Explain-Response-Surface-Methodology

Aki, T., Nagahata, Y., Ishihara, K., Tanaka, Y., Morinaga, T., Higashiyama, K., Akimoto, K., Fujikawa, S., Kawamoto, S., Shigeta, S., Ono, K., & Suzuki, O. (2001). Production of arachidonic acid by filamentous fungus, *Mortierella alliacea* strain YN-15. *Journal of the American Oil Chemists' Society*, *78*(6), 599–604. https://doi.org/10.1007/s11746-001-0311-2

Antimanon, S., Chamkhuy, W., Sutthiwattanakul, S., & Laoteng, K. (2018). Efficient production of arachidonic acid of Mortierella sp. By solid-state fermentation using combinatorial medium with spent mushroom substrate. *Chemical Papers*, *72*(11), 2899–2908. https://doi.org/10.1007/s11696-018-0519-2

Arora, N., Lo, E., & Philippidis, G. P. (2022). A two-prong mutagenesis and adaptive evolution strategy to enhance the temperature tolerance and productivity of Nannochloropsis oculata. *Bioresource Technology*, *364*, 128101. https://doi.org/10.1016/j.biortech.2022.128101

Arora, N., & Philippidis, G. P. (2021). Microalgae strain improvement strategies: Random mutagenesis and adaptive laboratory evolution. *Trends in Plant Science*, *26*(11), 1199–1200. https://doi.org/10.1016/j.tplants.2021.06.005

Arora, N., Yen, H.-W., & Philippidis, G. P. (2020). Harnessing the Power of Mutagenesis and Adaptive Laboratory Evolution for High Lipid Production by Oleaginous Microalgae and Yeasts. *Sustainability*, *12*(12), 5125. https://doi.org/10.3390/su12125125

Artisan Technology Group. (n.d.). *UVP CL-1000 Ultraviolet Crosslinkers Operating Instructions and Service Manual*. Artisan Technology Group. https://www.artisantg.com/Scientific/90092-1/UVP-CL-1000L-Longwave-UV-Crosslinker

Asadi, S. Z., Khosravi-Darani, K., Nikoopour, H., & Bakhoda, H. (2018). Production of Arachidonic Acid and Eicosapentaenoic Acid by Mortierella alpina CBS 528.72 on Date Waste. *Food Technology and Biotechnology*, *56*(2), 197–207. https://doi.org/10.17113/ftb.56.02.18.5379

Barten, R., Peeters, T., Navalho, S., Fontowicz, L., Wijffels, R. H., & Barbosa, M. (2022). Expanding the upper-temperature boundary for the microalga *Picochlorum sp. (BPE23)* by adaptive laboratory evolution. *Biotechnology Journal*, *17*(5), 2100659. https://doi.org/10.1002/biot.202100659

Beacham, T. A., Macia, V. M., Rooks, P., White, D. A., & Ali, S. T. (2015). Altered lipid accumulation in Nannochloropsis salina CCAP849/3 following EMS and UV induced mutagenesis. *Biotechnology Reports*, *7*, 87–94. https://doi.org/10.1016/j.btre.2015.05.007

Bhavsar, K., Gujar, P., Shah, P., Kumar, V. R., & Khire, J. M. (2013). Combinatorial approach of statistical optimization and mutagenesis for improved production of acidic phytase by Aspergillus niger NCIM 563 under submerged fermentation condition. *Applied Microbiology and Biotechnology*, *97*(2), 673–679. https://doi.org/10.1007/s00253-012-3965-8

Bicas, J., Maróstica Jr., M., & Pastore, G. (Eds.). (2016). Microbial Single-Cell Oils: Precursors of Biofuels and Dietary Supplements. In *Biotechnological Production Of Natural Ingredients For Food Industry* (pp. 322–375). BENTHAM SCIENCE PUBLISHERS. https://doi.org/10.2174/978168108265311601001l

Borowitzka, M. A. (2010). Algae Oils for Biofuels: Chemistry, Physiology, and Production. In *Single Cell Oils* (pp. 271–289). Elsevier. https://doi.org/10.1016/B978-1-893997-73-8.50017-7

Botha, A., Paul, I., Roux, C., Kock, J. L. F., Coetzee, D. J., Strauss, T., & Maree, C. (1999). *An isolation procedure for arachidonic acid producing Mortierella species*. *75*(3), 253–256. https://doi.org/10.1023/A:1001848709005

Braun, S. (1991). Mycelial morphology and metabolite production. *Trends in Biotechnology*, *9*(1), 63–68. https://doi.org/10.1016/0167-7799(91)90020-I

Breig, S. J. M., & Luti, K. J. K. (2021). Response surface methodology: A review on its applications and challenges in microbial cultures. *Materials Today: Proceedings*, *42*, 2277–2284. https://doi.org/10.1016/j.matpr.2020.12.316

Buckling, A., Craig Maclean, R., Brockhurst, M. A., & Colegrave, N. (2009). The Beagle in a bottle. *Nature*, *457*(7231), 824–829. https://doi.org/10.1038/nature07892

Cao, G., Guan, Z., Liu, F. g, Liao, X., & Cai, Y. (2015). Arachidonic acid production by Mortierella alpina using raw crop materials. *Acta Scientiarum Polonorum Technologia Alimentaria*, *14*(2), 133–143. https://doi.org/10.17306/J.AFS.15

Certik, M. (1998). Desaturase-defective fungal mutants: Useful tools for the regulation and overproduction of polyunsaturated fatty acids. *Trends in Biotechnology*, *16*(12), 500–505. https://doi.org/10.1016/S0167-7799(98)01244-X

Chakravarti, L. J., Beltran, V. H., & Van Oppen, M. J. H. (2017). Rapid thermal adaptation in photosymbionts of reef-building corals. *Global Change Biology*, *23*(11), 4675–4688. https://doi.org/10.1111/gcb.13702

Chang, L., Chen, H., Tang, X., Zhao, J., Zhang, H., Chen, Y. Q., & Chen, W. (2021). Advances in improving the biotechnological application of oleaginous fungus Mortierella alpina. *Applied Microbiology and Biotechnology*, *105*(16–17), 6275–6289. https://doi.org/10.1007/s00253-021-11480-y

Chang, L., Lu, H., Chen, H., Tang, X., Zhao, J., Zhang, H., Chen, Y. Q., & Chen, W. (2022). Lipid metabolism research in oleaginous fungus Mortierella alpina: Current progress and future prospects. *Biotechnology Advances*, *54*, 107794. https://doi.org/10.1016/j.biotechadv.2021.107794

Charlesworth, B. (2012). The Effects of Deleterious Mutations on Evolution at Linked Sites. *Genetics*, *190*(1), 5–22. https://doi.org/10.1534/genetics.111.134288

Chen, H. C., Chang, C. C., & Chen, C. X. (1997). Optimization of arachidonic acid production by *Mortierella alpina* Wuji-H4 isolate. *Journal of the American Oil Chemists' Society*, *74*(5), 569–578. https://doi.org/10.1007/s11746-997-0182-1

Chen, Y.-H., Ong, C.-C., & Lin, T.-Y. (2022). Effect of Sea Salt and Taro Waste on Fungal Mortierella alpina Cultivation for Arachidonic Acid-Rich Lipid Production. *Fermentation*, *8*(2), 81. https://doi.org/10.3390/fermentation8020081

Choudhary, A. K., & Pramanik, H. (2021). Optimization and validation of process parameters via RSM for minimizing use of resources to generate electricity from a DEFC. *International Journal of Energy Research*, *45*(14), 20413–20429. https://doi.org/10.1002/er.7126

Cohen, Z., & Khozin-Goldberg, I. (2010). Searching for Polyunsaturated Fatty Acid-Rich Photosynthetic Microalgae. In *Single Cell Oils* (pp. 201–224). Elsevier. https://doi.org/10.1016/B978-1-893997-73-8.50014-1

Conrad, T. M., Lewis, N. E., & Palsson, B. Ø. (2011). Microbial laboratory evolution in the era of genome-scale science. *Molecular Systems Biology*, *7*(1), 509. https://doi.org/10.1038/msb.2011.42

Cornell, J. A. (2002). *Experiments with Mixtures: Designs, Models, and the Analysis of Mixture Data* (1st ed.). Wiley. https://doi.org/10.1002/9781118204221

Daskalaki, A., Perdikouli, N., Aggeli, D., & Aggelis, G. (2019). Laboratory evolution strategies for improving lipid accumulation in Yarrowia lipolytica. *Applied Microbiology and Biotechnology*, *103*(20), 8585–8596. https://doi.org/10.1007/s00253-019-10088-7

Data Bridge Market Research. (2021). *Global Arachidonic Acid Market – Industry Trends and Forecast to 2028*. https://www.databridgemarketresearch.com/reports/global-arachidonic-acid-market

de Castro, R. J. S., & Sato, H. H. (2013). Synergistic effects of agroindustrial wastes on simultaneous production of protease and α-amylase under solid state fermentation using a simplex centroid mixture design. *Industrial Crops and Products*, *49*, 813–821. https://doi.org/10.1016/j.indcrop.2013.07.002

de Jaeger, L., Verbeek, R. E., Draaisma, R. B., Martens, D. E., Springer, J., Eggink, G., & Wijffels, R. H. (2014). Superior triacylglycerol (TAG) accumulation in starchless mutants of Scenedesmus obliquus: (I) mutant generation and characterization. *Biotechnology for Biofuels*, *7*(1), 69. https://doi.org/10.1186/1754-6834-7-69

Dennis, D. A., & Armenta, R. E. (2017). *(71) Applicant: MARA Renewables Corporation,* (Mara Renewables Corp Patent No. US9745539B2).

Dhar, R., Sägesser, R., Weikert, C., Yuan, J., & Wagner, A. (2011). Adaptation of Saccharomyces cerevisiae to saline stress through laboratory evolution: Adaptation of S. cerevisiae to saline stress. *Journal of Evolutionary Biology*, *24*(5), 1135–1153. https://doi.org/10.1111/j.1420-9101.2011.02249.x

Dias, F. F. G., de Castro, R. J. S., Ohara, A., Nishide, T. G., Bagagli, M. P., & Sato, H. H. (2015). Simplex centroid mixture design to improve l -asparaginase production in solid-state fermentation using agroindustrial wastes. *Biocatalysis and Agricultural Biotechnology*, *4*(4), 528–534. https://doi.org/10.1016/j.bcab.2015.09.011

Dragosits, M., & Mattanovich, D. (2013). Adaptive laboratory evolution – principles and applications for biotechnology. *Microbial Cell Factories*, *12*(1), 64. https://doi.org/10.1186/1475-2859-12-64

Dzurendova, S., Zimmermann, B., Tafintseva, V., Kohler, A., Ekeberg, D., & Shapaval, V. (2020). The influence of phosphorus source and the nature of nitrogen substrate on the biomass production and lipid accumulation in oleaginous Mucoromycota fungi. *Applied Microbiology and Biotechnology*, *104*(18), 8065–8076. https://doi.org/10.1007/s00253-020-10821-7

Ekpenyong, M. G., Antai, S. P., Asitok, A. D., & Ekpo, B. O. (2017). Plackett-Burman Design and Response Surface Optimization of Medium Trace Nutrients for Glycolipopeptide Biosurfactant Production. *Iranian Biomedical Journal*, *21*(4), 249–260. https://doi.org/10.18869/acadpub.ibj.21.4.249

El-Enshasy, H. A. (2007). Filamentous Fungal Cultures – Process Characteristics, Products, and Applications. In *Bioprocessing for Value-Added Products from Renewable Resources* (pp. 225–261). Elsevier. https://doi.org/10.1016/B978-044452114-9/50010-4

Fageria, N. K., dos Santos, A. B., & Moraes, M. F. (2010). Influence of Urea and Ammonium Sulfate on Soil Acidity Indices in Lowland Rice Production. *Communications in Soil Science and Plant Analysis*, *41*(13), 1565–1575. https://doi.org/10.1080/00103624.2010.485237

Fang, X., Zhao, G., Dai, J., Liu, H., Wang, P., Wang, L., Song, J., & Zheng, Z. (2018). Macro-morphological characterization and kinetics of Mortierella alpina colonies during batch cultivation. *PLOS ONE*, *13*(8), e0192803. https://doi.org/10.1371/journal.pone.0192803

Fisher, K. J., & Lang, G. I. (2016). Experimental evolution in fungi: An untapped resource. *Fungal Genetics and Biology*, *94*, 88–94. https://doi.org/10.1016/j.fgb.2016.06.007

Food Standards Australia New Zealand. (2003). *Dhasco and arasco oils as sources of long-chain polyunsaturated fatty acids in infant formula: A safety assessment*. Food Standards Australia New Zealand.

Fortela, D. L., Hernandez, R., French, W. T., Zappi, M., Revellame, E., Holmes, W., & Mondala, A. (2016). Extent of inhibition and utilization of volatile fatty acids as carbon sources for activated sludge microbial consortia dedicated for biodiesel production. *Renewable Energy*, *96*, 11–19. https://doi.org/10.1016/j.renene.2016.04.068

Gachelin, M., Boutoute, M., Carrier, G., Talec, A., Pruvost, E., Guihéneuf, F., Bernard, O., & Sciandra, A. (2021). Enhancing PUFA-rich polar lipids in Tisochrysis lutea using adaptive laboratory evolution (ALE) with oscillating thermal stress. *Applied Microbiology and Biotechnology*, *105*(1), 301–312. https://doi.org/10.1007/s00253-020-11000-4

Ghobadi, Z., Hamidi-Esfahani, Z., & Azizi, M. H. (2022). Statistical optimization of arachidonic acid synthesis by *Mortierella alpina* CBS 754.68 in a solid-state fermenter. *Food Science & Nutrition*, *10*(2), 436–444. https://doi.org/10.1002/fsn3.2667

Goyzueta-Mamani, L. D., Carvalho, J. C., Magalhães, A. I., & Soccol, C. R. (2021). Production of arachidonic acid by *Mortierella alpina* using wastes from potato chips industry. *Journal of Applied Microbiology*, *130*(5), 1592–1601. https://doi.org/10.1111/jam.14864

Gunstone, F. D. (2001). Oilseed Crops with Modified Fatty Acid Composition. *Journal of Oleo Science*, *50*(5), 269–279. https://doi.org/10.5650/jos.50.269

Guthrie, W. F. (2020). *NIST/SEMATECH e-Handbook of Statistical Methods (NIST Handbook 151)* [Data set]. National Institute of Standards and Technology. https://doi.org/10.18434/M32189

Hansson, L., & Dostalek, M. (1988). Effect of culture conditions on mycelial growth and production of ?-linolenic acid by the fungus Mortierella ramanniana. *Applied Microbiology and Biotechnology*, *28*(3). https://doi.org/10.1007/BF00250448

Hao, G., Chen, H., Gu, Z., Zhang, H., Chen, W., & Chen, Y. Q. (2015). Metabolic engineering of Mortierella alpina for arachidonic acid production with glycerol as carbon source. *Microbial Cell Factories*, *14*(1), 205. https://doi.org/10.1186/s12934-015-0392-4

Hayashi, S., Naka, M., Ikeuchi, K., Ohtsuka, M., Kobayashi, K., Satoh, Y., Ogasawara, Y., Maruyama, C., Hamano, Y., Ujihara, T., & Dairi, T. (2019). Control Mechanism for Carbon-Chain Length in Polyunsaturated Fatty-Acid Synthases. *Angewandte Chemie International Edition*, *58*(20), 6605–6610. https://doi.org/10.1002/anie.201900771

Hemansi, Himanshu, Patel, A. K., Saini, J. K., & Singhania, R. R. (2022). Development of multiple inhibitor tolerant yeast via adaptive laboratory evolution for sustainable bioethanol production. *Bioresource Technology*, *344*, 126247. https://doi.org/10.1016/j.biortech.2021.126247

Higashiyama, K., Fujikawa, S., Park, E. Y., & Okabe, M. (1999). Image analysis of morphological change during arachidonic acid production by Mortierella alpina 1S-4. *Journal of Bioscience and Bioengineering*, *87*(4), 489–494. https://doi.org/10.1016/S1389-1723(99)80098-X

Higashiyama, K., Fujikawa, S., Park, E. Y., & Shimizu, S. (2002). Production of arachidonic acid byMortierella fungi. *Biotechnology and Bioprocess Engineering*, *7*(5), 252–262. https://doi.org/10.1007/BF02932833

Higashiyama, K., Yaguchi, T., Akimoto, K., Fujikawa, S., & Shimizu, S. (1998a). Enhancement of arachidonic acid production by *Mortierella alpina* 1S-4. *Journal of the American Oil Chemists' Society*, *75*(11), 1501–1505. https://doi.org/10.1007/s11746-998-0085-9

Higashiyama, K., Yaguchi, T., Akimoto, K., Fujikawaa, S., & Sakayu Shimizu. (1998b). Effects of mineral addition on the growth morphology of and arachidonic acid production by *Mortierella alpina* 1S-4. *Journal of the American Oil Chemists' Society*, *75*(12), 1815–1819. https://doi.org/10.1007/s11746-998-0336-9

HiMedia Laboratories. (2018). *Soy Peptone—Material Code RM007*. https://www.himediadownloads.com/MSDS/RM007.pdf

Hlavova, M., Turoczy, Z., & Bisova, K. (2015). Improving microalgae for biotechnology—From genetics to synthetic biology. *Biotechnology Advances*, *33*(6), 1194–1203. https://doi.org/10.1016/j.biotechadv.2015.01.009

Hoffman, D. R., Boettcher, J. A., & Diersen-Schade, D. A. (2009). Toward optimizing vision and cognition in term infants by dietary docosahexaenoic and arachidonic acid supplementation: A review of randomized controlled trials. *Prostaglandins, Leukotrienes and Essential Fatty Acids*, *81*(2–3), 151–158. https://doi.org/10.1016/j.plefa.2009.05.003

Hu, X., Luo, Y., Man, Y., Tang, X., Bi, Z., & Ren, L. (2022). Lipidomic and transcriptomic analysis reveals the self-regulation mechanism of Schizochytrium sp. In response to temperature stresses. *Algal Research*, *64*, 102664. https://doi.org/10.1016/j.algal.2022.102664

Hu, X., Tang, X., Bi, Z., Zhao, Q., & Ren, L. (2021). Adaptive evolution of microalgae Schizochytrium sp. Under high temperature for efficient production of docosahexaeonic acid. *Algal Research*, *54*, 102212. https://doi.org/10.1016/j.algal.2021.102212

Iacobazzi, V., & Infantino, V. (2014). Citrate – new functions for an old metabolite. *Biological Chemistry*, *395*(4), 387–399. https://doi.org/10.1515/hsz-2013-0271

ISixSigma. (2022). *STANDARDIZED RESIDUAL*. https://www.isixsigma.com/dictionary/standardized-residual/

Ji, X.-J., Ren, L.-J., Nie, Z.-K., Huang, H., & Ouyang, P.-K. (2014). Fungal arachidonic acid-rich oil: Research, development and industrialization. *Critical Reviews in Biotechnology*, *34*(3), 197–214. https://doi.org/10.3109/07388551.2013.778229

Jin, M.-J., Huang, H., Xiao, A.-H., Gao, Z., Liu, X., & Peng, C. (2009). Enhancing arachidonic acid production by Mortierella alpina ME-1 using improved mycelium aging technology. *Bioprocess and Biosystems Engineering*, *32*(1), 117–122. https://doi.org/10.1007/s00449-008-0229-1

Kavitha, M. D., Kathiresan, S., Bhattacharya, S., & Sarada, R. (2016). Culture media optimization of Porphyridium purpureum: Production potential of biomass, total lipids, arachidonic and eicosapentaenoic acid. *Journal of Food Science and Technology*, *53*(5), 2270–2278. https://doi.org/10.1007/s13197-016-2185-0

Kawashima, H. (2019). Intake of arachidonic acid-containing lipids in adult humans: Dietary surveys and clinical trials. *Lipids in Health and Disease*, *18*(1), 101. https://doi.org/10.1186/s12944-019-1039-y

Kikukawa, H., Sakuradani, E., Ando, A., Shimizu, S., & Ogawa, J. (2018). Arachidonic acid production by the oleaginous fungus Mortierella alpina 1S-4: A review. *Journal of Advanced Research*, *11*, 15–22. https://doi.org/10.1016/j.jare.2018.02.003

Kim, Z.-H., Kim, K., Park, H., Lee, C. S., Nam, S. W., Yim, K. J., Jung, J. Y., Hong, S.-J., & Lee, C.-G. (2021). Enhanced Fatty Acid Productivity by Parachlorella sp., a Freshwater Microalga, via Adaptive Laboratory Evolution Under Salt Stress. *Biotechnology and Bioprocess Engineering*, *26*(2), 223–231. https://doi.org/10.1007/s12257-020-0001-1

Koike, Y., Jie Cai, H., Higashiyama, K., Fujikawa, S., & Park, E. Y. (2001). Effect of consumed carbon to nitrogen ratio of mycelial morphology and arachidonic acid production in cultures of mortierella alpina. *Journal of Bioscience and Bioengineering*, *91*(4), 382–389. https://doi.org/10.1016/S1389-1723(01)80156-0

Kowluru, A., Chen, H.-Q., Modrick, L. M., & Stefanelli, C. (2001). Activation of Acetyl-CoA Carboxylase by a Glutamate- and Magnesium-Sensitive Protein Phosphatase in the Islet β-Cell. *Diabetes*, *50*(7), 1580–1587. https://doi.org/10.2337/diabetes.50.7.1580

Kraber, S. (2022, May). *Understanding Lack of Fit: When to Worry*. StatEase. https://www.statease.com/blog/understanding-lack-of-fit-when-to-worry/

Kyle, D. J. (2010). Future Development of Single Cell Oils. In *Single Cell Oils* (pp. 439–451). Elsevier. https://doi.org/10.1016/B978-1-893997-73-8.50024-4

LaCroix, R. A., Palsson, B. O., & Feist, A. M. (2017). A Model for Designing Adaptive Laboratory Evolution Experiments. *Applied and Environmental Microbiology*, *83*(8), e03115-16. https://doi.org/10.1128/AEM.03115-16

Lan, W.-Z., Qin, W.-M., & Yu, L.-J. (2002). Effect of glutamate on arachidonic acid production from Mortierella alpina. *Letters in Applied Microbiology*, *35*(4), 357–360. https://doi.org/10.1046/j.1472-765X.2002.01195.x

LaPanse, A. J., Krishnan, A., & Posewitz, M. C. (2021). Adaptive Laboratory Evolution for algal strain improvement: Methodologies and applications. *Algal Research*, *53*, 102122. https://doi.org/10.1016/j.algal.2020.102122

Lee, S., & Kim, P. (2020). Current Status and Applications of Adaptive Laboratory Evolution in Industrial Microorganisms. *Journal of Microbiology and Biotechnology*, *30*(6), 793–803. https://doi.org/10.4014/jmb.2003.03072

Leth, I. K., & McDonald, K. A. (2017). Media development for large scale *Agrobacterium tumefaciens* culture. *Biotechnology Progress*, *33*(5), 1218–1225. https://doi.org/10.1002/btpr.2504

Li, J., Liu, Y., Cheng, J. J., Mos, M., & Daroch, M. (2015). Biological potential of microalgae in China for biorefinery-based production of biofuels and high value compounds. *New Biotechnology*, *32*(6), 588–596. https://doi.org/10.1016/j.nbt.2015.02.001

Li, X., Liu, R., Li, J., Chang, M., Liu, Y., Jin, Q., & Wang, X. (2015). Enhanced arachidonic acid production from Mortierella alpina combining atmospheric and room temperature plasma (ARTP) and diethyl sulfate treatments. *Bioresource Technology*, *177*, 134–140. https://doi.org/10.1016/j.biortech.2014.11.051

Li, X., Pei, G., Liu, L., Chen, L., & Zhang, W. (2017). Metabolomic analysis and lipid accumulation in a glucose tolerant Crypthecodinium cohnii strain obtained by adaptive laboratory evolution. *Bioresource Technology*, *235*, 87–95. https://doi.org/10.1016/j.biortech.2017.03.049

Liang, M.-H., & Jiang, J.-G. (2013). Advancing oleaginous microorganisms to produce lipid via metabolic engineering technology. *Progress in Lipid Research*, *52*(4), 395–408. https://doi.org/10.1016/j.plipres.2013.05.002

Liao, W., Liu, Y., Frear, C., & Chen, S. (2007). A new approach of pellet formation of a filamentous fungus – Rhizopus oryzae. *Bioresource Technology*, *98*(18), 3415–3423. https://doi.org/10.1016/j.biortech.2006.10.028

Lina, L., Changqing, Y., & Yuxi, H. (2011). Enhancement of Arachidonic Acid Production by Mortierella isabellina Through Protoplast Regeneration Mutagenesis. *Journal of Northeast Agricultural University (English Edition)*, *18*(2), 65–72. https://doi.org/10.1016/S1006-8104(12)60012-9

Ling, X., Zeng, S., Chen, C., Liu, X., & Lu, Y. (2016). Enhanced arachidonic acid production using a bioreactor culture of Mortierella alpina with a combined organic nitrogen source. *Bioresources and Bioprocessing*, *3*(1), 43. https://doi.org/10.1186/s40643-016-0121-9

Liu, S., Zhao, Y., Liu, L., Ao, X., Ma, L., Wu, M., & Ma, F. (2015). Improving Cell Growth and Lipid Accumulation in Green Microalgae Chlorella sp. Via UV Irradiation. *Applied Biochemistry and Biotechnology*, *175*(7), 3507–3518. https://doi.org/10.1007/s12010-015-1521-6

Liu, X., Ji, X., Zhang, H., Fu, N., Yan, L., Deng, Z., & Huang, H. (2012). Development of a Defined Medium for Arachidonic Acid Production by Mortierella alpina Using a Visualization Method. *Applied Biochemistry and Biotechnology*, *168*(6), 1516–1527. https://doi.org/10.1007/s12010-012-9874-6

Lo, E., Arora, N., & Philippidis, G. P. (2022). Physiological insights into enhanced lipid accumulation and temperature tolerance by Tetraselmis suecica ultraviolet mutants. *Science of The Total Environment*, *839*, 156361. https://doi.org/10.1016/j.scitotenv.2022.156361

Lu, J., Peng, C., Ji, X.-J., You, J., Cong, L., Ouyang, P., & Huang, H. (2011). Fermentation Characteristics of Mortierella alpina in Response to Different Nitrogen Sources. *Applied Biochemistry and Biotechnology*, *164*(7), 979–990. https://doi.org/10.1007/s12010-011-9189-z

Malaiwong, N., Yongmanitchai, W., & Chonudomkul, D. (2016). Optimization of arachidonic acid production from Mortierella alpina PRAO7-10 by response surface methodology. *Agriculture and Natural Resources*, *50*(3), 162–172. https://doi.org/10.1016/j.anres.2016.06.003

Mamani, L. D. G., Magalhães, A. I., Ruan, Z., Carvalho, J. C. de, & Soccol, C. R. (2019). Industrial production, patent landscape, and market trends of arachidonic acid-rich oil of Mortierella alpina. *Biotechnology Research and Innovation*, *3*(1), 103–119. https://doi.org/10.1016/j.biori.2019.02.002

Mavrommati, M., Daskalaki, A., Papanikolaou, S., & Aggelis, G. (2022). Adaptive laboratory evolution principles and applications in industrial biotechnology. *Biotechnology Advances*, *54*, 107795. https://doi.org/10.1016/j.biotechadv.2021.107795

McDonald, M. J. (2019). Microbial Experimental Evolution – a proving ground for evolutionary theory and a tool for discovery. *EMBO Reports*, *20*(8). https://doi.org/10.15252/embr.201846992

Mhlongo, S. I., Ezeokoli, O. T., Roopnarain, A., Ndaba, B., Sekoai, P. T., Habimana, O., & Pohl, C. H. (2021). The Potential of Single-Cell Oils Derived From Filamentous Fungi as Alternative Feedstock Sources for Biodiesel Production. *Frontiers in Microbiology*, *12*, 637381. https://doi.org/10.3389/fmicb.2021.637381

Min, B., Kim, K., Li, V., Kim, Y., & Kim, H. (2019). *Adaptive laboratory evolution of heat tolerance in Streptococcus thermophilus BIOPOP-1 and BIOPOP-2 under gradually increasing heat temperature* [Preprint]. In Review. https://doi.org/10.21203/rs.2.14193/v1

Mironov, A., Nemashkalov, V., Stepanova, N., Kamzolova, S., Rymowicz, W., & Morgunov, I. (2018). The Effect of pH and Temperature on Arachidonic Acid Production by Glycerol-Grown Mortierella alpina NRRL-A-10995. *Fermentation*, *4*(1), 17. https://doi.org/10.3390/fermentation4010017

Moldes, A., Cendón, Y., & Barral, M. T. (2007). Evaluation of municipal solid waste compost as a plant growing media component, by applying mixture design. *Bioresource Technology*, *98*(16), 3069–3075. https://doi.org/10.1016/j.biortech.2006.10.021

Montone, C. M., Aita, S. E., Catani, M., Cavaliere, C., Cerrato, A., Piovesana, S., Laganà, A., & Capriotti, A. L. (2021). Profiling and quantitative analysis of underivatized fatty acids in *Chlorella vulgaris* microalgae by liquid chromatography-high resolution mass spectrometry. *Journal of Separation Science*, *44*(16), 3041–3051. https://doi.org/10.1002/jssc.202100306

Morales, M., Aflalo, C., & Bernard, O. (2021). Microalgal lipids: A review of lipids potential and quantification for 95 phytoplankton species. *Biomass and Bioenergy*, *150*, 106108. https://doi.org/10.1016/j.biombioe.2021.106108

Moussa, S. H., Tayel, A. A., Al-Hassan, A. A., & Farouk, A. (2013). Tetrazolium/Formazan Test as an Efficient Method to Determine Fungal Chitosan Antimicrobial Activity. *Journal of Mycology*, *2013*, 1–7. https://doi.org/10.1155/2013/753692

Muthuraj, M., Selvaraj, B., Palabhanvi, B., Kumar, V., & Das, D. (2019). Enhanced lipid content in Chlorella sp. FC2 IITG via high energy irradiation mutagenesis. *Korean Journal of Chemical Engineering*, *36*(1), 63–70. https://doi.org/10.1007/s11814-018-0180-z

Myers, R. H., Montgomery, D. C., & Anderson-Cook, C. M. (2009). *Response Surface Methodology: Process and Product Optimization Using Designed Experiments* (3rd Edition). John Wiley & Sons.

National Center for Biotechnology Information. (2023a). *PubChem Compound Summary for CID 24268, Sodium Nitrate*. https://pubchem.ncbi.nlm.nih.gov/compound/Sodium-Nitrate

National Center for Biotechnology Information. (2023b). *PubChem Compound Summary for CID 6097028, Ammonium Sulfate*. https://pubchem.ncbi.nlm.nih.gov/compound/Ammonium-Sulfate

National Center for Biotechnology Information. (2023c). *PubChem Compound Summary for CID 23672308, Monosodium Glutamate*. https://pubchem.ncbi.nlm.nih.gov/compound/Monosodium-Glutamate

Nisha, A. (2009). *Biotechnological Studies for the Production of Arachidonic Acid from Mortierella Alpina.pdf* [PhD thesis, University of Mysore]. http://ir.cftri.res.in/id/eprint/9961

Nisha, A., Rastogi, N. K., & Venkateswaran, G. (2011). Optimization of media components for enhanced arachidonic acid production by Mortierella alpina under submerged cultivation. *Biotechnology and Bioprocess Engineering*, *16*(2), 229–237. https://doi.org/10.1007/s12257-010-0294-6

Nisha, A., & Venkateswaran, G. (2011). Effect of Culture Variables on Mycelial Arachidonic acid Production by Mortierella alpina. *Food and Bioprocess Technology*, *4*(2), 232–240. https://doi.org/10.1007/s11947-008-0146-y

Obukowicz, M. G., Welsch, D. J., Salsgiver, W. J., Martin-Berger, C. L., Chinn, K. S., Duffin, K. L., Raz, A., & Needleman, P. (1998). Novel, selective delta6 or delta5 fatty acid desaturase inhibitors as antiinflammatory agents in mice. *The Journal of Pharmacology and Experimental Therapeutics*, *287*(1), 157–166.

Oladosu, Y., Rafii, M. Y., Abdullah, N., Hussin, G., Ramli, A., Rahim, H. A., Miah, G., & Usman, M. (2016). Principle and application of plant mutagenesis in crop improvement: A review. *Biotechnology & Biotechnological Equipment*, *30*(1), 1–16. https://doi.org/10.1080/13102818.2015.1087333

Olawoye, Babatunde. (2016). *A comprehensive handout on central composite design (ccd)*. Springer.

Onipchenko, V. G. (Ed.). (2004). *Alpine Ecosystems in the Northwest Caucasus*. Springer Netherlands. https://doi.org/10.1007/978-1-4020-2383-5

Ozimek, E., & Hanaka, A. (2020). Mortierella Species as the Plant Growth-Promoting Fungi Present in the Agricultural Soils. *Agriculture*, *11*(1), 7. https://doi.org/10.3390/agriculture11010007

Papagianni, M. (2004). Fungal morphology and metabolite production in submerged mycelial processes. *Biotechnology Advances*, *22*(3), 189–259. https://doi.org/10.1016/j.biotechadv.2003.09.005

Patrovsky, M., Sinovska, K., Branska, B., & Patakova, P. (2019). Effect of initial pH, different nitrogen sources, and cultivation time on the production of yellow or orange *Monascus purpureus* pigments and the mycotoxin citrinin. *Food Science & Nutrition*, *7*(11), 3494–3500. https://doi.org/10.1002/fsn3.1197

Peng, C., Huang, H., Ji, X., Liu, X., You, J., Lu, J., Cong, L., Xu, X., & Ouyang, P. (2010). A temperature-shift strategy for efficient arachidonic acid fermentation by Mortierella alpina in batch culture. *Biochemical Engineering Journal*, *53*(1), 92–96. https://doi.org/10.1016/j.bej.2010.09.014

Posch, A. E., Herwig, C., & Spadiut, O. (2013). Science-based bioprocess design for filamentous fungi. *Trends in Biotechnology*, *31*(1), 37–44. https://doi.org/10.1016/j.tibtech.2012.10.008

Rastogi, R. P., Richa, Kumar, A., Tyagi, M. B., & Sinha, R. P. (2010). Molecular Mechanisms of Ultraviolet Radiation-Induced DNA Damage and Repair. *Journal of Nucleic Acids*, *2010*, 1–32. https://doi.org/10.4061/2010/592980

Ratledge, C., & Hopkins, S. (2006). Lipids from microbial sources. In *Modifying Lipids for Use in Food* (pp. 80–113). Elsevier. https://doi.org/10.1533/9781845691684.1.80

Rayaroth, A. C., Tomar, R. S., & Mishra, R. K. (2017). Arachidonic Acid Synthesis in Mortierella alpina: Origin, Evolution and Advancements. *Proceedings of the National Academy of Sciences, India Section B: Biological Sciences*, *87*(4), 1053–1066. https://doi.org/10.1007/s40011-016-0714-2

Rayaroth, A., Tomar, R. S., & Mishra, R. K. (2021). One step selection strategy for optimization of media to enhance arachidonic acid production under solid state fermentation. *LWT*, *152*, 112366. https://doi.org/10.1016/j.lwt.2021.112366

Ren, L., Sun, X., Zhang, L., Huang, H., & Zhao, Q. (2020). Exergy analysis for docosahexaenoic acid production by fermentation and strain improvement by adaptive laboratory evolution for Schizochytrium sp. *Bioresource Technology*, *298*, 122562. https://doi.org/10.1016/j.biortech.2019.122562

Rispoli, F., & Shah, V. (2009). A new efficient mixture screening design for optimization of media. *Biotechnology Progress*, *25*(4), 980–985. https://doi.org/10.1002/btpr.225

Rocky-Salimi, K., Hamidi-Esfahani, Z., & Abbasi, S. (2011). Statistical optimization of arachidonic acid production by Mortierella alpina CBS 754.68 in submerged fermentation. *IRANIAN JOURNAL of BIOTECHNOLOGY*, *9*(2), 7.

Ryan, A. S., Zeller, S., & Nelson, E. B. (2010). Safety Evaluation of Single Cell Oils and the Regulatory Requirements for Use as Food Ingredients. In *Single Cell Oils* (pp. 317–350). Elsevier. https://doi.org/10.1016/B978-1-893997-73-8.50019-0

Saelao, S., Kanjana-Opas, A., & Kaewsuwan, S. (2011). Optimization of Biomass and Arachidonic Acid Production by Aureispira maritima Using Response Surface Methodology. *Journal of the American Oil Chemists' Society*, *88*(5), 619–629. https://doi.org/10.1007/s11746-010-1710-y

Sakuradani, E. (2010). Advances in the Production of Various Polyunsaturated Fatty Acids through Oleaginous Fungus *Mortierella alpina* Breeding. *Bioscience, Biotechnology, and Biochemistry*, *74*(5), 908–917. https://doi.org/10.1271/bbb.100001

Sakuradani, E., Ando, A., Ogawa, J., & Shimizu, S. (2010). Arachidonic Acid-Producing Mortierella alpina: Creation of Mutants, Isolation of the Related Enzyme Genes, and Molecular Breeding. In *Single Cell Oils* (pp. 29–49). Elsevier. https://doi.org/10.1016/B978-1-893997-73-8.50006-2

Sakuradani, E., Ando, A., Shimizu, S., & Ogawa, J. (2013). Metabolic engineering for the production of polyunsaturated fatty acids by oleaginous fungus Mortierella alpina 1S-4. *Journal of Bioscience and Bioengineering*, *116*(4), 417–422. https://doi.org/10.1016/j.jbiosc.2013.04.008

Salem, N., & Van Dael, P. (2020). Arachidonic Acid in Human Milk. *Nutrients*, *12*(3), 626. https://doi.org/10.3390/nu12030626

Samadlouie, H.-R., Hamidi-Esfahani, Z., Alavi, S.-M., Soltani-Najafabadi, M., Sahari, M. A., & Abbasi, S. (2012). Statistical approach to optimization of fermentative production of oil and arachidonic acid from Mortierella alpine CBS 754.68. *Afr. J. Microbiol. Res.*, *6*(7), 1559–1567. https://doi.org/10.5897/AJMR11.1552

Sandberg, T. E., Salazar, M. J., Weng, L. L., Palsson, B. O., & Feist, A. M. (2019). The emergence of adaptive laboratory evolution as an efficient tool for biological discovery and industrial biotechnology. *Metabolic Engineering*, *56*, 1–16. https://doi.org/10.1016/j.ymben.2019.08.004

Sarayloo, E., Simsek, S., Unlu, Y. S., Cevahir, G., Erkey, C., & Kavakli, I. H. (2018). Enhancement of the lipid productivity and fatty acid methyl ester profile of Chlorella vulgaris by two rounds of mutagenesis. *Bioresource Technology*, *250*, 764–769. https://doi.org/10.1016/j.biortech.2017.11.105

Sathish, T., Lakshmi, G. S., Rao, Ch. S., Brahmaiah, P., & Prakasham, R. S. (2008). Mixture design as first step for improved glutaminase production in solid-state fermentation by isolated *Bacillus* sp. RSP-GLU. *Letters in Applied Microbiology*, *47*(4), 256–262. https://doi.org/10.1111/j.1472-765X.2008.02413.x

Schaum, C.-E., Buckling, A., Smirnoff, N., Studholme, D. J., & Yvon-Durocher, G. (2018). Environmental fluctuations accelerate molecular evolution of thermal tolerance in a marine diatom. *Nature Communications*, *9*(1), 1719. https://doi.org/10.1038/s41467-018-03906-5

Shanab, S. M. M., Hafez, R. M., & Fouad, A. S. (2018). A review on algae and plants as potential source of arachidonic acid. *Journal of Advanced Research*, *11*, 3–13. https://doi.org/10.1016/j.jare.2018.03.004

Shariati, S., Zare, D., & Mirdamadi, S. (2019). Screening of carbon and nitrogen sources using mixture analysis designs for carotenoid production by Blakeslea trispora. *Food Science and Biotechnology*, *28*(2), 469–479. https://doi.org/10.1007/s10068-018-0484-0

Shinmen, Y., Shimizu, S., Akimoto, K., Kawashima, H., & Yamada, H. (1989). Production of arachidonic acid by Mortierella fungi: Selection of a potent producer and optimization of culture conditions for large-scale production. *Applied Microbiology and Biotechnology*, *31*(1). https://doi.org/10.1007/BF00252518

Shofiul Azam, Md., Zhennan, G., Haiqin, C., & Yong Q., C. (2015). Using Mortierella alpina as a Novel Platform for Lipid Synthesis Inhibitor Screening. *Advances in Bioscience and Bioengineering*, *3*(1), 1–10. https://doi.org/10.11648/j.abb.20150301.11

Sigma-Aldrich. (2020). *Yeast Extract—Y1625*. https://www.sigmaaldrich.com/specification-sheets/549/569/Y1625-BULK_____SIGMA____.pdf

Sigma-Aldrich. (2022). *Urea—08582*. https://www.sigmaaldrich.com/CA/en/sds/sial/08582

Sinclair, A. J., & Jayasooriya, A. (2010). Nutritional Aspects of Single Cell Oils: Applications of Arachidonic Acid and Docosahexaenoic Acid Oils. In *Single Cell Oils* (pp. 351–368). Elsevier. https://doi.org/10.1016/B978-1-893997-73-8.50020-7

Singh, A., & Ward, O. P. (1997). Production of high yields of arachidonic acid in a fed-batch system by Mortierella alpina ATCC 32222. *Applied Microbiology and Biotechnology*, *48*(1), 1–5. https://doi.org/10.1007/s002530051005

Singh, V., Haque, S., Niwas, R., Srivastava, A., Pasupuleti, M., & Tripathi, C. K. M. (2017). Strategies for Fermentation Medium Optimization: An In-Depth Review. *Frontiers in Microbiology*, *7*. https://doi.org/10.3389/fmicb.2016.02087

Smith, N. M. H. (2020). *Screening novel marine fungal strains for the production of polyunsaturated fatty acids, specifically, eicosapentaenoic acid and arachidonic acid.* [Acadia University]. https://scholar.acadiau.ca/islandora/object/theses:3432

Streekstra, H. (2010). Arachidonic Acid: Fermentative Production by Mortierella Fungi. In *Single Cell Oils (Second Edition)* (Zvi Cohen, Colin Ratledge, pp. 97–114). https://doi.org/10.1016/B978-1-893997-73-8.50009-8

Sun, B., Han, P., Tao, R., Pang, Q., & Jia, S. (2015). Optimization of Cultural Conditions for Extracellular Polymeric Substances (EPS) Production by Burkholderia Using Response Surface Methodology. In T.-C. Zhang & M. Nakajima (Eds.), *Advances in Applied Biotechnology* (Vol. 333, pp. 295–303). Springer Berlin Heidelberg. https://doi.org/10.1007/978-3-662-46318-5_32

Sun, D., Zhou, C., Zhu, C., & Sun, Y. (2015). Effects of Culture Medium on PUFAs Production by Mortierella isabellinas. In T.-C. Zhang & M. Nakajima (Eds.), *Advances in Applied Biotechnology* (Vol. 333, pp. 219–228). Springer Berlin Heidelberg. https://doi.org/10.1007/978-3-662-46318-5_24

Sun, X.-M., Ren, L.-J., Bi, Z.-Q., Ji, X.-J., Zhao, Q.-Y., Jiang, L., & Huang, H. (2018). Development of a cooperative two-factor adaptive-evolution method to enhance lipid production and prevent lipid peroxidation in Schizochytrium sp. *Biotechnology for Biofuels*, *11*(1), 65. https://doi.org/10.1186/s13068-018-1065-4

Sun, X.-M., Ren, L.-J., Ji, X.-J., Chen, S.-L., Guo, D.-S., & Huang, H. (2016). Adaptive evolution of Schizochytrium sp. By continuous high oxygen stimulations to enhance docosahexaenoic acid synthesis. *Bioresource Technology*, *211*, 374–381. https://doi.org/10.1016/j.biortech.2016.03.093

Sun, X.-M., Ren, L.-J., Zhao, Q.-Y., Ji, X.-J., & Huang, H. (2018). Microalgae for the production of lipid and carotenoids: A review with focus on stress regulation and adaptation. *Biotechnology for Biofuels*, *11*(1), 272. https://doi.org/10.1186/s13068-018-1275-9

Tababa, H. G., Hirabayashi, S., & Inubushi, K. (2012). Media optimization of Parietochloris incisa for arachidonic acid accumulation in an outdoor vertical tubular photobioreactor. *Journal of Applied Phycology*, *24*(4), 887–895. https://doi.org/10.1007/s10811-011-9709-9

Takeno, S., Sakuradani, E., Tomi, A., Inohara-Ochiai, M., Kawashima, H., Ashikari, T., & Shimizu, S. (2005). Improvement of the Fatty Acid Composition of an Oil-Producing Filamentous Fungus, *Mortierella alpina* 1S-4, through RNA Interference with Δ12-Desaturase Gene Expression. *Applied and Environmental Microbiology*, *71*(9), 5124–5128. https://doi.org/10.1128/AEM.71.9.5124-5128.2005

Tallima, H., & El Ridi, R. (2018). Arachidonic acid: Physiological roles and potential health benefits – A review. *Journal of Advanced Research*, *11*, 33–41. https://doi.org/10.1016/j.jare.2017.11.004

Tapia V, E., Anschau, A., Coradini, A. L., T Franco, T., & Deckmann, A. C. (2012). Optimization of lipid production by the oleaginous yeast Lipomyces starkeyi by random mutagenesis coupled to cerulenin screening. *AMB Express*, *2*(1), 64. https://doi.org/10.1186/2191-0855-2-64

Teng, Y., Xu, Y., & Wang, D. (2009). Changes in morphology of Rhizopus chinensis in submerged fermentation and their effect on production of mycelium-bound lipase. *Bioprocess and Biosystems Engineering*, *32*(3), 397–405. https://doi.org/10.1007/s00449-008-0259-8

Totani, N., Yamaguchi, A., Yawata, M., & Ueda, T. (2002). The Role of Morphology during Growth of <I>Mortierella alpina</I> in Arachidonic Acid Production. *Journal of Oleo Science*, *51*(8), 531–538. https://doi.org/10.5650/jos.51.531

Trovão, M., Schüler, L. M., Machado, A., Bombo, G., Navalho, S., Barros, A., Pereira, H., Silva, J., Freitas, F., & Varela, J. (2022). Random Mutagenesis as a Promising Tool for Microalgal Strain Improvement towards Industrial Production. *Marine Drugs*, *20*(7), 440. https://doi.org/10.3390/md20070440

Turnbull, P. C. B., Reyes, A. E., Chute, M. D., & Mateczun, A. J. (2008). Effectiveness of UV Exposure of Items Contaminated with Anthrax Spores in a Class 2 Biosafety Cabinet and a Biosafety Level 3 Laboratory Pass-Box. *Applied Biosafety*, *13*(3), 164–168. https://doi.org/10.1177/153567600801300306

Vanaja, K., & Shobha Rani, R. H. (2007). Design of Experiments: Concept and Applications of Plackett Burman Design. *Clinical Research and Regulatory Affairs*, *24*(1), 1–23. https://doi.org/10.1080/10601330701220520

Wan, M., Zhang, J., Hou, D., Fan, J., Li, Y., Huang, J., & Wang, J. (2014). The effect of temperature on cell growth and astaxanthin accumulation of Haematococcus pluvialis during a light–dark cyclic cultivation. *Bioresource Technology*, *167*, 276–283. https://doi.org/10.1016/j.biortech.2014.06.030

Wang, J., Wang, Y., Wu, Y., Fan, Y., Zhu, C., Fu, X., Chu, Y., Chen, F., Sun, H., & Mou, H. (2021). Application of Microalgal Stress Responses in Industrial Microalgal Production Systems. *Marine Drugs*, *20*(1), 30. https://doi.org/10.3390/md20010030

Wang, L., Chen, W., Feng, Y., Ren, Y., Gu, Z., Chen, H., Wang, H., Thomas, M. J., Zhang, B., Berquin, I. M., Li, Y., Wu, J., Zhang, H., Song, Y., Liu, X., Norris, J. S., Wang, S., Du, P., Shen, J., … Chen, Y. Q. (2011). Genome Characterization of the Oleaginous Fungus Mortierella alpina. *PLoS ONE*, *6*(12), e28319. https://doi.org/10.1371/journal.pone.0028319

Wang, S., Wan, W., Wang, Z., Zhang, H., Liu, H., Arunakumara, K. K. I. U., Cui, Q., & Song, X. (2021). A Two-Stage Adaptive Laboratory Evolution Strategy to Enhance Docosahexaenoic Acid Synthesis in Oleaginous Thraustochytrid. *Frontiers in Nutrition*, *8*, 795491. https://doi.org/10.3389/fnut.2021.795491

Wice, B. M., Reitzer, L. J., & Kennell, D. (1981). The continuous growth of vertebrate cells in the absence of sugar. *The Journal of Biological Chemistry*, *256*(15), 7812–7819.

Winkler, J. D., & Kao, K. C. (2014). Recent advances in the evolutionary engineering of industrial biocatalysts. *Genomics*, *104*(6), 406–411. https://doi.org/10.1016/j.ygeno.2014.09.006

Wynn, J. P., Hamid, A. bin A., & Ratledge, C. (1999). The role of malic enzyme in the regulation of lipid accumulation in filamentous fungi. *Microbiology*, *145*(8), 1911–1917. https://doi.org/10.1099/13500872-145-8-1911

Xu, K., Lv, B., Huo, Y.-X., & Li, C. (2018). Toward the lowest energy consumption and emission in biofuel production: Combination of ideal reactors and robust hosts. *Current Opinion in Biotechnology*, *50*, 19–24. https://doi.org/10.1016/j.copbio.2017.08.011

Yadav, D. R., Kim, S. W., Adhikari, M., Um, Y. H., Kim, H. S., Kim, C., Lee, H. B., & Lee, Y. S. (2015). Three New Records of *Mortierella* Species Isolated from Crop Field Soil in Korea. *Mycobiology*, *43*(3), 203–209. https://doi.org/10.5941/MYCO.2015.43.3.203

Yadav, D. R., Kim, S. W., Babu, A. G., Adhikari, M., Kim, C., Lee, H. B., & Lee, Y. S. (2014). First Report of *Mortierella alpina* (Mortierellaceae, Zygomycota) Isolated from Crop Field Soil in Korea. *Mycobiology*, *42*(4), 401–404. https://doi.org/10.5941/MYCO.2014.42.4.401

Yang, J., John J Peterson, Andre I Khuri, Heidi B Goldfarb, Siuli Mukhopadhyay, Greg F Piepel, & Walter H Carter. (2006). *Response Surface Methodology And Related Topics*. World Scientific; eBook Academic Collection (EBSCOhost). http://ezproxy.library.dal.ca/login?url=https://search.ebscohost.com/login.aspx?direct=true&db=e000xna&AN=210782&site=ehost-live

Yang, L., Zhou, N., & Tian, Y. (2019). Characterization and application of dextranase produced by Chaetomium globosum mutant through combined application of atmospheric and room temperature plasma and ethyl methyl sulfone. *Process Biochemistry*, *85*, 116–124. https://doi.org/10.1016/j.procbio.2019.06.026

Yang, S.-T., Liu, X., & Zhang, Y. (2007). Metabolic Engineering – Applications, Methods, and Challenges. In *Bioprocessing for Value-Added Products from Renewable Resources* (pp. 73–118). Elsevier. https://doi.org/10.1016/B978-044452114-9/50005-0

Yao, Q., Chen, H., Wang, S., Tang, X., Gu, Z., Zhang, H., Chen, W., & Chen, Y. Q. (2019). An efficient strategy for screening polyunsaturated fatty acid-producing oleaginous filamentous fungi from soil. *Journal of Microbiological Methods*, *158*, 80–85. https://doi.org/10.1016/j.mimet.2018.12.023

Yuan, C., Wang, J., Shang, Y., Gong, G., Yao, J., & Yu, Z. (2002). Production of Arachidonic Acid by Mortierella alpina I49-N18. *Food Technology and Biotechnology*, *40*(4), 311–315.

Zeng, Y., Ji, X.-J., Chang, S.-M., Nie, Z.-K., & Huang, H. (2012). Improving arachidonic acid accumulation in Mortierella alpina through B-group vitamin addition. *Bioprocess and Biosystems Engineering*, *35*(5), 683–688. https://doi.org/10.1007/s00449-011-0648-2

Zhang, H., Cui, Q., & Song, X. (2021). Research advances on arachidonic acid production by fermentation and genetic modification of Mortierella alpina. *World Journal of Microbiology and Biotechnology*, *37*(1), 4. https://doi.org/10.1007/s11274-020-02984-2

Zhang, H., Lu, D., Li, X., Feng, Y., Cui, Q., & Song, X. (2018). Heavy ion mutagenesis combined with triclosan screening provides a new strategy for improving the arachidonic acid yield in Mortierella alpina. *BMC Biotechnology*, *18*(1), 23. https://doi.org/10.1186/s12896-018-0437-y

Zheng, Y., Hong, K., Wang, B., Liu, D., Chen, T., & Wang, Z. (2021). Genetic Diversity for Accelerating Microbial Adaptive Laboratory Evolution. *ACS Synthetic Biology*, *10*(7), 1574–1586. https://doi.org/10.1021/acssynbio.0c00589

Zhu, M., Yu, L. J., Liu, Z., & Xu, H. B. (2004). Isolating Mortierella alpina strains of high yield of arachidonic acid. *Letters in Applied Microbiology*, 4.

Zhu, M., Yu, L.-J., & Wu, Y.-X. (2003). An inexpensive medium for production of arachidonic acid by Mortierella alpina. *Journal of Industrial Microbiology & Biotechnology*, *30*(1), 75–79. https://doi.org/10.1007/s10295-002-0013-1

Zhu, S., Bonito, G., Chen, Y., & Du, Z.-Y. (2021). Oleaginous Fungi in Biorefineries. In *Encyclopedia of Mycology* (pp. 577–589). Elsevier. https://doi.org/10.1016/B978-0-12-819990-9.00004-4

Appendix A: Supplementary Figures

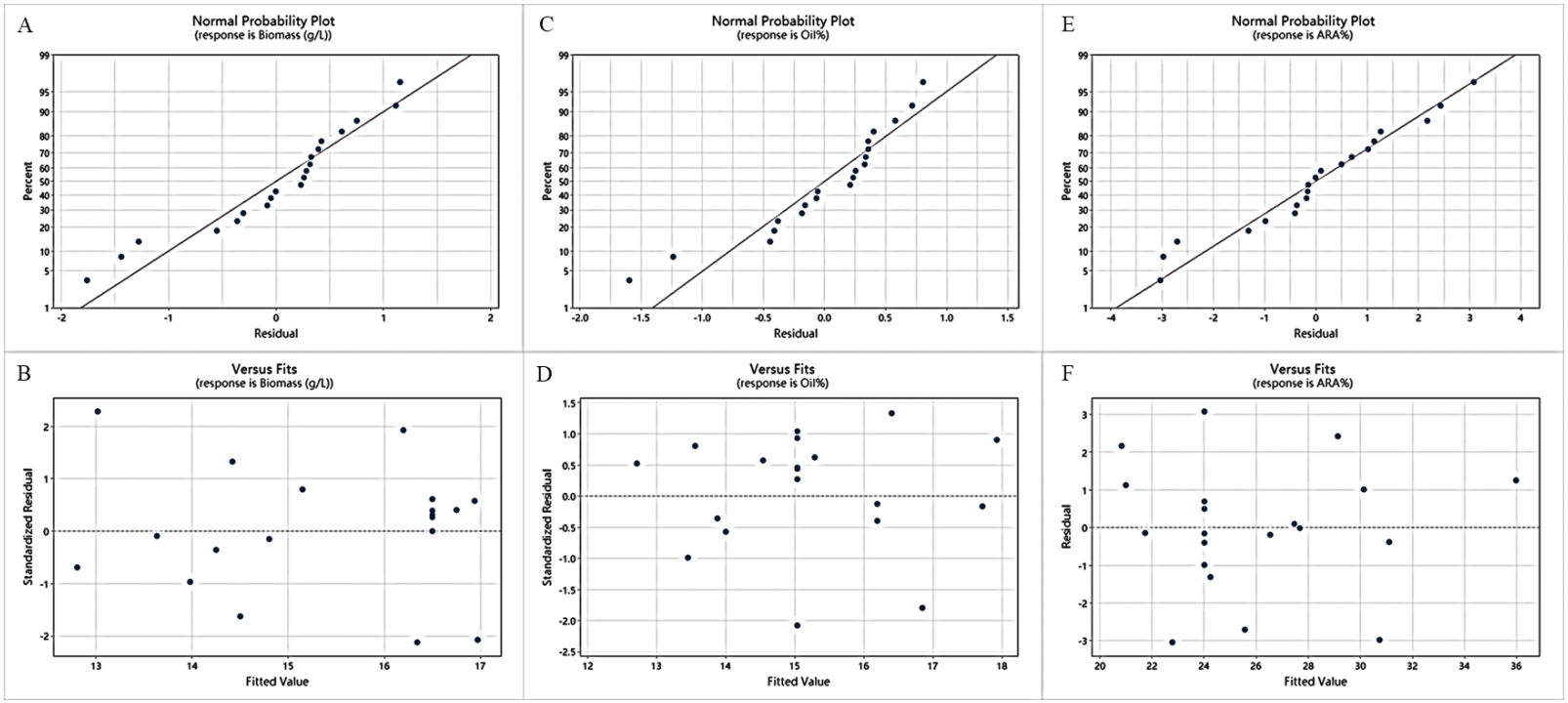

Figure A.1: (A, C, E) Normal probability plot of the residuals for significant response variables: A) Biomass DCW (g L^{-1}); C) TFA or total oil content w/w% in biomass; E) ARA w/w% in TFA. (B, D, F) Residual plots for residual versus fit for significant response variables: B) Biomass DCW (g L^{-1}); D) TFA or total oil content w/w% in biomass; F) ARA w/w% in TFA.

Analysis of Variance

Source	DF	Seq SS	Adj SS	Adj MS	F-Value	P-Value
Model	9	53053.3	53053.3	5894.8	4.27	0.021
Linear	3	24224.8	25682.5	8560.8	6.19	0.014
KH2PO4	1	7446.6	8904.3	8904.3	6.44	0.032
MgSO4	1	497.3	497.3	497.3	0.36	0.563
CaCl2	1	16280.9	16280.9	16280.9	11.78	0.007
Square	3	16508.3	16508.3	5502.8	3.98	0.047
KH2PO4*KH2PO4	1	186.6	8.2	8.2	0.01	0.940
MgSO4*MgSO4	1	1834.5	3553.3	3553.3	2.57	0.143
CaCl2*CaCl2	1	14487.1	14487.1	14487.1	10.48	0.010
2-Way Interaction	3	12320.2	12320.2	4106.7	2.97	0.089
KH2PO4*MgSO4	1	9131.1	9131.1	9131.1	6.61	0.030
KH2PO4*CaCl2	1	1904.2	1904.2	1904.2	1.38	0.271
MgSO4*CaCl2	1	1284.9	1284.9	1284.9	0.93	0.360
Error	9	12438.8	12438.8	1382.1		
Lack-of-Fit	4	8632.3	8632.3	2158.1	2.83	0.142
Pure Error	5	3806.5	3806.5	761.3		
Total	18	65492.1				

Figure A.2: ANOVA analysis for quadratic model of ARA concentration when removing the outlier (run no. # 9) in the 2nd RSM design. The figure was sourced from Minitab software.

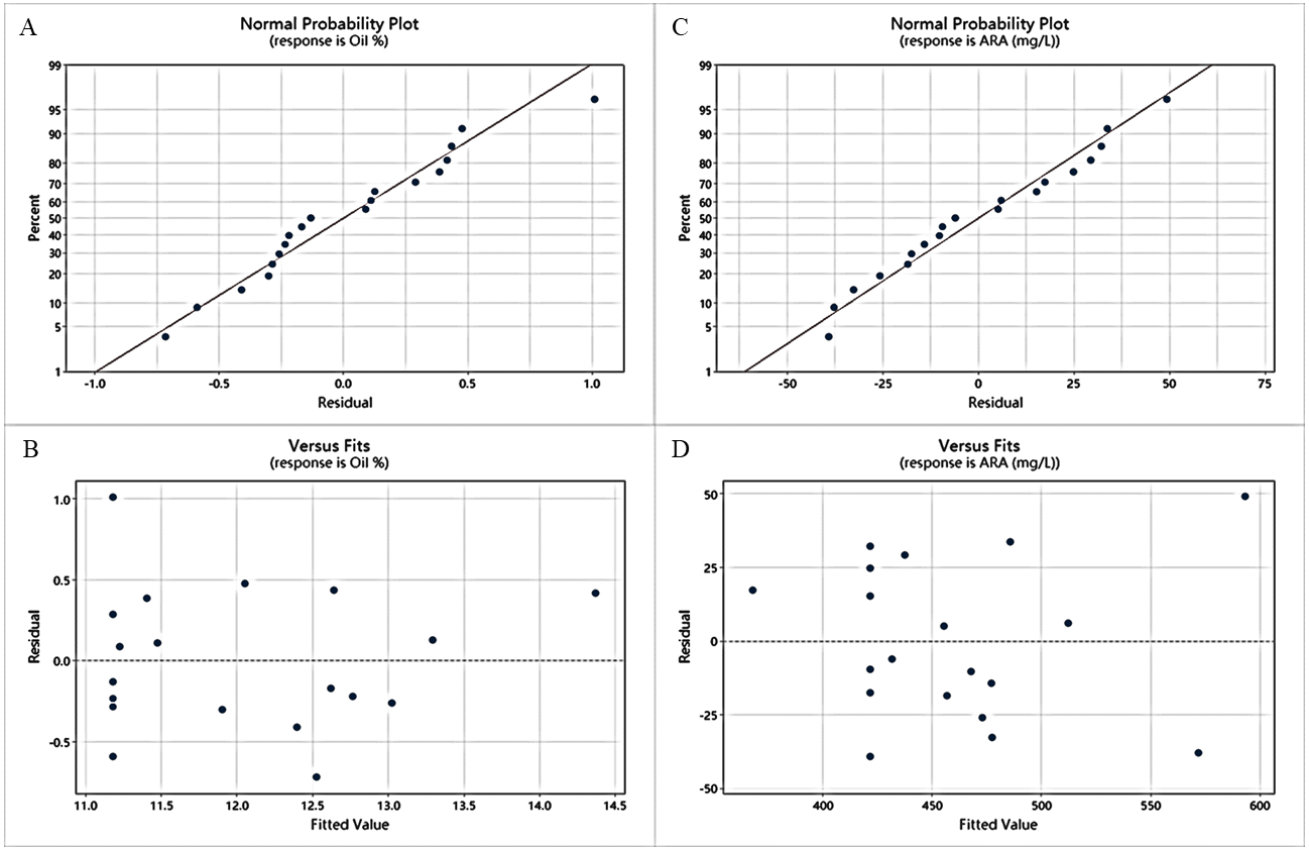

Figure A.3: (A and C) Normal probability plot of the residuals for significant response variables: A) Total oil content w/w%; C) ARA concentration (mg L^{-1}). (B and D) Residual plots for residual versus fit for significant response variables: B) Total oil content w/w%; D) ARA concentration (mg L^{-1}).

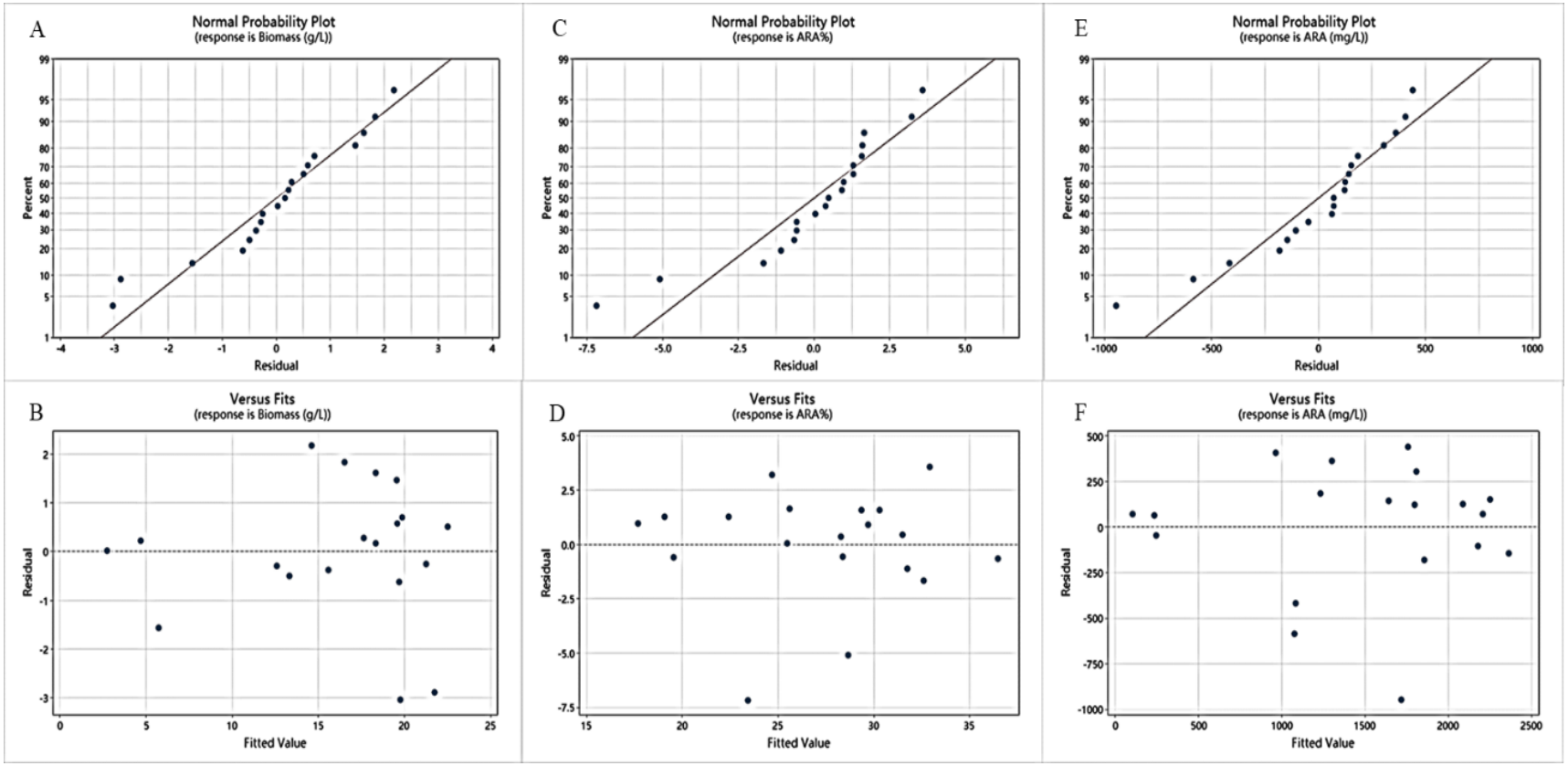

Figure A.4: (A, C, E) Normal probability plot of the residuals for significant response variables: A) Biomass DCW (g L^{-1}); C) ARA w/w% in TFA; E) ARA concentration (mg L^{-1}). (B, D, F) Residual plots for residual versus fit for significant response variables: B) Biomass DCW (g L^{-1}); D) ARA w/w% in TFA; F) ARA concentration (mg L^{-1}).

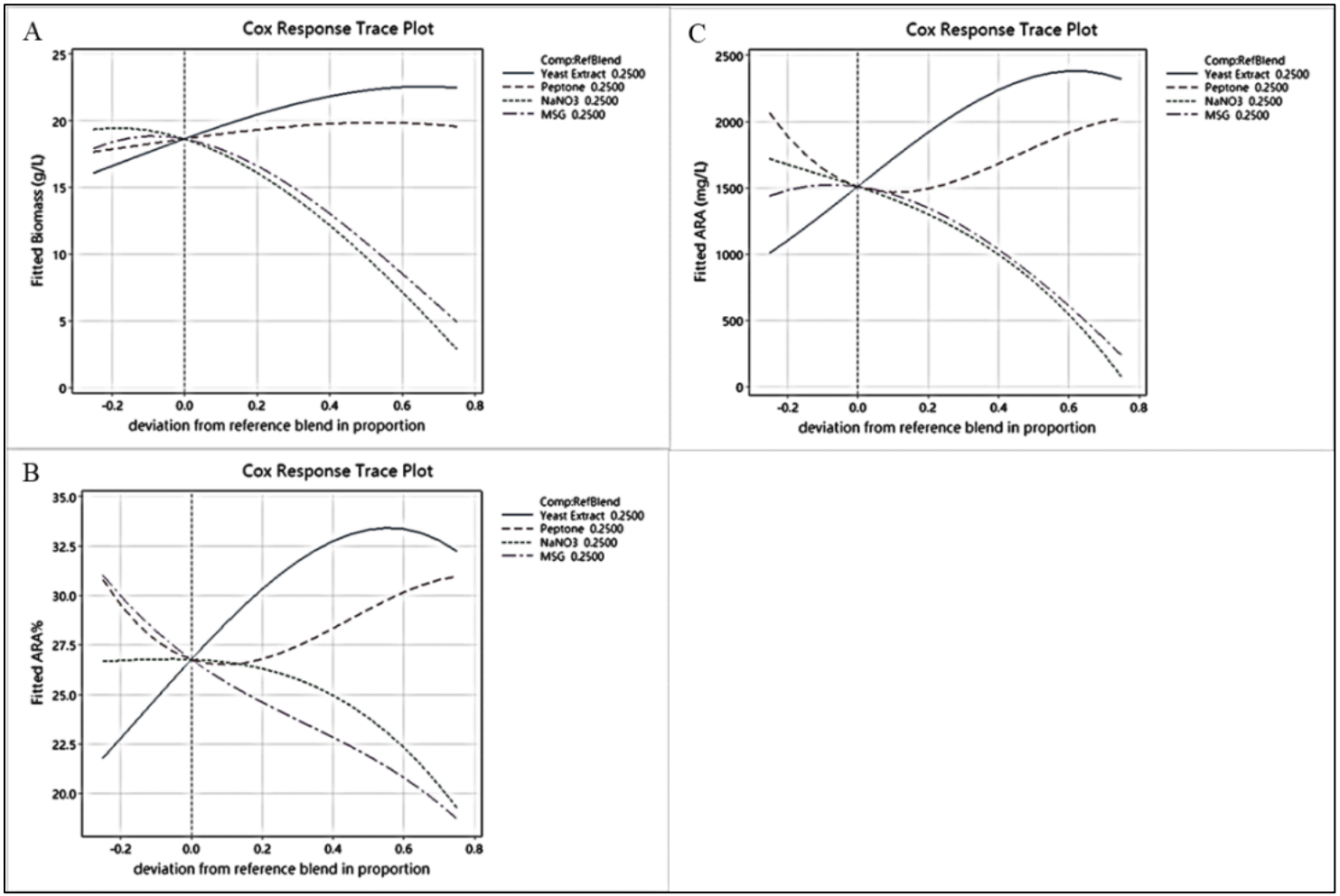

Figure A.5: Response trace plot (Cox direction) of four nitrogen sources. A) in response to biomass DCW (g L^{-1}); B) ARA w/w% in TFA; C) ARA concentration (mg L^{-1})

Appendix B: Supplementary Tables

Table B.1: Experimental design for screening nitrogen sources using mixture design, and the experimental values of the responses (biomass, oil content and ARA content and concentration) of *M. alpina* MA2-2

StdOrder	Yeast Extract	Peptone	$NaNO_3$	MSG	Biomass [b]	Oil %	ARA%	ARA
1	11 (100) [a]	0	0	0	23.0 ± 1.71[c]	31.0 ± 1.38	30.9 ± 1.2	2213.6 ± 348
2	0	10.58(100)	0	0	20.2 ± 0.45	34.3 ± 0.46	32.0 ± 0.62	2212.2 ± 35.6
3	0	0	6.68(100)	0	2.8 ± 1.39	33.8 ± 2.57	19.0 ± 2.06	174.4 ± 83.2
4	0	0	0	13.27(100)	4.9 ± 1.47	29.4 ± 1.35	20.3 ± 1.01	298.0 ± 116
5	5.5(50)	5.29(50)	0	0	21.0 ± 0.35	31.5 ± 1.47	31.9 ± 1.85	2109.6 ± 186
6	5.5(50)	0	3.34(50)	0	17.9 ± 0.79	35.5 ± 0.44	35.8 ± 0.03	2277.3 ± 127
7	5.5(50)	0	0	6.63(50)	21.0 ± 0.31	32.2 ± 1.11	30.6 ± 1.31	2070.3 ± 190
8	0	5.29(50)	3.34(50)	0	18.5 ± 0.15	33.0 ± 2.4	27.2 ± 0.4	1661.1 ± 82.4
9	0	5.29(50)	0	6.63(50)	15.2 ± 0.64	23.9 ± 2.64	27.9 ± 10.6	1417.5 ± 640
10	0	0	3.34(50)	6.63(50)	4.2 ± 3.4	24.6 ± 3.27	18.7 ± 0.76	197.6 ± 173
11	3.67(33.3)	3.53(33.3)	2.23(33.3)	0	19.1 ± 0.34	28.6 ± 2.07	30.6 ± 0.17	1671.3 ± 160
12	3.67(33.3)	3.53(33.3)	0	4.42(33.3)	20.6 ± 0.45	33.6 ± 0.23	27.8 ± 0.93	1920.5 ± 35.4
13	3.67(33.3)	0	2.23(33.3)	4.42(33.3)	18.3 ± 0.94	38.8 ± 1.46	30.9 ± 1.6	2196.0 ± 143
14	0	3.53(33.3)	2.23(33.3)	4.42(33.3)	16.8 ± 2.73	34.2 ± 3.14	23.7 ± 0.01	1369.2 ± 345
15	2.75(25)	2.64(25)	1.67(25)	3.32(25)	19.9 ± 0.07	31.2 ± 0.92	28.6 ± 3.1	1785.0 ± 252
16	6.88(62.5)	1.32(12.5)	0.835(12.5)	1.66(12.5)	18.8	34.9	36.5	2400.5
17	1.38(12.5)	6.61(62.5)	0.835(12.5)	1.66(12.5)	16.7 ± 1.42	19.5 ± 4.91	23.6 ± 1.11	771.6 ± 222
18	1.38(12.5)	1.32(12.5)	4.17(62.5)	1.66(12.5)	12.3 ± 0.44	15.6 ± 0.16	25.51 ± 0.4	488.94 ± 15
19	1.38(12.5)	1.32(12.5)	0.835(12.5)	8.29(62.5)	12.8 ± 2.58	31.6 ± 3.5	16.2 ± 0.33	666.48 ± 219

[a] Uncoded variable with the total N source maintained at 1.1 g L^{-1}, with 100 % Ratio of components (%); [c] Mean ± Standard Deviation (SD), n = 2

[b] Represents mean of the responses for biomass DCW production (g L^{-1}), Oil content (%), ARA content (%) and ARA production (mg L^{-1})

Table B.2: Plackett-Burman design table.

No.	X_1 [a]	X_2	X_3	X_4	X_5	X_6	X_7	X_8	DCW [b]	TFA % [c]	ARA % [d]	ARA [e]
1	7.5 (+)	0 (-)	2.7 (+)	0 (-)	0 (-)	0 (-)	24 (+)	10 (+)	13.52± 0.52[f]	17.15 ± 0.05	19.58 ± 1.45	454.4 ± 46
2	7.5 (+)	15 (+)	0 (-)	0.5 (+)	0 (-)	0 (-)	0 (-)	10 (+)	11.74 ± 0.09	14.23 ± 0.10	25.86 ± 0.18	432.3 ± 1.8
3	0 (-)	15 (+)	2.7 (+)	0 (-)	5.4 (+)	0 (-)	0 (-)	0 (-)	7.50 ± 0.01	11.80 ± 0.70	21.64 ± 0.21	191.6 ± 19.7
4	7.5 (+)	0 (-)	2.7 (+)	0.5 (+)	0 (-)	2 (+)	0 (-)	0 (-)	14.72 ± 0.21	16.49 ± 0.17	31.31 ± 1.03	760.3 ± 26
5	7.5 (+)	15 (+)	0 (-)	0.5 (+)	5.4 (+)	0 (-)	24 (+)	0 (-)	14.87 ± 0.54	16.08 ± 0.28	24.52 ± 0.48	586.1 ± 2.8
6	7.5 (+)	15 (+)	2.7 (+)	0 (-)	5.4 (+)	2 (+)	0 (-)	10 (+)	14.10 ± 1.51	14.13 ± 0.16	19.75 ± 0.47	393.5 ± 47
7	0 (-)	15 (+)	2.7 (+)	0.5 (+)	0 (-)	2 (+)	24 (+)	0 (-)	14.62 ± 0.59	13.14 ± 0.49	21.47 ± 1.32	412.2 ± 30
8	0 (-)	0 (-)	2.7 (+)	0.5 (+)	5.4 (+)	0 (-)	24 (+)	10 (+)	12.09 ± 0.34	12.42 ± 0.05	23.05 ± 3.80	345.2 ± 26
9	0 (-)	0 (-)	0 (-)	0.5 (+)	5.4 (+)	2 (+)	0 (-)	10 (+)	13.40 ± 0.88	14.00 ± 0.51	23.07 ± 5.25	433.5 ± 109
10	7.5 (+)	0 (-)	0 (-)	0 (-)	5.4 (+)	2 (+)	24 (+)	0 (-)	11.09 ± 0.32	12.11 ± 0.31	21.21 ± 0.65	285.1 ± 24
11	0 (-)	15 (+)	0 (-)	0 (-)	0 (-)	2 (+)	24 (+)	10 (+)	3.61 ± 0.11	8.10 ± 1.48	21.24 ± 1.06	62.5 ± 27
12	0 (-)	0 (-)	0 (-)	0 (-)	0 (-)	0 (-)	0 (-)	0 (-)	9.81 ± 0.66	18.17 ± 0.25	22.33 ± 3.50	396.4 ± 38

[a] $X_1 = KH_2PO_4$ (g L^{-1}); X_2 = NaCl (g L^{-1}); $X_3 = MgSO_4.7H_20$ (g L^{-1}); $X_4 = CaCl_2.2H_20$ (g L^{-1}); $X_5 = MgCl_2.6H_20$ (g L^{-1}); X_6 = Sodium Citrate (g L^{-1}); X_7 = Trace Mineral Solution (TMS) (mL L^{-1}); X_8 = Vitamin Solution (mL L^{-1})

[b] Represents mean of the responses for biomass DCW production (g L^{-1}) based on duplicate experiments.

[c] Represents mean of the responses for oil TFA content (%) based on duplicate experiments.

[d] Represents mean of the responses for ARA content (%) based on duplicate experiments.

[e] Represents mean of the responses for ARA production (mg L^{-1}) based on duplicate experiments.

[f] Mean ± Standard Deviation (SD), n = 2.

Table B.3: Central composite design in uncoded and coded units (parentheses), and the experimental values of the responses (biomass, oil content and ARA content and concentration) for *M. alpina* MA2-2 in the 1st RSM design

No.	KH_2PO_4 (g L^{-1})	$MgSO_4.7H_20$ (g L^{-1})	$CaCl_2.2H_20$ (g L^{-1})	**Biomass** g L^{-1} [a]	**Oil %** [c]	**ARA%** [d]	**ARA mg** L^{-1} [e]
1	0.5 (-1)	0.5 (-1)	0.05 (-1)	14.2 ± 0.16 [b]	18.3 ± 0.22	27.56 ± 0.07	713.6 ± 18.4
2	7.5 (+1)	0.5 (-1)	0.05 (-1)	15.6 ± 0.27	17.6 ± 0.92	21.60 ± 0.77	593.2 ± 41.9
3	0.5 (-1)	5 (+1)	0.05 (-1)	12.4 ± 0.40	13.9 ± 1.37	31.56 ± 2.11	548.5 ± 107.6
4	7.5 (+1)	5 (+1)	0.05 (-1)	14.7 ± 0.24	17.0 ± 0.80	22.13 ± 0.29	553.6 ± 42.1
5	0.5 (-1)	0.5 (-1)	2 (+1)	13.6 ± 0.63	13.0 ± 0.11	27.67 ± 8.94	486.1 ± 131.6
6	7.5 (+1)	0.5 (-1)	2 (+1)	17.0 ± 0.08	13.7 ± 0.85	22.94 ± 0.47	534.7 ± 46.7
7	0.5 (-1)	5 (+1)	2 (+1)	13.4 ± 0.12	12.9 ± 0.53	37.23 ± 1.60	646.6 ± 4.39
8	7.5 (+1)	5 (+1)	2 (+1)	15.7 ± 1.11	16.0 ± 0.85	31.14 ± 1.94	780.5 ± 62.2
9	0 (-1.683)	2.75 (0)	1.025 (0)	13.9 ± 0.94	13.6 ± 0.49	27.75 ± 2.80	524.8 ± 1.24
10	9.886 (+1.683)	2.75 (0)	1.025 (0)	17.3 ± 0.02	16.1 ± 0.12	26.35 ± 0.67	734.2 ± 25.3
11	4 (0)	0 (-1.683)	1.025 (0)	14.6 ± 0.23	15.7 ± 1.53	23.02 ± 4.41	530.1 ± 143.9
12	4 (0)	6.534 (+1.683)	1.025 (0)	17.3 ± 0.08	13.0 ± 0.66	22.86 ± 0.40	515.1 ± 32.8
13	4 (0)	2.75 (0)	0 (-1.683)	13.1	15.6	19.76	402.4
14	4 (0)	2.75 (0)	2.665 (+1.683)	15.2 ± 0.19	14.8 ± 0.66	30.73 ± 0.23	689.4 ± 27.4
15	4 (0)	2.75 (0)	1.025 (0)	16.8 ± 0.14	15.8 ± 0.02	24.71 ± 0.37	658.0 ± 5.07
16	4 (0)	2.75 (0)	1.025 (0)	16.8 ± 0.42	15.8 ± 0.75	27.09 ± 3.06	715.7 ± 96.8
17	4 (0)	2.75 (0)	1.025 (0)	16.5 ± 0.97	13.4 ± 1.76	24.51 ± 4.63	544.9 ± 141.4
18	4 (0)	2.75 (0)	1.025 (0)	17.1 ± 0.13	15.4 ± 0.63	23.85 ± 0.23	627.4 ± 27.1
19	4 (0)	2.75 (0)	1.025 (0)	16.9 ± 0.13	15.4 ± 0.49	23.02 ± 0.21	598.4 ± 8.82
20	4 (0)	2.75 (0)	1.025 (0)	16.8 ± 0.11	15.2 ± 0.68	23.61 ± 1.64	604.7 ± 65.0

[a] Represents mean of the responses for biomass DCW production (g L^{-1}); TFA or Oil content (%); ARA content (%) and ARA production (mg L^{-1}) based on duplicate experiments. [b] Mean ± SD, n = 2

Table B.4: Central composite design in uncoded and coded units (parentheses), and the experimental values of the responses (biomass, oil content and ARA content and concentration) of *M. alpina* MA2-2 in the 2nd RSM design

No.	KH_2PO_4 (g L^{-1})	$MgSO_4.7H_20$ (g L^{-1})	$CaCl_2.2H_20$ (g L^{-1})	**Biomass g L^{-1}** [a]	**Oil %**	**ARA%**	**ARA mg L^{-1}**
1	1 (-1)	2.5 (-1)	1 (-1)	16.6 ± 0.0[b]	12.45 ± 0.0	20.58 ± 0.0	425.47 ± 0.0
2	4 (+1)	2.5 (-1)	1 (-1)	15.31 ± 0.5	13.42 ± 0.0	31.21 ± 2.72	642.20 ± 77.2
3	1 (-1)	7.5 (+1)	1 (-1)	15.56 ± 1.3	12.55 ± 0.6	26.68 ± 1.90	519.39 ± 29.9
4	4 (+1)	7.5 (+1)	1 (-1)	16.78 ± 0.3	12.76 ± 0.0	24.22 ± 4.21	518.19 ± 83.0
5	1 (-1)	2.5 (-1)	3 (+1)	12.90 ± 0.5	12.53 ± 0.1	23.83 ± 0.21	385.26 ± 14.6
6	4 (+1)	2.5 (-1)	3 (+1)	15.69 ± 1.0	13.08 ± 0.8	22.34 ± 2.08	457.49 ± 41.2
7	1 (-1)	7.5 (+1)	3 (+1)	15.08 ± 0.2	11.32 ± 0.3	26.21 ± 0.13	447.08 ± 4.20
8	4 (+1)	7.5 (+1)	3 (+1)	15.43 ± 0.6	11.79 ± 1.4	25.44 ± 7.75	466.96 ± 176
9	0 (-1.683)	5 (0)	2 (0)	5.34 ± 1.1	9.80 ± 0.8	18.53 ± 1.62	99.04 ± 36.5
10	5.023 (+1.683)	5 (0)	2 (0)	15.34 ± 0.3	11.60 ± 0.5	25.20 ± 7.17	444.62 ± 98.2
11	2.5 (0)	0.796 (-1.683)	2 (0)	14.60 ± 0.1	11.98 ± 0.8	25.07 ± 0.29	438.44 ± 25.6
12	2.5 (0)	9.204 (+1.683)	2 (0)	15.33±0.7	11.59 ± 0.3	26.16 ± 9.33	462.95 ± 158
13	2.5 (0)	5 (0)	0.318 (-1.683)	15.13 ± 0.3	14.78 ± 0.6	23.85 ± 1.37	533.69 ± 44.2
14	2.5 (0)	5 (0)	3.682 (+1.683)	14.98 ± 0.1	11.81 ± 0.8	25.99 ± 1.44	460.51 ± 52.5
15	2.5 (0)	5 (0)	2 (0)	14.93 ± 0.0	10.59 ± 0.3	28.68 ± 0.96	453.67 ± 25.9
16	2.5 (0)	5 (0)	2 (0)	15.08 ± 0.1	11.47 ± 0.4	22.08 ± 1.42	382.29 ± 35.7
17	2.5 (0)	5 (0)	2 (0)	14.62 ± 0.6	12.19 ± 0.1	23.16 ± 2.07	411.99 ± 15.2
18	2.5 (0)	5 (0)	2 (0)	14.85 ± 0.1	10.90 ± 0.2	27.60 ± 1.35	446.27 ± 15.5
19	2.5 (0)	5 (0)	2 (0)	14.84 ± 0.0	10.95 ± 0.2	24.83 ± 3.35	404.06 ± 62.9
20	2.5 (0)	5 (0)	2 (0)	14.88 ± 0.4	11.05 ± 0.2	26.54 ± 0.70	436.74 ± 29.9

[a] Represents mean of the responses for biomass DCW production (g L^{-1}); TFA or Oil content (%); ARA content (%) and ARA production (mg L^{-1}) based on duplicate experiments. [b] Mean ± SD, n = 2